

ENERGY REQUIREMENTS AND PRODUCTIVITY OF MACHINERY USED TO
HARVEST HERBACEOUS ENERGY CROPS

BY

PHILLIP C. JOHNSON

THESIS

Submitted in partial fulfillment of the requirements
for the degree of Master of Science in Agricultural and Biological Engineering
in the Graduate College of the
University of Illinois at Urbana-Champaign, 2012

Urbana, Illinois

Adviser:

Professor Alan Hansen

ABSTRACT

Herbaceous energy crops (miscanthus, switchgrass, and tallgrass prairie) are promising biomass feedstocks, but are difficult to harvest with traditional machinery. In this study, energy required for harvesting novel herbaceous crops was evaluated in both field and laboratory settings. Previous work on harvesting concluded that crop flow and parasitic losses accounted for the majority of harvesting power requirements. In mowing, for example, research has shown that cutting of plant material accounted for only 3% energy usage. Investigations of single stem cutting of traditional forages (timothy, alfalfa, wheat straw, maize) have identified a critical cutting speed at which energy requirements are minimized and ideal cut quality occurs. This critical speed is believed to occur when blade velocity is high enough to sever the stem without moving it, which occurs when inertia forces equal or outweigh the external force imposed by cutting.

Results of high speed cutting experiments in this study confirm the low influence of crop cutting on total harvest energy. Energy requirements of single stem cutting in miscanthus were 9.30 ± 2.60 J per stem, which represented only 2.1% of in-field mowing requirements. A critical cutting speed for miscanthus was not found and may occur above the range considered (10-20 m/s). Mowing and baling power demands ranged from 25-63 kW. Parasitic energy, required to power the machine without crop input, was high by multiple estimates, and averaged 56% of power usage. Due to these losses, harvest efficiency is favored by maximizing machine groundspeed and throughput, which increases instantaneous power requirements but accomplishes more useful work per unit of energy lost. Mowing productivity (23.6 Mg/h) was higher than baling (16 Mg/h), which may complicate the design of single-pass harvesting machinery. Due to the influence of ground speed on energy usage, modern hay and forage

equipment will benefit from tractor-baler integration and self-controlled groundspeed. Overall, energy requirements of baled crop on a dry basis were 18.2, 10.9, 19.4, and 13.4 MJ/Mg for the large square baler, pull-type rotary mower, self-propelled rotary, and sickle, respectively. Based on these results, electronic throughput control shows promise as means of reducing energy usage. Conversely, advances in single stem cutting efficiency are not likely to reduce harvest power, since cutting represents a small percentage of overall power demands. In-field power measurements would benefit from additional work aimed at decreasing uncertainty using higher resolution yield measurements and considerations of draft power.

ACKNOWLEDGEMENTS

This research was financially supported by the Energy Bioscience Institute (EBI) and the Jonathan Baldwin Turner fellowship, which is provided by the college of ACES at the University of Illinois. Material and technical support were provided by Case New Holland (CNH). I am indebted to my advisor, Dr. Alan Hansen for his patience, wisdom and guidance. In addition, I acknowledge the support of my committee, Dr. Tony Grift and Dr. Luis Rodríguez.

Invaluable technical support was provided by members of the EBI Research Farm, including Dr. Tom Voigt, Tim Mies, Chris Rudisill, Emily Thomas, and Drew Shilling (Voigt et al. 2010). I am also grateful for the help of Dr. Chris Foster and Jeff Fay of CNH. Field trials in Miscanthus and switchgrass were orchestrated and performed entirely by these members of EBI with assistance from CNH. My recording system was a comparatively small addition.

Dr.s Clairmont Clementson, Sunil Mathanker, and Zewei Miao provided invaluable mentoring and advice in the design of cutting experiments and processing of the resulting data.

I am especially indebted to Amanda Valentine, who constructed the high speed cutting apparatus and took a personal interest in my success and growth as a professional.

Finally I am grateful for my parents and friends, who have appropriately nurtured, guided, and inspired me.

TABLE OF CONTENTS

CHAPTER 1: INTRODUCTION.....	1
CHAPTER 2: OBJECTIVES	2
CHAPTER 3: REVIEW OF LITERATURE.....	3
3.1 Brief Introduction to Herbaceous Energy Crops.....	3
3.1.1 Switchgrass (<i>Panicum virgatum</i>)	5
3.1.2 Miscanthus (<i>Miscanthus x giganteus</i>)	7
3.1.3 Mixed Tallgrass Prairie	9
3.2 Harvesting of Herbaceous Energy Crops.....	10
3.2.1 Mowing.....	11
3.2.1.1 Reciprocating Sickle Bar Mowers	12
3.2.1.2 Vertical Axis Rotary Mowers (Disc and Drum).....	15
3.2.1.3 Horizontal Axis Rotary Mowers (Flail)	19
3.2.2 Baling	20
3.3 Theoretical Cutting Mechanics of Forage and Herbaceous Energy Crops.....	23
3.3.1 Modes of Cutting Plant Material.....	24
3.3.2 Critical Cutting Speed	25
3.3.3 Geometry of Cutting Knives.....	29
3.4 Laboratory Based Cutting Experiments.....	30
3.4.1 Cutting of Grass-Like Stems.....	31
3.4.2 Cutting of Cane-Like Stems	33
CHAPTER 4: MATERIALS AND METHODS	35
4.1 Evaluation of Current Two-Pass Harvest Technique	35
4.1.1 Harvesting Equipment Used.....	36
4.1.1.1 Mowing Equipment.....	37
4.1.1.2 Baling Equipment	38
4.1.2 Harvest Monitoring System.....	39
4.1.3 Processing of Harvest Data.....	42
4.2 Development and Testing of High-speed Cutting Apparatus	43
4.2.1 Moment of Inertia of Single Stem Cutter	45

4.2.2 Determination of Cutting Speed	49
4.2.3 Characterization of Miscanthus Used In Cutting Trials	52
4.2.4 Design Iterations of Single Stem Cutter	53
4.2.5 Safety Considerations	53
CHAPTER 5: RESULTS AND DISCUSSION	55
5.1 In-Field Performance Monitoring	56
5.1.1 Variation in Engine Load.....	57
5.1.2 Aggregate Results	57
5.1.2.1 Machine Power Usage.....	59
5.1.2.2 Average Machine Speed.....	60
5.1.2.3 Crop Conditions	61
5.1.2.4 Average Harvest Energy	62
5.1.3 Effect of Yield on Engine Power	63
5.1.4 Effect of Ground Speed on Engine Power.....	66
5.1.5 Relationship Between Engine Power, Yield, and Harvest Speed.....	68
5.2 Laboratory Based Cutting of Miscanthus	71
5.2.1 Effect of Cutting at Node and Internode	72
5.2.2 Effect of Miscanthus Diameter	74
5.2.3 Statistical Interpretation of Results	74
CHAPTER 6: SUMMARY AND CONCLUSIONS	76
CHAPTER 7: RECOMMENDATIONS FOR FUTURE WORK.....	78
REFERENCES	79
APPENDIX A: MEASUREMENT RESULTS.....	87
A.1 Summarized Results of Harvesting Field Trials.....	87
A.2 Data Files Recorded During Harvesting Field Trials	88
APPENDIX B: PROGRAMS USED IN DATA ACQUISITION	102
APPENDIX C: PROGRAMS USED IN DATA PROCESSING.....	117
C.1 Main Matlab® (Mathworks) Script Used to Process High Speed Cutting Data	117
C.2 Main Matlab® (Mathworks) Script Used To Process In-Field Harvest Data	120

CHAPTER 1: INTRODUCTION

In the United States alone, farmers harvest approximately 60 million acres of grass, alfalfa, and other forages each year (National Agriculture Compliance Assistance Center 2012). The area devoted to forage production is equivalent to the combined footprint of corn and soybeans, which occupy 146 million acres. Forage crops typically have a lower value, producing \$56 per acre, where corn and soybeans average \$200. Despite this, hay and forage production has played an important role in the development of society. Storage of forage as hay allowed pre-industrial societies to nourish their sources of food and transportation (livestock and draft animals) throughout the winter in densely populated areas (Dyson 1989). The invention of hay is believed to have been a necessary precursor to the birth of Rome, Paris, London, and later Berlin, Moscow and New York.

Following a projected decline in global oil reserves, researchers are pursuing a means of converting cellulosic forages and other feedstock into ethanol, to once again fuel society's transportation needs. Ethanol production has increased rapidly in the past decade, but questions remain about the sustainability of current, first-generation biofuels. Generation of ethanol from high value crops (corn, beans, and cane) is believed unsustainable due to the amount of net energy produced and possible competition with food crops (Perlack et al. 2005). Second-generation biofuels offer a promising alternative, as low-input biomass feedstocks can be used to produce cellulosic ethanol. The aim of this work is to facilitate and optimize the collection of herbaceous energy crops, a promising feedstock for second-generation biofuels.

CHAPTER 2: OBJECTIVES

The feasibility of large scale biofuel production is sensitive to the amount of energy required to harvest biomass feedstocks (Giampietro et al. 1997). The objective of this study was to evaluate current harvesting techniques and provide recommendations for reducing the amount of energy required to harvest herbaceous energy crops. Harvesting was evaluated in two ways. First, a holistic view of the process was considered, by monitoring the energy requirements and productivity of several types of existing machinery. This provided an estimate of harvesting energy requirements that was dependent on the particular machinery in use. Second, laboratory experiments were conducted to fundamentally evaluate the cutting of plant stems. This evaluation provided a much narrower view of the harvesting process, but was independent of the equipment in use and allowed experiments to take place in a controlled, repeatable fashion.

In particular, the objectives of field trials with harvesting machinery were to:

- measure the energy consumed at harvest by each machine, per unit of biomass
- evaluate the relationship between throughput and power usage
- determine the average productivity of each machine

The objectives of laboratory cutting experiments were to:

- determine the amount of energy required to sever individual miscanthus stems
- evaluate the effect of blade speed and oblique angle on cutting energy

The results of field and laboratory experiments were combined to estimate the fraction of energy that field harvesting machinery expended in cutting plant stems. These results were used to evaluate the overall importance of stem cutting on the harvesting process, in terms of the fraction of overall energy consumed.

CHAPTER 3: REVIEW OF LITERATURE

Recent interest in the large scale production of biomass-based fuels has led researchers to reevaluate the effectiveness of traditional hay and forage machinery in novel, forage-like energy crops. This machinery, which has remained relatively unchanged since its development (Stone 1977), would be used to harvest an unprecedented volume of biomass (Richard 2010). Prior to interest in herbaceous energy crops, significant work has been done to evaluate the energy requirements of hay and forage machinery in existing crops (Chancellor 1958; Karpenko 1968; Mcrandal and McNulty 1978b; Srivastava et al. 2006). This previous work includes field testing of production machines as well as laboratory experiments on machine components and fundamental processes, such as the cutting of plant stems. While existing hay and forage machinery works relatively well with herbaceous energy crops (Heaton et al. 2004), the higher yield and maturity of these crops will necessitate design changes to handle greater crop volumes (Shinners et al. 2010). The following sections provide an overview of the energy crops considered in this study, existing harvest options, design consideration of harvesting equipment, and results of laboratory-based evaluations of crop cutting.

3.1 Brief Introduction to Herbaceous Energy Crops

This study considers the harvesting of three herbaceous energy crops: miscanthus (*Miscanthus x giganteus*), switchgrass (*Panicum virgatum*), and mixed tallgrass prairie. All three crops were grown in Illinois in research efforts directed by the Feedstock Production and Agronomy program at the Energy Bioscience Institute (Voigt et al. 2010). Herbaceous energy crops are known for their efficiency in converting sunlight to cellulose with low agronomic inputs such as fertilizer, herbicide, and intensive management (Perlack et al. 2005). These crops

also have environmental benefits; they provide resistance against soil erosion and can be used to buffer cropland near waterways.

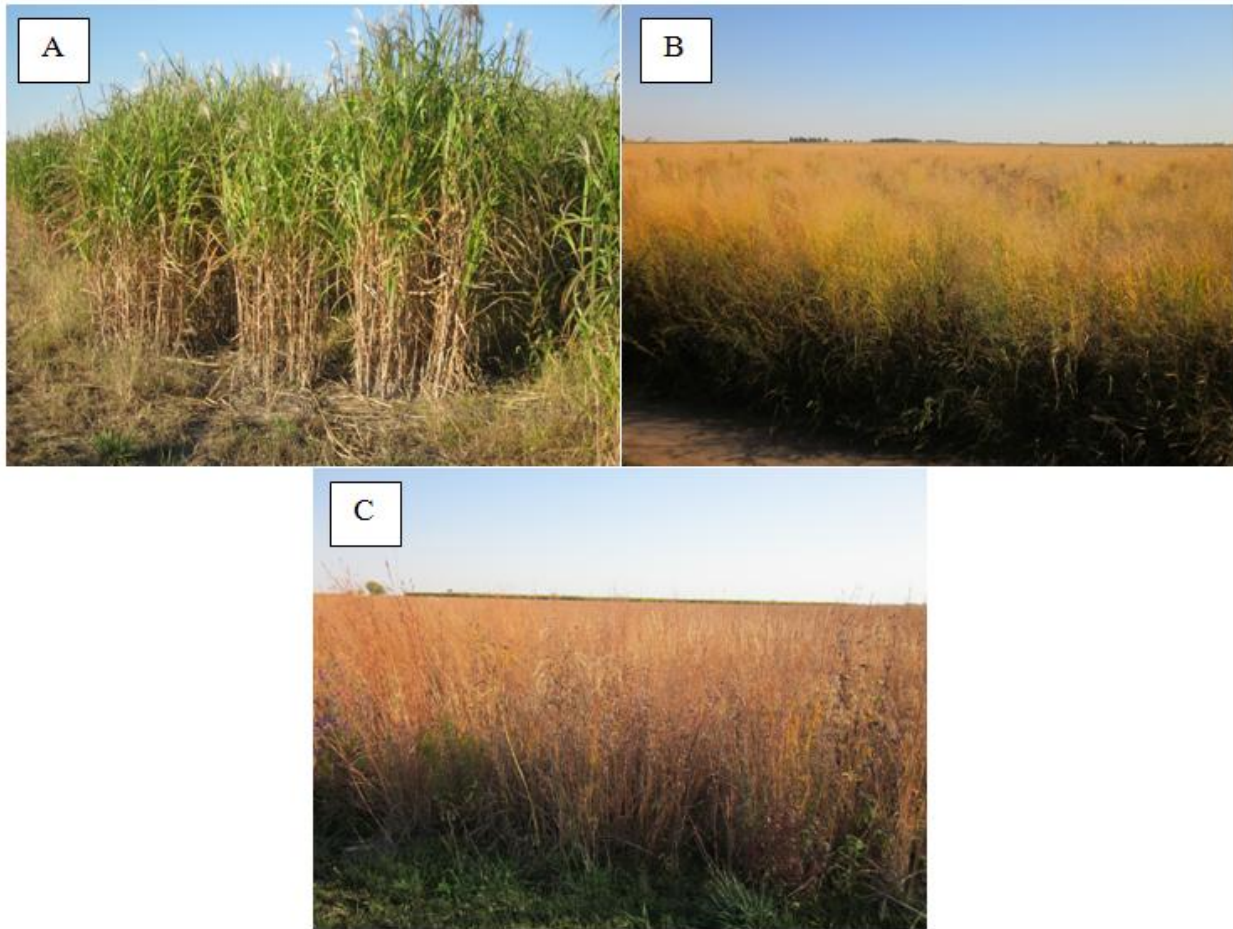


Figure 1 Miscanthus (A), switchgrass (B), and tallgrass prairie(C).

While the ideal frequency and time of biomass harvest is under debate (Hohenstein and Wright 1994, Thomason et al. 2004, Fike et al. 2006), it is believed that a single late season harvest minimizes nutrient removal because crops transport nitrogen and other nutrients into their roots after a killing frost. This leads to a single-cutting strategy that contrasts the handling of conventional forage, which is collected three to four times per year. While beneficial from an agronomic standpoint, a single annual harvest places additional stress on harvesting machinery, since yields are greater, and the crop itself more mature and resilient to cutting (Vogel et al.

2010). The following sections provide a brief background of the herbaceous energy crops considered in this study, as well as their relevant mechanical properties and traditional yield expectations. This review considers specifically the aspects of these crops most relevant to harvest operations. Factors such as the chemical composition of the crop are ignored. A full discussion of the agronomics and management of these energy crops is provided by Hohenstein and Wright 1994, Giampietro et al. 1997, Lewandowski et al. 2000, Thomason et al. 2004, Heaton et al. 2004, and Yu et al. 2006. Figure 1 depicts the herbaceous energy crops considered in this study.

3.1.1 Switchgrass (*Panicum virgatum*)

Switchgrass has shown considerable promise as an energy crop due to its high yield, ability to propagate by seed, and tolerance for domestic conditions as a native grass species (Yu et al. 2006). Three cultivars typically considered are Cave-In-Rock, Shawnee, and Trailblazer (Adler et al. 2006). Switchgrass can be harvested with existing hay equipment and can be planted on marginal land (Vogel 1996). Other advantages include its tolerance to droughts, low fertilizer requirements, low risk, and simple farm integration (Hohenstein and Wright 1994). Switchgrass is believed to have evolved under low nitrogen conditions. Trials conducted by Thomason et al. (2004) indicated that switchgrass growth was not greatly increased by heavy nitrogen fertilization. Yields from 4-14 Mg/ha/year have been cited (Thomason et al. 2004, Adler et al. 2006, Fike et al. 2006, Yu et al. 2006, Shinnars et al. 2010). Yields greater than 20 Mg/ha have been reported, and 12 Mg/ha is considered a conservative estimate of production (Richard 2010). Previous studies of the internal energy content and economics of harvest have indicated that switchgrass production is comparable to wood on the basis of cost per unit of heat generation (Thomason et al. 2004).

Although existing machinery can be used to harvest switchgrass, yields are much higher than traditional forage crops (Thomason et al. 2004). Shinnars et al. (2010) note that the ground speed of baling equipment was severely limited by the volume of crop material collected. Harvesting two or three times annually can ease these concerns by decreasing the volume at each collection and allowing earlier cuttings to be used as animal feed. Thomason et al. (2004) note that the number of harvests had a strong impact on yield, with three, two, and one annual harvests producing 16.3, 14.7, and 12.9 Mg/ha per year, respectively. Shinnars et al. (2010) reported an increase in yield of 31% with two cuttings. Thomason et al. (2004) also note that increased harvest frequency tends to decrease the density of the plant stand over time, which may eventually result in lower yields.

The timing of switchgrass harvest also has a significant impact on yield, and may place additional stress on harvesting machinery. Shinnars et al. (2010) report a 17% loss in yield due to harvesting in spring rather than late fall. Another study reports yield losses in spring harvests of 40% after a winter of heavy snow accumulation (Shinnars et al. 2010). Disagreement exists over sources for this loss of yield. Adler et al. (2006) report that 90% of switchgrass losses due to overwintering are due to inability of the harvester to gather lodged crop material. However, Shinnars et al. (2010) argue that reduced collection in spring harvest is due to loss in plant matter as leaves shed during the winter decompose. The amount of snow received during the winter may also be a factor, yield losses as high as 40% have been reported over heavy winters with 150cm of snowfall (Adler et al. 2006). The decision to harvest in winter rather than late fall also affects the quality of harvested material, because winter harvests result in lower mineral content. It has therefore been suggested that biomass harvested for direct combustion may be favorable in

the winter or spring, while harvest for conversion to cellulosic ethanol should take place in late autumn (Adler et al. 2006).

3.1.2 Miscanthus (*Miscanthus x giganteus*)

Miscanthus x giganteus, hereafter referred to as miscanthus, is a perennial warm-season (C4) grass that produces bamboo-like shoots that are 12-20mm in diameter and 3m tall (Pyter et al. 2007). Like switchgrass, miscanthus is very efficient at capturing and retaining nitrogen. Research plots in Illinois consistently produced 6.2-14.8 Mg/ha, with yields as high as 40 Mg/ha reported under ideal conditions (Pyter et al. 2007, Anderson et al. 2011). Lewandowski et al. (2003) report yields of 30 Mg DM/ha under ideal conditions and 12-15 Mg DM/ha consistently. Cultivation and harvesting of miscanthus is well known in Europe, where it has been commercially grown to provide feedstock for combined heat and power facilities. The sterile hybrid of two miscanthus species, giant miscanthus (*Miscanthus x giganteus*) is propagated asexually by dividing and replanting rhizomes. Establishment costs are high, as planting and propagation remains an open area of research and commercial innovation. The growing season in Illinois begins in April and harvest typically occurs after the first killing frost in October. Yields increase each year after planting as the miscanthus stand matures. Establishment can take 5-7 years in poor soils. Final crop density is approximately 50-100 stems per m² (Pyter et al. 2007). Anderson et al. (2011) provide a comprehensive review of the growth and agronomy of miscanthus.



Figure 2 Effect of conditioning roll pressure on windrow characteristics. The windrow on the left is unconditioned and difficult to pickup because stems are lying flat. The properly conditioned windrow on the right stands up taller and is easier to bale.

As with switchgrass, the ideal frequency and maturity at harvest is still under debate. Current thinking is that miscanthus should be harvested once, in late autumn or winter-spring, after its nutrients have translocated to the roots (Lewandowski and Heinz 2003) . As with other biomass crops, harvesting later in winter tends to produce lower yields, but makes the crop more attractive for an end use of combustion, since it tends to have a lower mineral content (Kristensen 2003). Harvest management will therefore depend on end use as well as field accessibility. Winter harvesting by mowing and baling can be especially difficult to accommodate, since the ground must be frozen with little or no snow present. A single-pass harvester will allow mild snow accumulation, since the crop will not have to be grounded between mowing and baling or chopping. Whenever harvesting takes place, it is clear that the harvesting window will be small and the throughput of harvesting machinery critical (Greenlees

et al. 2000, Vogel et al. 2002). As with switchgrass, delayed harvest due to snow or rain reduces yield by up to 18% (Lewandowski and Heinz 2003).

Relative to other herbaceous energy crops, miscanthus presents the greatest challenge to existing equipment. Its high yield and stalk rigidity make it difficult to cut and convey. Conditioning after mowing has been found to break stems and improve crop flow into the baler in two-pass harvest operations (Kristensen 2003). Metal crimping rolls appear to perform this task better than rubber. Kristensen (2003) has found that a lack of uniform crimping at mowing will lead to frequent stops and plugging of the baler. A similar outcome in crop conditioning was observed in harvest trials conducted during this study, as indicated in Figure 2. Mowing and baling operations of miscanthus are further complicated by its elevated silica content, which increases wear on machinery (Greenlees et al. 2000).

3.1.3 Mixed Tallgrass Prairie

Mixed tallgrass prairie is an assortment of native grass species that have historically comprised the flora of the plains. While feedstock production from miscanthus and switchgrass has been extensively studied in the US and Europe, less is known about these native species (Voigt et al. 2010). Mixed tallgrass prairie constitutes a dynamic planting that changes throughout the growing season as the most aptly suited species exploit current conditions (DeHaan et al. 2010). From a harvesting standpoint, prairie grass mixtures resemble conventional crops and do not require significant harvesting innovation. Research has shown that the diversity of mixed tallgrass prairie plantings may allow them to produce more biomass than monocultures of other grasses (Tilman et al. 2006). Biomass yields from mixed tallgrass prairie plantings are strongly dependent on the species present, with yields from 2.7 to 3 Mg/ha (DeHaan et al. 2010). Tilman et al. (2006) demonstrated a logarithmic relationship between

biomass yield and the number of species within the plot. Further research into plant species and their role within the ecosystem may lead to higher yielding combinations.

3.2 Harvesting of Herbaceous Energy Crops

Traditional forage crops, such as grasses and legumes have been mechanically harvested for centuries to supplement animal nutrition and eliminate the need for animals to graze (Stone 1977). Forages are traditionally harvested in two ways – *direct-cut* and *field wilting* (Srivastava et al. 2006). Direct cut methods harvest the forage in a single-pass, and are usually performed by a flail mower or forage chopper. Direct cutting requires storage at the moisture content present during harvest. Field wilting requires several harvesting passes (mowing, conditioning, raking, tedding, and baling), and reduces the moisture content of the forage by laying it in the field before collection and storage. Traditional field wilted forage is cut at 70-80% moisture and reduced to 50-65% for ensilage and 15-23% for hay. Reducing the moisture content of forage often results in crop loss as leaves and stems fall apart during subsequent field operations (Rees 1982). Herbaceous energy crops differ from traditional forages in that they are typically dry enough (15- 23% moisture) to be direct-cut and stored. This eliminates the need for wilting, unless multiple harvests per year are considered. Most herbaceous energy crops can therefore be harvested by direct-cut mowing and baling or direct-cut field chopping (Lewandowski et al. 2000).

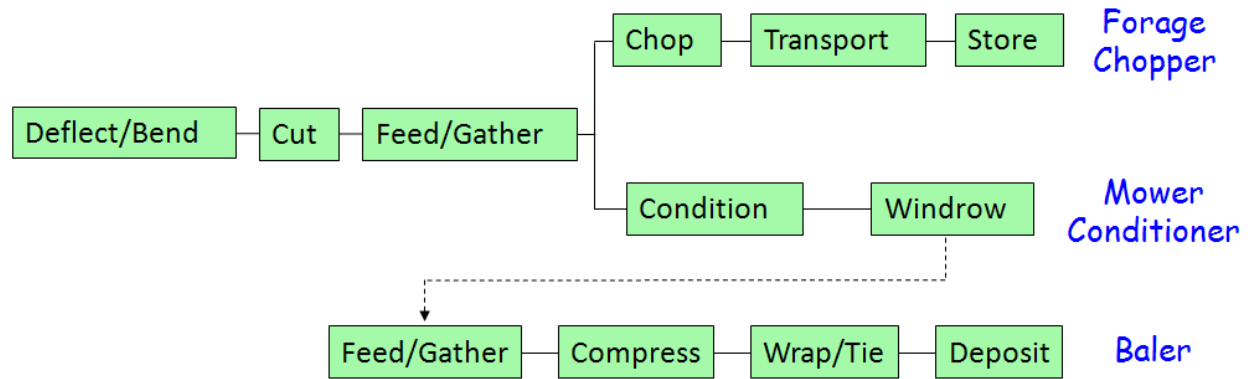


Figure 3 Functional processes required to harvest herbaceous energy crops and traditional forages. Single pass baling equipment combines mowing and baling in a single machine.

Single-pass harvesting is possible with direct-cut field choppers or combined mowing and baling machines. Either pathway requires harvesting equipment that is not usually employed, since direct-cutting of traditional crops is uncommon due to the poor storage characteristics of unwilted forage. The advantages of direct-cutting energy crops must therefore be weighed against an increase in machinery cost. Figure 3 depicts the functional processes required to harvest forage crops.

3.2.1 Mowing

Whether direct-cutting or field wilting, harvesting begins with a mowing operation. Mowing is often combined with conditioning, hence the term mower-conditioner. During conditioning, the crop is passed through axial rollers or drum-mounted flails. Conditioning crushes plant stems, allowing them to dry at the same rate as the plant's leaves, which reduces overall drying time (Srivastava et al. 2006). While drying is usually unnecessary in herbaceous energy crops, conditioning can increase flowability in subsequent conveying and densification processes (Kristensen 2003). Mower-conditioners can be employed as headers on self-propelled machines, towed implements, or direct-cut headers on forage harvesters and single-pass balers. Current mowers can be categorized by their cutting mechanisms as: reciprocating blades (sickle

bar mowers), horizontal rotary blades (flail mowers), or vertical rotary blades (discbines and omni-directional heads). The following sections describe the relevant features of these machine variations. A full engineering analysis is omitted here, but can be found in Srivastava et al. (2006).

Mechanized mowing of forage crops dates back at least to Roman times, when Pliny the elder observed that the Gauls made use of reciprocating blades on mule-powered “vallus” cutting machines (Plinius Gaius AD 77-79). Horse powered sickle bar mowers were developed in the 1820’s by Baily, Hussey, Moore, and McCormick, and tractor drawn models were available by 1930. The design of sickle mowers continued to evolve throughout the 1950’s as the drive mechanism changed to eliminate wooden pitman driving rods. Rotary disc mowers are the most recent innovation, and were developed after 1950 (Stone 1977).

3.2.1.1 Reciprocating Sickle Bar Mowers

Sickle bar mowers sever the crop by slicing it between a moving blade and counter shear (Srivastava et al. 2006). The reciprocating mower is composed of the moving blades, an oscillatory drive mechanism, and the stationary frame and guards that support and protect the mechanism (Guarnieri et al. 2007). The reciprocating motion of the blades is approximately sinusoidal, and can be represented by (Srivastava et al. 2006)

$$v_{km} = \frac{L_s w_c}{2} \cos(w_c t) \quad (1)$$

where: v_{km} = velocity of knife relative to mower, m/s

L_s = stroke length of knife, m

w_c = sickle frequency, rad/s

t = time measured from center of stroke, s

Uniform stubble height requires that cutting occurs throughout a large portion of the knife's stroke, before it reaches the ledger plate. Mid-stroke cutting is aided by increased blade speed, and occurs using a combination of impact and shear. Sickle bar cutters tend to cut the crop at low speeds, 1.5-3 m/s (Kepner 1952). Energy is required to overcome inertia forces associated with moving the blades and cutting the crop (Karpenko 1968). Previous work in hay crops has shown that when the blades are sharp, more energy is required to overcome inertial forces than is used in cutting crop material (Chancellor 1958; Srivastava et al. 2006). These inertial forces increase with the cutterbar's frequency of oscillation, and limit the realistic forward speed of most reciprocating mowers to 8-10 mph. Elfes (1954) notes that only 30% of power requirements went toward cutting plant material when operating at 942 cycles/minute. Perhaps counter intuitively, cutting a large amount of forage can reduce power requirements by dampening the motion of the knives and decreasing inertial losses. Inertial forces can also be reduced using counterweights, although complete balancing is unnecessary, since some vibration aids crop flow and keeps the cutterbar clean (Srivastava et al. 2006). Unlike rotary cutters, the sickle bar mechanism does not achieve 100% field coverage. Instead, the blunt ends of the sickle bar knives are protected by the guards, and crop material in these areas is deflected by the guard tips to areas where cutting may be accomplished. This and the reciprocating motion of the blades can cause plant material to be expelled forward rather than cut, especially at low ground speeds (Kepner 1952, Srivastava et al. 2006). These factors significantly limit the maximum forward speed of sickle mowers, especially in dense crop stands. A complete analysis of the vibratory phenomena present in sickle bar mowers is provided by Kepner (1952) and Guarnieri et al. (2007).

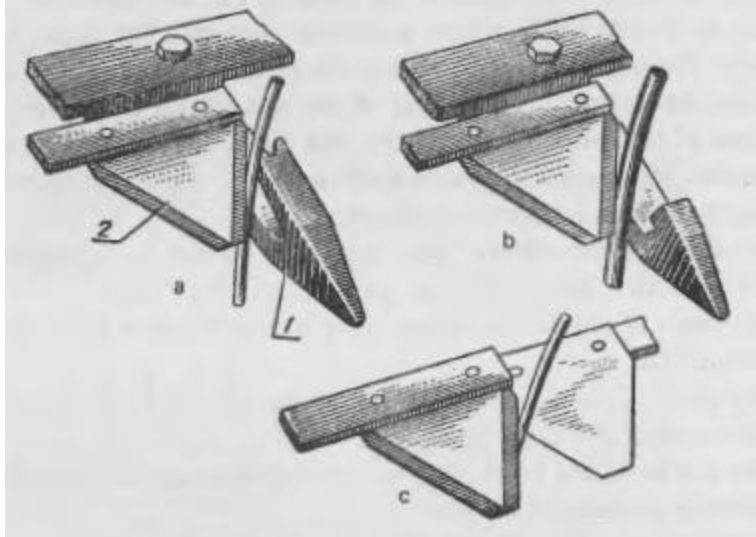


Figure 4: Types of sickle bar cutters: finger bar with lip (a), finger bar without lip (b), and dual-action cutterbar (c), Srivastava et al. 2006.

The design of sickle mowers may be modified for better performance in thick stemmed crops like miscanthus. Sickle mechanisms have been used in heavier applications than forage crops, such as shrub pruning (Guarnieri et al. 2007). Monroe et al. (1977) discuss the design and development of an oversized mower cutter bar for pruning trees. Here the forward speed of the cutter is greatly reduced relative to its use in field crops. Similar design changes may be required to adapt traditional sickle mowers to miscanthus. Karpenko (1968) notes that sickle bar guards can be employed with or without a lip above the reciprocating blade, as shown in Figure 4. This support ensures that crop is supported at two points during cutting. While this prevents bending in thin stemmed crops, it impedes the flow of larger plants (Karpenko 1968). Increased guard pitch, from 76.2mm to 90mm, has also been shown to enhance the performance of sickle bar mowers in heavier crops, such as corn and sunflowers, and may improve performance in switchgrass and miscanthus.

Power requirements for sickle mechanisms are estimated at 1.2 kW per meter of cutterbar when mowing alfalfa. Total requirements for mowing, conditioning, rolling resistance, and crop

flow are estimated at 4.5 kW/m for sickle type mower-conditioners (ASABE D497.7 2011). McGechan (1989) provides a similar estimate of 3.7-5.9 kW/m for mower conditioners and 0.9-1.5 kW/m for the cutterbar alone. The theoretical power requirements of sickle mowers with a counter shear can be calculated in terms of the average cutting force, number of cuts per second, and length of material being cut. Srivastava et al. (2006) give a relationship for calculating theoretical cutting power in mowers,

$$P_{cut} = C_f F_{max} X_{bu} f_{cut} \quad (2)$$

where: P_{cut} = mowing power requirement, W

C_f = ratio of average to peak cutting force

F_{max} = maximum cutting force, N

X_{bu} = depth of material at initial contact with knife, m

f_{cut} = cutting frequency, Hz

The ratio of average to peak cutting force (C_f) is typically 0.64 for traditional forage crops.

3.2.1.2 Vertical Axis Rotary Mowers (Disc and Drum)

Vertical axis mowers avoid many of the complications of reciprocating machines by cutting the crop with freely pivoting blades attached to rotating disks (Srivastava et al. 2006). The pivoting action of the blades allows them to swing away from rocks and other obstacles. In all rotary mowers, the crop is unsupported during cutting. Thus for a clean cut, the force of cutting must be absorbed by the rigidity of the plant's stem and its neighbors—there is no counter shear to hold the stem in place. There are two types of vertical axis rotary mowers, disc and drum. Drive mechanisms in disc mowers are located beneath the cutting blades, so crop flows more easily through the machine. This is believed to reduce energy requirements for crop conveyance. Blades may be counter rotating to leave the material in distinct bands or co-rotating

for uniform distribution across the cutting width. Drum mowers have their drive mechanism above the blades, and crop is required to pass in the narrower spaces between or under the drums, resulting in higher energy requirements.

The combination of the mowers revolution and forward velocity causes the blade to move in a cycloidal path. The ends of blades may be beveled so that the flat portion of the blade does not push into standing crop as the machine advances (Srivastava et al. 2006). Some manufacturers ignore this effect, opting instead to produce blades that reveal a second cutting edge when flipped, and possess no bevel. In general, the tangential velocity of the blade is much greater than the forward velocity of the mower, so the oblique angle of cutting is near zero. This reduces the number of stems that slide forward and off the blade's edge, since the cutting surface is oriented perpendicular to the direction of travel.

Power requirements of rotary mowers are generally 2-4 times greater than sickle machines of the same width. Reported fuel requirements of drum mowers were higher than disc mowers (Rotz and Sprott 1984). ASABE D497.7 (2011) cites a power requirement of 5.0 kW/m of rotary cutting width. The power requirement for rotary mower-conditioners is 8.0 kW/m. Other studies report even higher energy requirements, with 11 to 16 kW/m consumed by the mower at 15 km/h (Srivastava et al. 2006). Tuck et al. (1991b) cite power requirements of 10-12 kW/m as the blades wear. Mcrandal et al. (1978b) reported a power usage of 3.5-6.5 kW/m for mower conditioners, and 5 kW/m for mowing alone. In another study, mowing and conditioning required an average of 8.0 kW/m, with a range of 5.6-10.4 kW/m (Srivastava et al. 2006). Persson (1987) suggests the following relationship for the power requirements of a rotary mower:

$$P_{mow} = (P_{Ls} + E_{sc}v_f)w_c \quad (3)$$

where: P_{mow} = total power requirement of power, kW

P_{LS} = specific power loss due to air, stubble, and gear-train friction, kW/m

E_{sc} = specific cutting energy, kJ/m^2

v_f = forward velocity of mower, m/s

w_c = width of mower, m

Specific power losses (P_{LS}) range from 1.5-4.0 kW/m, with drum mowers experiencing higher losses than disc-type (Persson 1987). Specific cutting energy (E_{sc}) ranged from 1.5-2.1 kJ/m^2 , depending on blade sharpness.

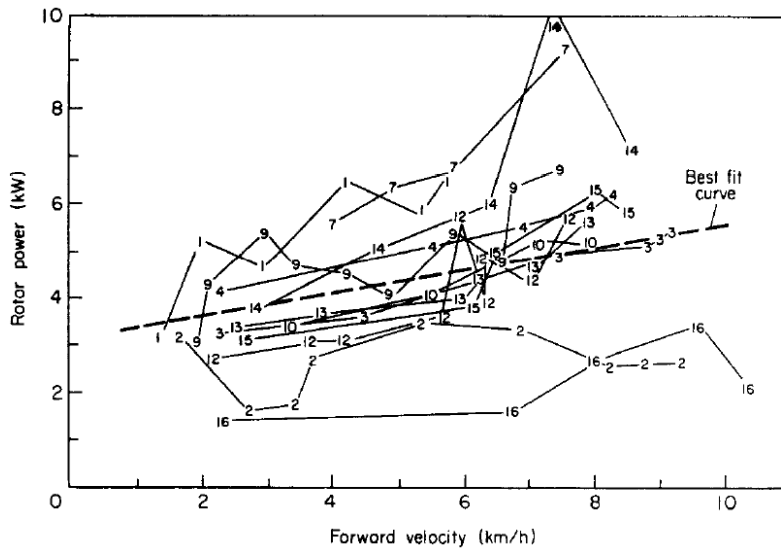


Figure 5: Effect of forward velocity on mowing power, with constant blade velocity of 78 m/s. Numbers indicate fields (Mcrahdal and McNulty 1978b).

Energy losses in rotary mowers are identified as windage, mower drag, friction within the drive train, and friction with the stubble beneath the blades (Mcrahdal and McNulty 1978b). Experiments with a vertical drum disk indicated that 50% of input energy was used for crop conveyance; while only 3% of the input energy was used in shearing plant stems (Mcrahdal and McNulty 1978a). These experiments were performed in grass forage with blade speeds of 78 m/s and a forward velocity of 5.5 km/h. Crop density, specifically the mass of crop per unit area,

was the most important factor in determining power consumption, explaining 46% of the observed variation. Stem shearing strength, number of stems per unit area, and crop height had a comparatively small effect, accounting for 14, 13, 6, and 2% of power variation, respectively. Mowing power increased as forward velocity increased (Mcrcandal and McNulty 1978b), as shown in Figure 5. This relationship may be due to an increase in energy requirements for crop flow, which have been related to the square of forward velocity.

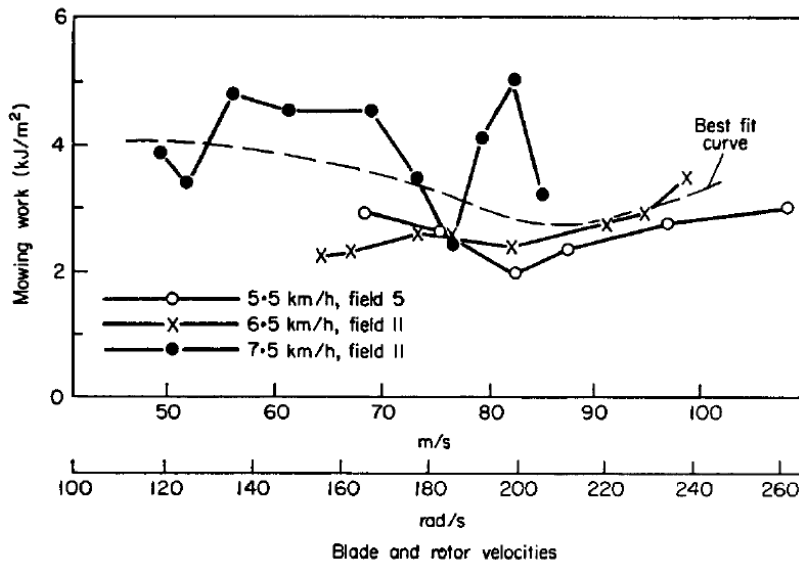


Figure 6: Effect of cutting and forward velocities on mowing work. Each data point is the average of four field measurements (Mcrcandal and McNulty 1978b).

As shown in Figure 6, the power required per unit area (kW/m^2) decreased with forward velocity, within the range of 2-9 km/h, implying that total power use can be reduced by increasing groundspeed (Mcrcandal and McNulty 1978b). This trend is likely due to a higher proportion of useful work accomplished per unit of energy lost to parasitics.

Blade usage is another important factor in rotary mower performance. Laboratory studies demonstrated clean cutting of grass at speeds as low as 25 m/s (Mcrcandal and McNulty 1978b), while field mowers required 40-60 m/s (Mcrcandal and McNulty 1978b). This discrepancy is

explained by the observation that kinetic energy of the blade was fully consumed under field conditions, where plant density and frictional losses were greater.

In addition to bladed rotary disk and drum mowers, toothed disk mowing mechanisms have been evaluated by Tuck et al. (1991a) Power requirements for the mower were lower, as little as 65% of the requirements of a conventional bladed rotary mower. Tangential cutting speed was reduced to 40 m/s. Difficulty was encountered in some cases in achieving uniform stubble height, especially with worn blades or in lodged forage.

3.2.1.3 Horizontal Axis Rotary Mowers (Flail)

Flail mowers are used in direct-cut harvest operations to simultaneously cut, condition, and collect forage. Cutting is accomplished by freely pivoting blades attached to a horizontal rotating drum. Like all rotary cutters, flail mowers rely on impact cutting rather than countershear support. This means that cutting forces must be supported by the plant stem for a clean cut to occur (Srivastava et al. 2006). In addition to being cut, the crop is conditioned and conveyed as it passes over the high velocity blades. Forage can be collected directly behind the mower or allowed to drop into the field for wilting. In general, flail mowers tend to be less precise than sickle and disc type mowers, leading to 10-15% higher losses in standing crops. Conversely, flail mowers perform better than other mowers in firmly lodged crops, which may aid in the collection energy forages after overwintering. The main source of losses in flail mowers are uneven stubble heights due to plant deflection and re-cutting of the crop as it is being conditioned, which make plant stems too short to be collected. Both sources of loss are mitigated by a push bar in front of the mower, which bends the crop away from the machines as it approaches. This action pushes the upper portion of plant stems out of the path of the blade, which reduces losses by eliminating re-cutting (Srivastava et al. 2006). The push bar also puts

pressure on the stems, which immobilizes them and allows cutting at a lower velocity. Common blade velocities in traditional forages are 45 m/s, whereas vertical disk mowers tend to operate at 60 m/s. This reduction in cutter speed also reduces re-cutting within the mower.

Power requirements of flail mowers are significantly higher than sickle cutterbars. ASABE 497.7(2011) indicates a power requirement of 10 kW/m for flail mowers, the highest of any mower. A general formula for the energy requirements of a flail mower is (Srivastava et al. 2006):

$$P_{mow} = c_1 + c_2 m_f \quad (4)$$

where: m_f = mass feed rate of crop material, kg/s

c_1 = constant power requirement, kW

c_2 = feed rate energy requirement, kJ/kg

Typical values for c_1 and c_2 are 10 kW and 4.0 kJ/kg. In addition to flail mowers, other horizontal axis mowers have been developed and tested, such as a compound helical cutterbar (Coates and Porterfield 1975).

3.2.2 Baling

Baling is one method of collecting and compacting forage prior to transport and storage. Several baling technologies have been developed, including small square balers (SSB), large round balers (LRB), and large square balers (LSB). Herbaceous energy crops are typically baled at low moisture contents (18-23%) and stored aerobically without wrapping. Small square balers produce 25-40 kg bales that can be moved by hand or with somewhat specialized machinery. Round balers produce larger cylindrical bales 100 to 500 kg in mass that are moved with simple loader attachments. Large square balers produce rectangular bales that are similar in weight and density to round bales but are easier to stack and ship. Both large and small square bales do not

shed water and require covered storage. Large round bales shed water and can be stored outdoors with acceptable loss in quality. Balers may be equipped with crop processing knives to reduce the size of the material being collected. Bales deposited in the field must be collected and stored prior to crop regrowth.

Rees (1982) notes that the pickup operation in traditional haymaking is crucial, with losses from 4.4 – 11% possible in that stage alone. Shinnars et al. (2010) observed that baler speed was significantly limited by the sheer volume of crop material collected in mature energy crop harvests. They suggest modifications to the baler's throat to handle higher volumes. Shinnars et al. (2010) also note that the characteristics of the windrow can influence the ease of baling, with well-conditioned windrows tending to be smaller and easier to pick up. This effect is somewhat well known, and is illustrated in Figure 2.

Square and round balers compress hay differently. Both large and small square balers compact discrete charges of hay into a bale chamber with a reciprocating plunger. The plunger is fed by a stuffer fork, which pushes material into the chamber slightly before the plunger advances and compresses the bale. The re-expansion of hay in the bale chamber is prevented by fixed wedges and spring loaded dogs (Srivastava et al. 2006). In modern large square balers, hay from the pickup is first gathered in a pre-compression chamber, where it accumulates to a designated pressure before being advanced by an electronically triggered stuffer fork (New Holland 2009). Optimal baler throughput is obtained when enough hay is entering the chamber to produce slightly less than one stuffer cycle for each stroke of the main plunger. The baler's monitor indicates the ratio of stuffer to plunger strokes so that the operator can maintain performance. Square balers maintain the structure of each bale by wrapping it with twine which must be cut and knotted. The knotting mechanism is reliable, but somewhat complex and prone

to wear. Large round balers continuously add material to the bale as it is spun within a fixed or variable bale chamber. Fixed bale chambers result in bales with low density centers, since there is little pressure applied to the bales when they are small. When the windrow is narrower than the bale chamber, the operator must weave the baler across the windrow to ensure the bale is evenly formed. Round bales are held together with twine or a plastic mesh. Wrapping with twine takes longer as it must be longitudinally wrapped around the bale; whereas the plastic mesh or net is the same length as the bale and requires only a few revolutions. Bale ejection usually requires the tractor to be stopped and backed away from the windrow. Recently, balers have been equipped with ISO baler-tractor communication that allows the baler to stop the tractor automatically upon completion of the bale. In this case a bale ejector is used to push the bale away from the tractor, so that no backing up is required. Forward speed of round balers is generally limited by the pickup to 5-13 km/h in traditional forages (Srivastava et al. 2006).

Power requirements for large square balers are expressed with the following linear relationship (ASABE D497.7 2011),

$$P_{baler} = C_0 + C_1 m_f \quad (5)$$

where: P_{baler} = power requirement of baler, kW

C_0, C_1 are constants related to baler design and crop conditions, kW, kJ/kg

Typical values for (C_1, C_2) are (2, 3.6) and (4 kW, 4.7 kJ/kg) for small and large square balers, respectively (ASABE D497.7 2011). Power requirements for large round balers typically increase as the bale is forming, starting at 2-4 kW (Srivastava et al. 2006). When the bale has reached maximum size, power requirements range from 12 kW to 55 kW, depending on bale density and baler design. Single-pass mowing and baling machines are a recent commercial innovation intended for use in herbaceous energy crops. Direct harvesting without material

deposition on the ground is advantageous because it reduced losses and allows harvesting to continue in mild snow accumulations.

3.3 Theoretical Cutting Mechanics of Forage and Herbaceous Energy Crops

The mechanics of plant stems such differ significantly from manmade materials. Unlike iron or steel, biological materials are viscoelastic, meaning they possess no strictly defined relationship between stress and deformation. Methods used to analyze manmade materials such as low speed, static testing are therefore inappropriate in analyzing the high speed cutting that occurs in hay and forage machinery. Deformation in plant materials is a function of time (creep), and their modulus of elasticity (E) is non-constant (Persson 1987). They also behave differently under tensile and compressive forces as well as static and dynamic loading. Although the mechanics of plants are difficult to theoretically predict, they are often viewed as bundles of high strength fibers bound by materials of much lower strength (Srivastava et al. 2006). The diameter of the bundle of fibers rather than the stem determines bending and tensile strength. Large stems, such as those found in miscanthus and corn, are often composed of strong node and weak internode sections. Internode sections may be hollow or non-hollow and are typically more uniform than the nodes. Miscanthus possesses the later type of nodal stem with strong nodes and non-hollow internodes. Moisture content affects the strength of plant stems by changing the internal turgor pressure (Srivastava et al. 2006).

Cutting of plant stems is believed to occur when the pressure caused by the blade reaches a critical value, 9 to 30 N/mm² for most plant materials. Cutting results in multiple modes of tissue failure. Initial knife penetration results in localized plastic deformation, followed by significant buckling as the knife advances. The turgor pressure of moist stems will often resist initial compression in high speed cutting. As the knife continues to advance the fibers

composing the stem are deflected and eventually fail in tension. The plant stem is deformed and compressed ahead of and to the sides of the knife. These compression effects alone may account for 40-60% of total cutting energy (Srivastava et al. 2006). Stem compression tends to propagate at a finite rate, and low speed cutting may require more energy because it causes additional compression and deformation. Forces in low speed cutting are also higher (Persson 1987).

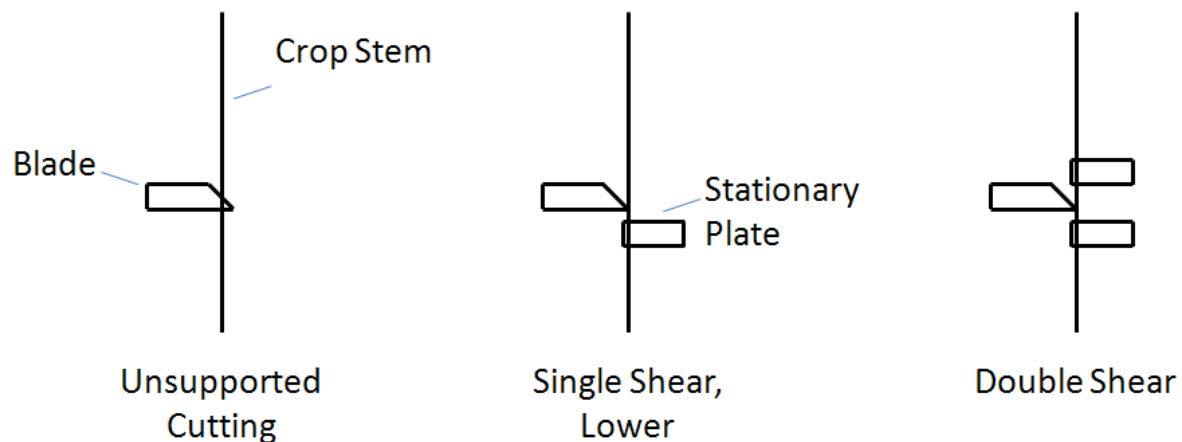


Figure 7: Methods of stalk support in crop cutting – unsupported, single and double shear.

3.3.1 Modes of Cutting Plant Material

Cutting processes in hay and forage machinery can be supported or unsupported, as depicted in Figure 7. Unsupported cutting requires high speeds (60-80 m/s), and is often referred to as inertial or impact cutting, since the cutting force is supported by the inertia of the plant (Srivastava et al. 2006). Supported cutting occurs at lower speeds (3 m/s) in a scissor-like action as the crop is sheared between the blade and ledger plate (Tuck et al. 1991b). Commercial rotary mowers cut in unsupported modes, whereas reciprocating mowers tend to employ supported cutting. In practice both mowers may employ a mixture of both as plants can immobilize their neighbors, and some cutting in reciprocating mowers occurs before the knife reaches the ledger plate (Kepner 1952). Cutting throughout the stroke of the reciprocating mower is believed to aid

in the creation of uniform stubble height and reduces peak cutting forces. Stems can be held during supported cutting in three different ways: upper shear, lower shear, and double shear (Figure 7). Impact cutting typically requires more energy, but does not require sharp blades or ideal crop conditions (Tuck et al. 1991b). Cutting of grass stems in shear can require as little as 30 mJ per stem, whereas impact cutting energy can be as high as 100-1000 mJ / stem (O'Dogherty and Gale 1986). This increase in energy is attributed to increased blade-stem friction, as well as the increased acceleration of the plant stem. High speed unsupported cutting may result in greater plant compression and deformation leading to elevated power usage (Persson 1987).

3.3.2 Critical Cutting Speed

Unsupported and partially supported cutting requires that cutting force to be reacted by the plants structural rigidity or inertia (Persson 1987). Hence cutting can only occur when the resistive forces of the plant exceed the force imposed by the blade. Since cutting force generally decreases with speed in grass-like stems (Chancellor 1958, Mcrandal and McNulty 1978a, Persson 1987, Tuck et al. 1991b), it is possible to define a critical cutting speed in which cutting force equals the reactive force of the plant. A clean cut requires the stem to be severed above the critical speed, since significantly less stem deflection occurs. By equating cutting forces with the expected rigidity of the plant, Persson (1987) provides an equation for this critical speed,

$$v_k = \sqrt{d_s \frac{F_x - F_b}{m_p} \left(1 + \frac{z_{cg}}{r_g^2} \right)} \quad (6)$$

where: v_k = critical knife velocity, m/s

d_s = stalk diameter, m

F_x = cutting force, N

F_b = bending resistance of stump, N

z_{eg} = height of center of gravity of cut plant, m

r_g = radius of gyration of cut portion of plant, m

m_p = mass of cut portion of plant, kg

A simple approximation to this equation can be obtained by assuming that $r_g = z_{cg}$ (Srivastava et al. 2006). Absolute minimum cutting speeds in conventional forage crops such as timothy are around 6-10 m/s (Karpenko 1968). Critical cutting speeds in grass are typically 25 m/s.

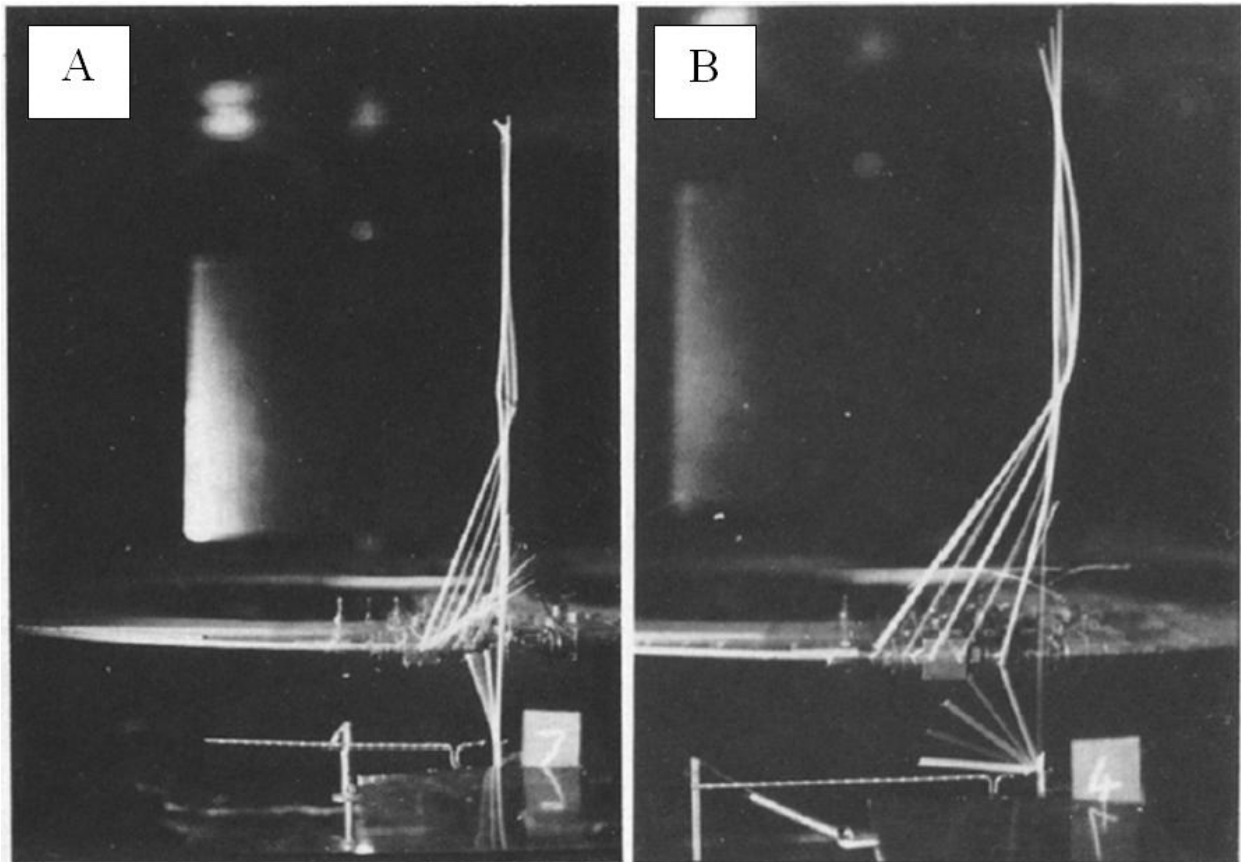


Figure 8: High speed photography of grass stem cutting. In A, the stem is cut inertially above the critical speed, (35 m/s, blunt blade). In B, the stem is cut below the critical speed with large deflection (20 m/s, sharp blade). Each frame corresponds to 15mm of blade movement (Tuck et al. 1991b).

Figure 8 depicts the difference in deflection of a grass stem observed above and below the critical cutting speed. In practice, cutting machinery employs speeds of 60 m/s or more, as deflected stems tend to require higher cutting speeds (O'Dogherty and Gale 1986, O'dogherty and Gale 1991). Cutting forces and power requirements tend to decrease substantially from the critical cutting speed, at which point the plant's resistance to cutting begins to decrease more gradually (Karpenko 1968).

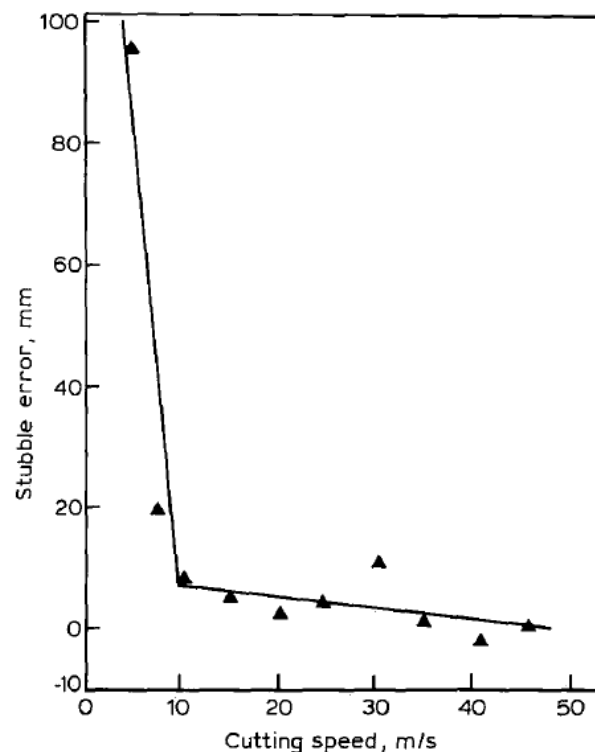


Figure 9: Effect of cutting speed on stubble error showing discontinuity at the critical speed when using blunt blades and over shear on a single stem (Tuck et al. 1991b).

The critical cutting speed is generally associated with an increase in cut consistency and quality (O'Dogherty and Gale 1986, Tuck et al. 1991b). O'Dogherty et al. (1986) note that cutting seems to occur by differing mechanisms above and below the critical speed, with low speeds more likely to result in stem movement and poor cut quality. Cutting below the critical speed increases the probability that the structure of the stem will fail, and it will wrap about the

cutting blade. When cutting below the critical speed, O'Dogherty et al. (1986) observed dragging of the stem across the blade and acceleration of the stem downwards. The critical cutting speed was measured by Mcrandal et al. (1978), by determining the point at which cut quality tended to drastically increase. Cut quality was measured in terms of stubble error, the total length of stem left above the intended cutting height. Figure 9 depicts the determination of critical cutting speed based on stubble error.

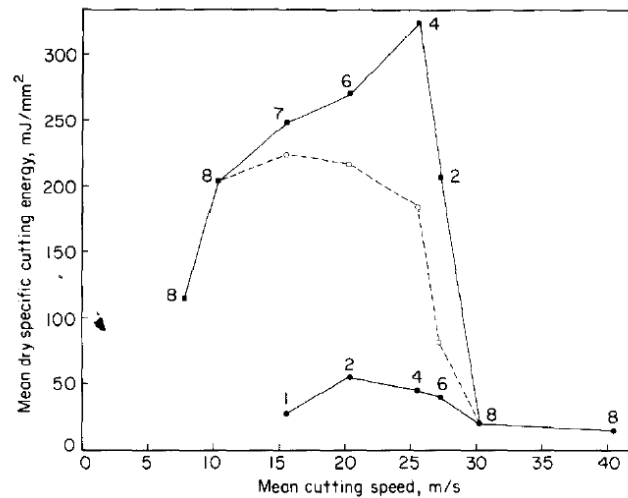


Figure 10: Results illustrating population of results above and below the critical cutting speeds. Numbers indicate stems cut at either high or low energy values (O'Dogherty and Gale 1986).

In addition to cut quality, cutting above and below the critical speed results in noticeable differences in cutting energy. O'Dogherty et al. (1986) indicate two populations of results, one above and one below the critical cutting speed. Below the critical speed, the stem wrapped or slid along the cutting blade resulting in increased cutting energy as depicted in Figure 10. While the critical speed applies to small grasses (timothy, rye, straw), cutting forces in larger cane-like plants may increase with speed. Section 3.4 further discusses this discrepancy.

3.3.3 Geometry of Cutting Knives

Blade geometry has a significant influence on the quality and energy requirements of cutting.

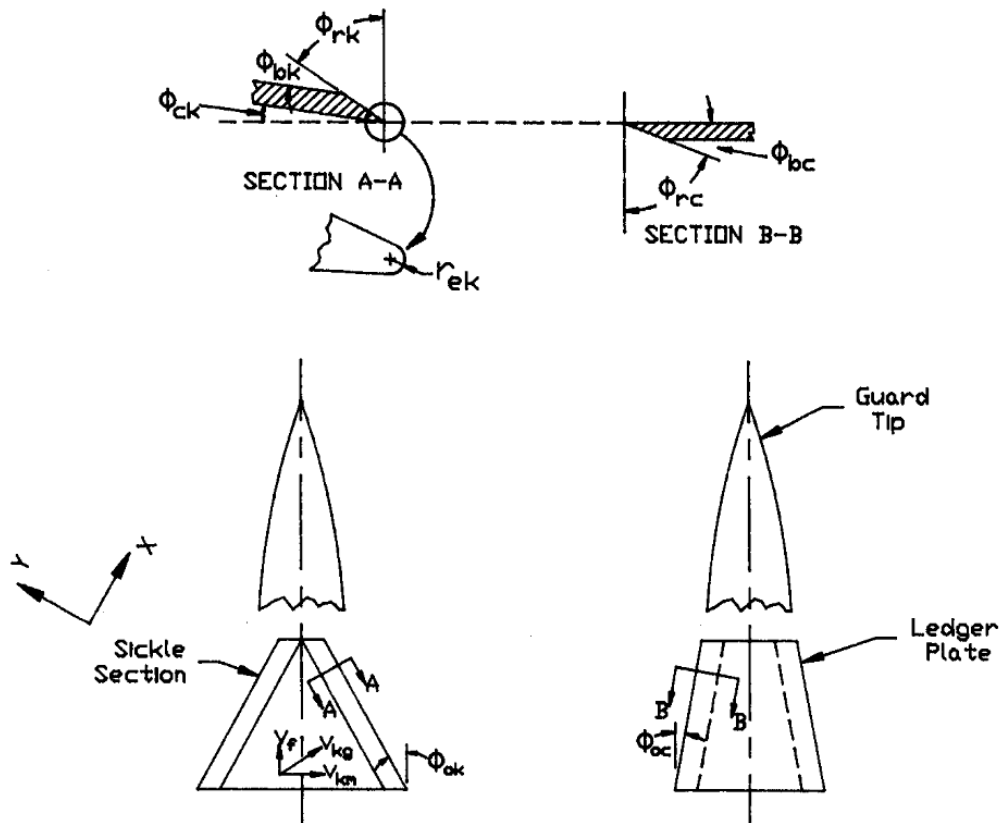


Figure 11: Cutting geometry of blade and counter shear (62).

Figure 11 depicts the geometry of a sickle blade knife (Karpenko 1968). The sharpness of the knife is defined by the end radius, r_{ek} . Cutting is aided by sharper knives, until the point where r_{ek} is reduced below $80\mu\text{m}$, at which point the blades must be sharpened every few hours (Persson 1987). Initial plant penetration is strongly influenced by the fineness of the blade, which is defined by the rake angle, ϕ_{rk} . Increasing the oblique angle tends to change the nature of cutting from impact to slicing (Srivastava et al. 2006). Slicing cuts generally require less energy, but increase the tendency for crop material to slide along the blade. Serrated blades increase friction between the blade and stem, reducing the tendency for material to slide out of

the cutting area. An oblique angle of 0° implies complete impact cutting with minimal risk for sliding. Oblique angles in reciprocating mowers range from $10\text{-}30^\circ$, whereas rotary mowers have pivoting blades with varying oblique angles. A full analysis of blade geometry, the influence of the forward motion of the mower, and the tendency for crop material to slide out of the cutterbar can be found in Srivastava et al. (2006).

3.4 Laboratory Based Cutting Experiments

Many have investigated the effects of cutting speed and geometry on cutting energy and force. Most studies have considered small stems, and have observed that cutting is more consistent and efficient at high speeds above a critical value. Contrary to the behavior of grass stems, energy requirements for larger, cane-like stems have been known to increase with cutting speed (Prasad and Gupta 1975, Taghijarah et al. 2011). A study of the literature suggests that this is an unresolved discrepancy. One possibility is that cane-like stems have a much greater critical velocity, which has not been observed in cutting experiments to date. Igathinathane et al. (2010) provide a different possible explanation. They argue that stress waves propagating at 400 m/s will reach the ground in 0.125 ms , before cutting is complete. Large stems will therefore behave like beams stabilized by quasi-static forces, even at low cutting speeds.

The following sections present the results of laboratory based evaluations of cutting experiments performed with grasses and larger cane-like stems. Investigators consider cutting geometry, blade speed, and various modes of supporting the stem during cutting. The emphasis on energy requirements may be of little consequence, since experiments by many indicate that power required for stem cutting is a small portion of mower power consumption, as little as 3-5% (McCrandal and McNulty 1978a). Quality of cut, however, remains a legitimate concern, and

cuts that require less energy have been shown to produce more uniform stubble, with fewer uncut stems (O'Dogherty and Gale 1991).

3.4.1 Cutting of Grass-Like Stems

The measurement of cutting energy in grass stems has led to a wide variety of values due to the variability in conditions used by investigators (O'Dogherty and Gale 1986). O'Dogherty et al. (1991) observed a peak cutting force of 18 N/mm when cutting grass at 20-60 m/s. Research by Dobler et al. (1972) supports this finding, and notes that there was no significant change in cutting force with changes in blade speed. In contrast, Mcrandal et al. (1978) observed that the average impact cutting energy for grasses fell from 2.38 kJ/m² at 20 m/s to 1.8 kJ/m² at 60 m/s in unsupported cutting. These results agree relatively well with force requirements of larger crops; Igathinathane et al. (2010) observed cutting forces of 11.3 - 23.5 N/mm in low speed cutting of corn stalks.

O'Dogherty et al. (1991) considered several factors relevant to the performance of rotary mowers. Their objectives were to incorporate ledger plates in the design of rotary cutters, so that cutting speeds could be reduced. Ledger plates were used to vary the nature of cutting from impact to slicing. The extent to which either mode occurred was determined by recording the duration of each cut, since impact cutting occurs more quickly (Tuck et al. 1991b). The effect of clearance between the blade and counter shear, rake angle, and blade sharpness were considered. O'Dogherty et al. (1991) found that double shear was the most effective means of supporting stems, with cutting occurring as low as 7.5 m/s under idealized conditions. Use of ledger plates was more effective for single stems; degradation of performance was noted when groups of stems were cut. Upper shear was the least effective means of support, resulting in the highest critical cutting speed and most uncut stems. The distance between blade and counter shear was

also considered, and had little effect (O'Dogherty and Gale 1986). Increasing the blade's rake angle improved the energy efficiency of cutting, but only at low speeds, below the critical cutting velocity. For free standing stems, sharp blades performed well, even at cutting speeds as low as 20 m/s. Furthermore, when compared to dull cutting surfaces, sharp blades reduced specific cutting energy by two thirds and specific force by half. Blunt blades also resulted in significantly higher stem deflection (up to 60°) and stubble loss (O'Dogherty and Gale 1986).

Many authors have measured the critical cutting speed of grasses, and have found a significant reduction in cutting energy above the critical speed. O'Dogherty et al. (1991) found a critical speed of 15-30 m/s for rye and grass. Mcrandal et al. (1978) determined a minimum critical cutting velocity of 20 m/s for grass and wheat straw, with energy requirements decreasing by 25% as cutting speed was increased from 20 to 60 m/s (Mcrandal and McNulty 1978a). O'Dogherty et al. (1991) reported a critical cutting speed of 25-30 m/s in grass and polystyrene tubes, but no evidence of a critical speed when cutting wheat straw. Instead, cutting energy in straw increased with cutting speed until 25 m/s, where it reached a constant value 4 times less than the energy expected for grass stems. The suspected difference in behavior was attributed to brittle straw stems failing in a different mode than the supple grass. O'Dogherty et al. (1991) noted that specific cutting energy was related to the resulting stubble length and duration of cut, both of which were favored in cutting with low energy requirements. Low and high energy regimes were observed, with requirements of 50 J/mm² and 400 J/mm², respectively. Cutting above the critical speed resulted in lower cutting energies and stubble losses, while cutting below led to significant "hair pinning" or wrapping of the plant stem around the cutting blade (O'Dogherty and Gale 1986). Tuck et al. (1991b) reported that critical cutting speeds were significantly lower than speeds used on commercial equipment. This discrepancy was attributed

to the non-ideal conditions encountered in the field, specifically the inclination of plant stems relative to the cutter. In further experiments, critical cutting speeds were increased by as much as 40 m/s when stems were inclined 60° (McCrandal and McNulty 1978b, O'Dogherty and Gale 1986). Researchers also considered the extent of blade utilization, or the percentage of the blade's length that was encountering new, uncut stems. At 100% blade utilization, the forward velocity of the cutter was such that the entire length of the blade was subjected to uncut stems each revolution. Surprisingly, Tuck et al. (1991) found that lower blade utilization worsened performance, because more stems were being cut at the tip of the blade where they were deflected. As expected, there were a greater number of uncut stems in sparse stands (Tuck et al. 1991b). This occurred even with ledger plates. High speed film indicated that the stems at the trailing edge of bundles were deflected away from the blade by the blunt ends of the plates. The number of uncut stems ranged from 0-16%, with the most uncut stems occurring with blunted cutting blades. Tuck et al. (1991b) also noted that mower skids could push stems away from the blade, and recommended a blade length at least as long as the skid.

3.4.2 Cutting of Cane-Like Stems

While the majority of cutting studies have considered grasses, some work has been done on larger, cane-like stems. Kroes et al. (1996) measured cutting forces and energy during the impact cutting of sugarcane stalks at 20 m/s. Cutting force and energy were obtained by recording the output of a piezoelectric force sensor and measuring the momentum lost by the cutting blade. Peak cutting forces ranged from 300-600 N and varied with stem diameter and cane variety. Cutting energy ranged from 5-25 J, again depending on stem size and variety (Kroes and Harris 1996). A significant portion of energy (7.5 ± 2.1 J) was devoted to accelerating the stem. Other researchers have alluded to a similar effect in measurements of cutting forces

and energy in maize (Prasad and Gupta 1975). Prasad et al. (1975) observed an increase in cutting energy with increasing speed at relatively low cutting speeds (0.5-3 m/s). Taghijarah et al. (2011) noted that the increase in cutting energy with speed was not well understood and reasoned that “at a higher velocity, the kinetic energy imparted by the impact of the machine is just wasted because more energy is transmitted to the separated parts of the stem after cutting.” The opposite trend, a decrease in cutting energy with speed, has also been observed in sorghum stalks, with cutting energy decreasing from 6 to 3 mJ/mm² as blade speed was increased from 20 to 60 m/s (Chattopadhyay and Pandey 2001). Kroes et al. (1996) also observed lower cutting forces as they increased the rotational speed of their cutting apparatus.

From the research reported above it is not clear whether cutting of large, cane-like stems is favored at high or low speeds. While some have observed an increase of cutting energy with speed in the range 0-20 m/s, others have observed the opposite phenomenon at higher speeds, from 20-60 m/s. This behavior is consistent with the trend in cutting energy reported in Figure 10 (O'Dogherty and Gale 1986). Here cutting energy increases with speed far below the critical speed, where cutting is ill defined and stochastic, but then sharply declines to a minimum value when the critical speed is reached. It remains to be seen whether the same behavior is occurring in cane-like stems.

CHAPTER 4: MATERIALS AND METHODS

Research efforts in crop harvesting are inherently complicated by limited harvesting windows and highly variable field conditions. The approach taken here was therefore to augment in-field data collection with repeatable experiments. Section 4.1 describes the in-field portion of this study, in which commercially available machinery was used to harvest approximately 50 hectares (120 acres) of herbaceous energy crops. Harvesting was performed in a two-pass mowing and baling operation. Harvest energy was determined from CAN messages for engine torque and speed. A detailed background of agronomic practices for these herbaceous energy crops is provided by Christian (2008), Fike (2006), and Vento et al. (2010), for miscanthus, switchgrass, and prairie grass, respectively. Section 4.2 describes the apparatus and procedure used for high-speed single stem cutting experiments. This equipment was designed and built specifically for this study and consisted of a swinging blade propelled by a customized pneumatic cannon. Cutting energy was determined by measuring the loss in velocity and kinetic energy of the blade, before and after cutting. System identification techniques were used to determine the blade's moment of inertia.

4.1 Evaluation of Current Two-Pass Harvest Technique

The two pass, mowing and baling harvest of miscanthus, switchgrass, and tallgrass prairie was evaluated by monitoring the speed and power consumption of harvesting equipment. Mowing was accomplished with a towed rotary mower and a self-propelled mower with rotary and sickle heads. Each machine was equipped with conditioning rolls. Baling was accomplished with a single large square baler. A computer-based data logger recorded the location, ground speed, and power use of the machinery at a collection rate of 1 Hz. Crop yield was determined

by summing the weight of the large square bales produced in each plot. In all cases, moisture measurements were used to convert yield numbers to a dry matter basis. In some areas, moisture measurements were not recorded and average moisture values for similar crops and conditions were used. Two years of crop growth were considered, with the first harvest occurring in March 2010 and the second taking place in November 2010 and March 2011.



Figure 12: Mowers used in energy crop harvest: Case Puma 210 powering DC 132 rotary disc mower-conditioner (A), self-propelled H8080 with rotary (B), and sickle mower-conditioner heads (C).

4.1.1 Harvesting Equipment Used

The miscanthus, switchgrass, and tallgrass prairie harvested in this study were collected in a two-pass mowing and baling operation. No tedding or raking was used as the crops were dry enough at harvest. The following sections describe the mowing and baling equipment used.

4.1.1.1 Mowing Equipment

Three mowers were evaluated. In the first harvest (March 2010), a pull-type Case DC 132 rotary mower-conditioner was used. The DC 132 had an operating width of 4 m, and cut using 10 rotary discs. The rotary blades operated at 3000 rpm. Steel conditioning rolls were used at 740 rpm. The minimum PTO requirement of the mower was 67 kW (Case New Holland Agriculture 2011). This mower was equipped with a cane package, which increased its performance in tall crops. Swath width was variable between 0.9 and 2.4 m, and was adjusted to match the size of the baler's pickup. The mower-conditioner was pulled by a Case Puma 210 tractor with a power of 142 kW at its rated speed of 2200 rpm (Hoy et al. 2007). This corresponds to a rated torque of 616.4 Nm. The Puma tractor and DC 132 mower are depicted in Figure 12 (A).

In the second harvest (November 2010, March 2011), a self-propelled H8080 windrower was used for mowing with rotary and sickle heads. The H8080 was powered by a 168 kW engine with a rated torque of 729.2 Nm. As with the Case Puma tractor, engine power consumption was monitored via an ISO-bus connector in the cab. The rotary disc head was model 750HD Specialty, with 12 discs revolving at 3000 rpm. Two blades were mounted on each 0.4 m disc, with a peripheral blade speed of 83.6 m/s (Case New Holland Agriculture 2008, Case New Holland Agriculture 2008). Maximum cut width was 4.67 m. The 750HD header was equipped with rubber, chevron type conditioning rolls. The sickle head used was model 14HS with a maximum cut width of 4.34 meters. The sickle cutterbar operated at 1810 cycles per minute with a stroke length of 76 mm. Steel conditioners were used at 717 rpm (Case New Holland Agriculture 2008). The H8080 is depicted in Figure 12 with rotary and sickle heads in (B) and (C), respectively.



Figure 13: Large square baler used in harvesting trials: Case Puma 210 tractor powering BB9080R large square baler.

4.1.1.2 Baling Equipment

In both harvests, baling was performed with a New Holland BB9080R. This baler was powered by a Case Puma 210 tractor in the first year of harvesting (see Figure 13), then by a John Deere 7930 in the second. Bale dimensions were 1.2x0.9 m, with a maximum bale length of 2.6 meters. The manufacturer-specified PTO power requirement of the baler was 112 kW. Pickup width was 2.4 m {{185 Case New Holland Agriculture 2008}}. The baler was equipped with rotor cutters and a main plunger operating at 42 strokes per minute, with a stroke length of 0.7 m. The power, speed, and rated engine torque of the John Deere 7930 were 136.5 kW, 2100 RPM, and 620.9 Nm respectively {{184 Hoy, Roger M. 2007}}.

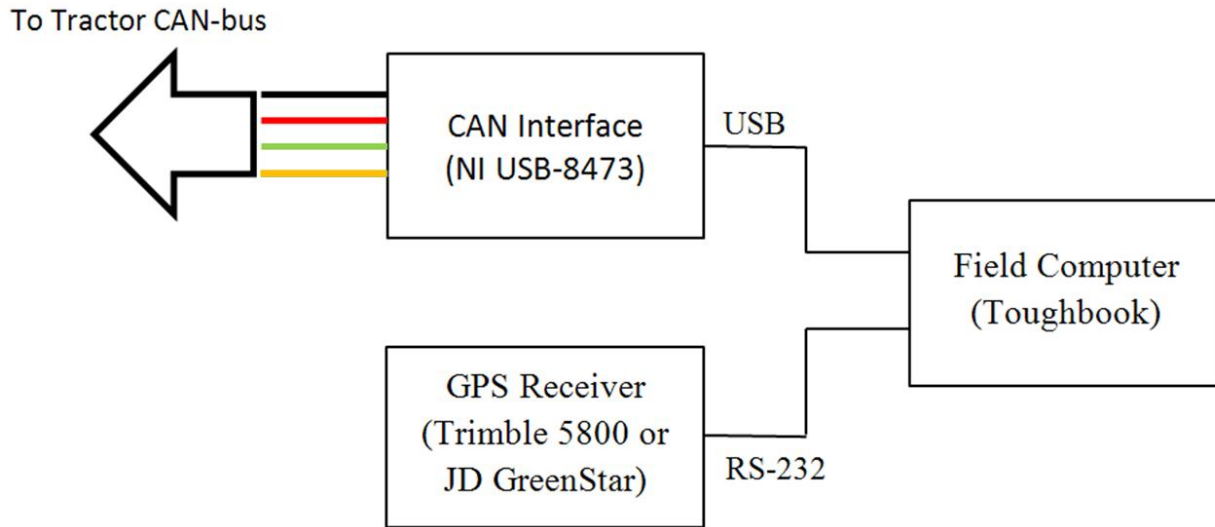


Figure 14: Schematic of in-field CAN and GPS data logging system.

4.1.2 Harvest Monitoring System

The electronics used to monitor harvest performance are depicted in Figure 14. Position and speed were recorded at 1 Hz with RTK-GPS, provided by the Trimble 5800 or John Deere Greenstar receivers. Engine speed and load were obtained from the engine control unit (ECU) via messages on the machine’s controller area network (CAN). In this fashion the CAN interface of the data logger was “listening-in” on messages sent between the ECU and periphery controllers on the tractor’s CAN-bus. Engine speed and load messages were transmitted at a rate of 200 Hz. The CAN messages received each second were averaged to produce an overall data rate of 1 Hz. The output of the GPS receiver was used to time the acquisition of CAN messages, so that incoming data from the CAN-bus and GPS receiver were synchronized. The instantaneous power consumption of each machine was calculated using

$$P_{harvest} = \omega_{engine} \frac{t_{percent}}{100} T_{rated} \quad (7)$$

where: $P_{harvest}$ = use of harvester, kW

ω_{engine} = engine speed, rad/s

$t_{percent}$ = engine torque, %

T_{rated} = rated engine torque, kNm

The rated engine torque for harvesting machinery considered in this study is given in the preceding section. The spatial work rate of each machine was determined using

$$W_{spatial} = \frac{vw}{10} \quad (8)$$

where: $W_{spatial}$ = spatial work rate of harvester, m²/s

v = harvester speed, m/s

w = harvester width, m

The mass work rate was calculated by dividing by the average yield of each crop. The energy required per megagram of harvested material was determined using

$$E_{specific} = \frac{P_{harvest}}{W_{mass}} \quad (9)$$

where: $E_{harvest}$ = specific energy of harvest, MJ/Mg

W_{mass} = mass work rate of harvester, Mg/s

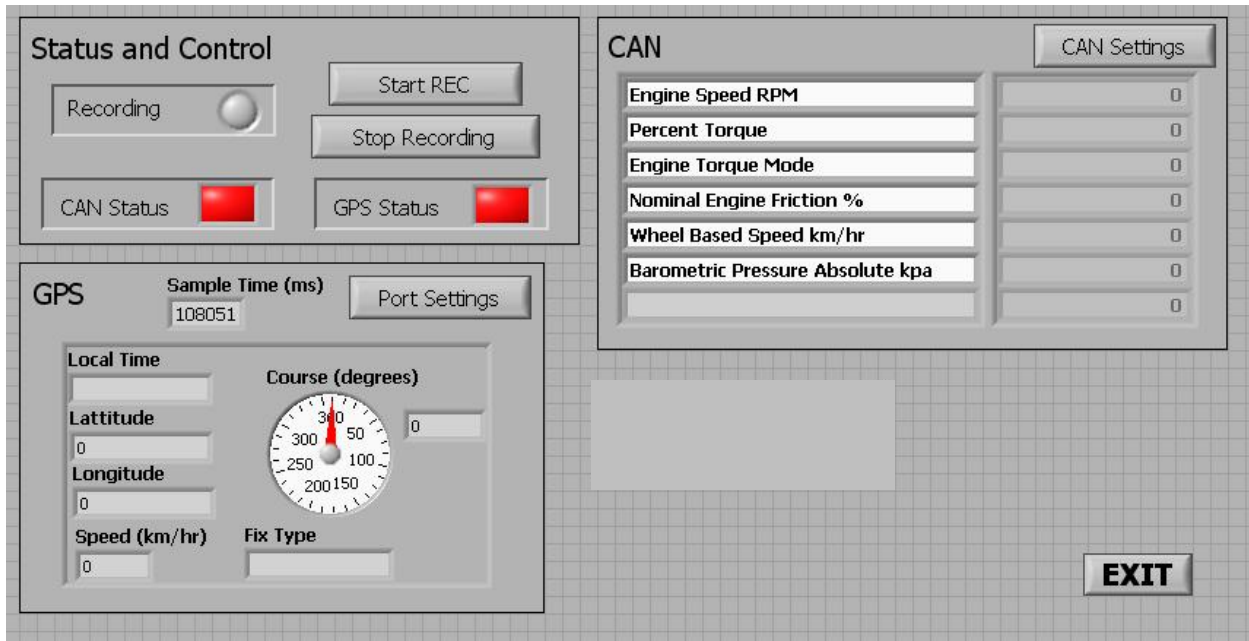


Figure 15: LabVIEW® (National Instruments) program used to collect in-field performance data from CAN and GPS.

A LabVIEW® (National Instruments) program was used to manage data acquisition. Collection of CAN messages was greatly simplified by the frame to channel conversion library, which parsed the raw CAN frames and returned engine speed and load data in physical units. Figure 15 depicts the LabVIEW® (National Instruments) program used to acquire field data. A portion of the code used in this program can be found in Appendix B. Due to the large number of incoming CAN messages, a producer-consumer architecture was employed. The producer loop ran with a high priority, saving incoming messages to the computer's RAM. The consumer loop processed the received data and saved it to the computer's hard drive. An audible alarm alerted the operator to fault conditions, such as loss of GPS signal.

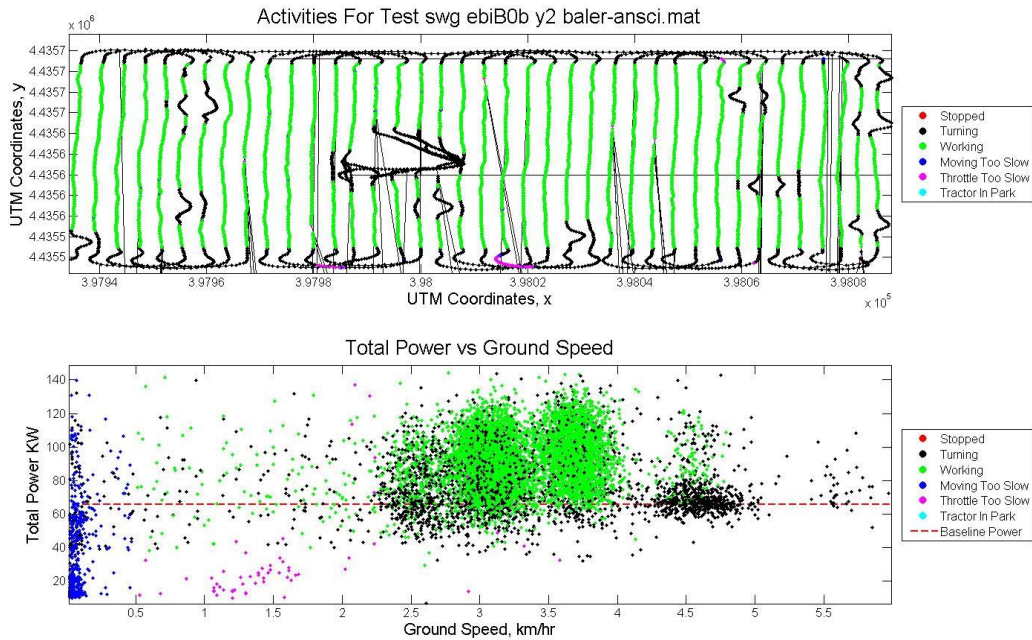


Figure 16 Data processing performed to remove stoppages and turning points from in-field performance data.

4.1.3 Processing of Harvest Data

The performance data collected during harvest was processed to categorize intervals in which the harvesting machinery was stopped or turning. Figure 16 illustrates the removal of data points in which the harvester was stopped, turning, or collecting an area less than its full width. Since the plots harvested were small (1.6 acres), it was necessary to eliminate turning time from performance measurements. The power use and capacities given here reflect 100% field efficiency, with turning time and stoppages removed. Data processing was conducted in a semi-automated fashion, using Matlab® (Mathworks). A validation report was generated to demonstrate that data from each plot was processed correctly. These reports are given in Appendix A.2.

4.2 Development and Testing of High-speed Cutting Apparatus

A high-speed cutting apparatus was constructed in order to quantify the energy requirements of cutting individual stalks of miscanthus. This device was constructed in the spirit of previous work by Kroes et al. (1996) and Chancellor (1958), who measured cutting forces in sugarcane and timothy with similar devices.

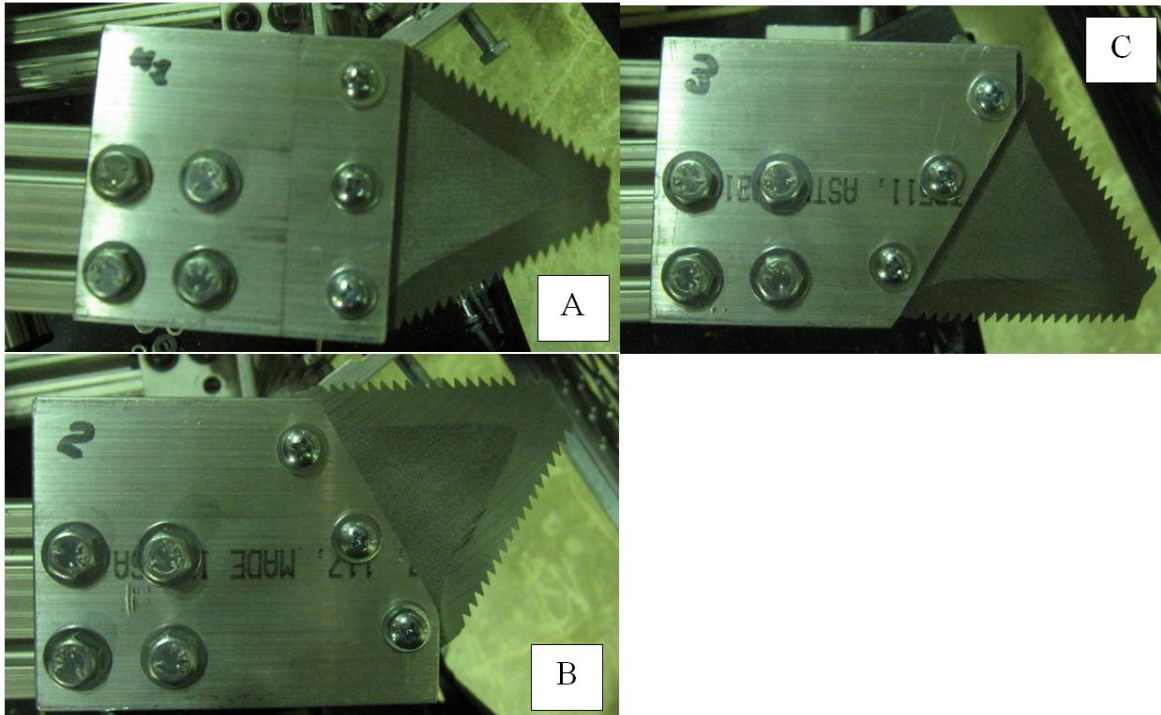


Figure 17 Blade configurations of single stem cutter: intermediate cuttings at 30° (A), impact cutting at 0° (B), and slicing cut at 60° (C).

A standard serrated sickle blade was used, and the oblique angle, the angle of the blade's edge relative to its forward velocity, was adjusted to 0, 30 and 60° (see Figure 17). The blade was mounted to a freely pivoting arm, and was initially accelerated to cutting speeds of 10-20 m/s. The blade's position and speed were estimated using a US digital 1028 count optical encoder (0.175° angular resolution), which was sampled at 100 kHz. Initial acceleration to the desired cutting speed was provided by an air cannon, which launched a tennis ball that impacted with and accelerated the cutting arm. The pressure within the cannon before this release was adjusted

to 15, 20, and 25 psi to apply different levels of cutting speed. Energy requirements for cutting were considered at and between nodes on the miscanthus plant. Three replications were targeted for each combination of factors. Trials at an oblique angle of 30° occurred only between nodes, since there was an insufficient number of stems to consider testing at nodes.

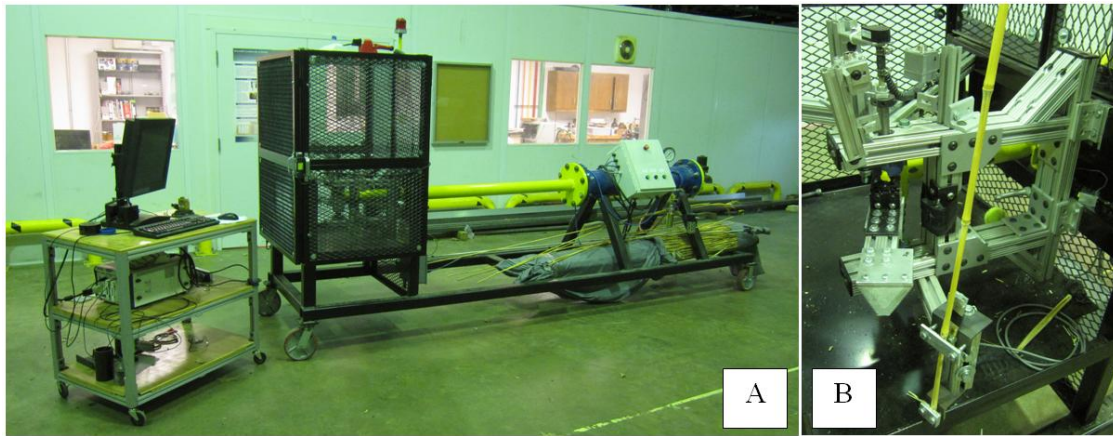


Figure 18 Cannon-powered cutting apparatus and data acquisition system (A). Close up of rotating cutting apparatus (B), configured for an impact angle of 30°.

Figure 18 depicts the single stem cutting apparatus, along with the cannon and encoder.

Cutting energy was determined by measuring the blade's loss of kinetic energy before and after cutting, namely (Ruina and Pratap 2012)

$$E_{cutting} = \frac{1}{2} I (\omega_i^2 - \omega_f^2) \quad (10)$$

where: $E_{cutting}$ = energy required to cut the miscanthus stalk, J

I = moment of inertia of arm, kgm^2

ω_i = initial speed of cutting arm, rad/s

ω_f = final speed of cutting arm, rad/s

A precise characterization of the cutter's mass properties and its motion are given in the following sections.



Figure 19 Compression caused in stalk prior to cutting event in Willow. Similar but less pronounced effects to occurred in miscanthus.

In addition to cutting energy, a substantial portion of the decrease in cutterhead speed was due to deflection of and friction with the stem, as shown in Figure 19. This study made no attempt to decouple cutting energy from the energy required to compress the stalk. Friction between the cutting blade and the underside of the blade was considered a part of the cutting energy, as in Kroes et al. (1996). Since cutting force was not monitored, it was not possible to distinguish these parasitic losses from the energy required to sever the stalk.

4.2.1 Moment of Inertia of Single Stem Cutter

As indicated in Equation (10), an accurate measure of the cutter's moment of inertia is required to determine the energy lost by the arm and therefore required to cut the crop. The arm's moment of inertia was calculated for all three blade configuration using the following general procedure:

- 1) The mass of the cutter's rotating components was recorded.

- 2) The distance between the arm's center of gravity and its center of rotation (L_e) was estimated by recording the partial weight of the arm on a scale.
- 3) The arm's natural pendulum-like motion was recorded, and a dynamic model that included the moment of inertia was fitted to this response.

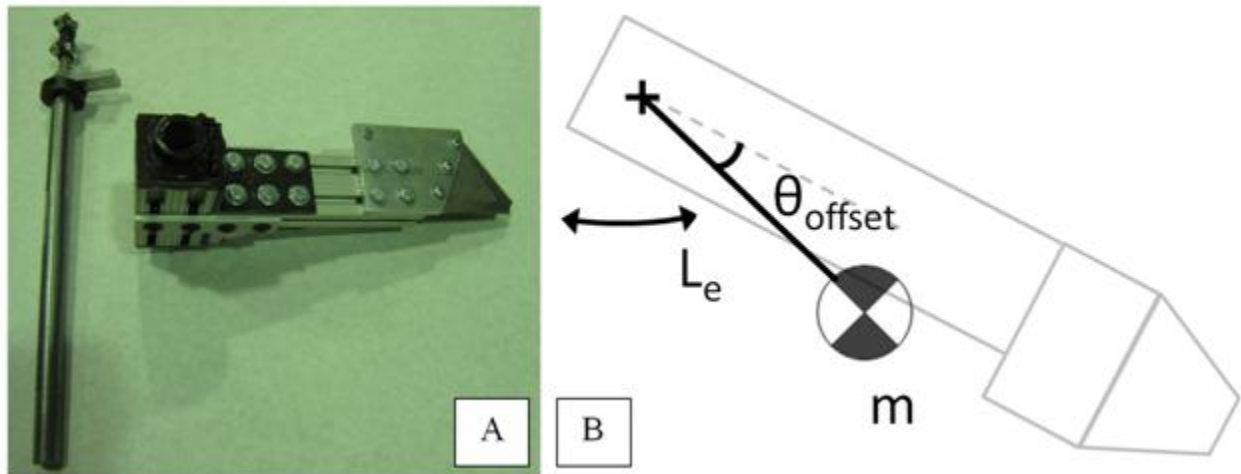


Figure 20 Rotating components of single stem cutter (A) and simplified dynamic representation of cutting arm and blade (B).

Figure 20 depicts the rotating components of the arm (A) and its dynamic representation (B).

The arm was modeled as an ideal pendulum composed of a massless rod connected to a concentrated point mass. Note that the moment of inertia was not equal to that of an ideal pendulum (mL_e^2), due to its non-uniform density (Ruina and Pratap 2012). Instead, a solution for the arm's equation of motion was fitted to its response, yielding a best fit value for, $\frac{mgL_e}{I}$, one of the coefficients in this dynamic equation. The results for effective length L_e and mass measured in previous experiments were then used to solve for the moment of inertia of the arm, I .

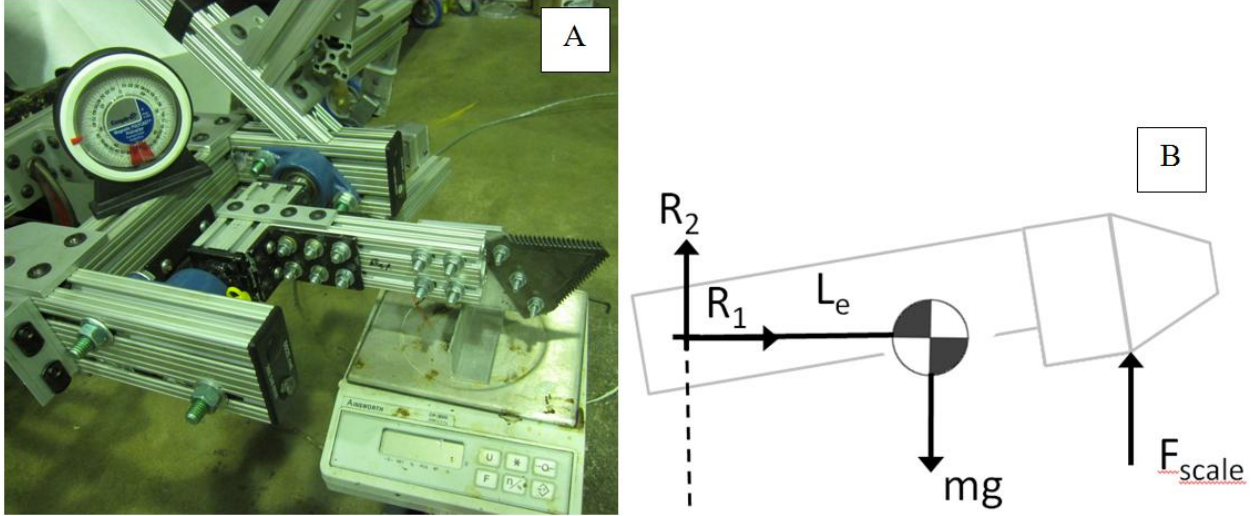


Figure 21 Experiment used to locate cutting arm's center of mass L_e (A) and free body diagram of cutting arm in this configuration (B).

Figure 21 illustrates the experiment used to locate the cutting arm's center of mass, in which one end of the cutting arm rested on a scale. Before balancing on the scale, the arm was allowed to swing freely and come to rest several times to ensure that its center of mass was directly below its axis of rotation. The encoder values for the arm's final resting point for several of these swings were averaged with a standard deviation of 0.32° . Following this, a level was used to hold the arm vertically, so θ_{offset} could be determined. The height of the scale in Figure 21 (A) was carefully adjusted until the arm was perpendicular to its rest position based on the encoder output. Summing moments about the arm's axis of rotation in Figure 21 (B) gives

$$mgL_e = F_{scale}L_{scale} \quad (11)$$

where: F_{scale} = force applied by scale, N

L_{scale} = length from axis of rotation to force application point on scale, m

g = acceleration due to gravity, 9.81 m/s^2

Equation (11) was used to locate the arms center of mass by determining L_e .

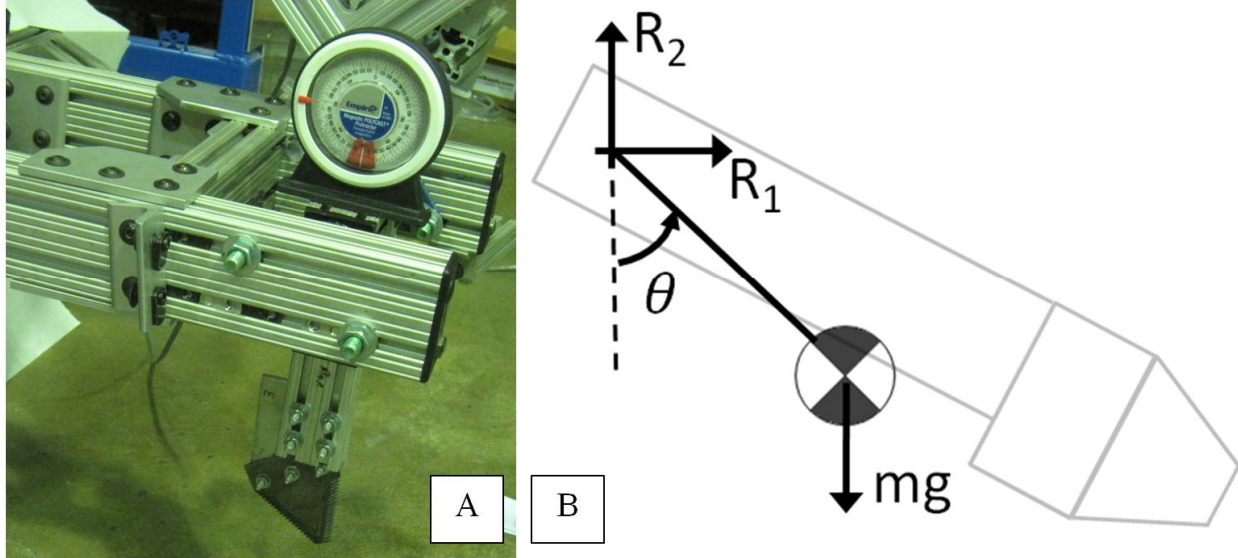


Figure 22 System identification experiment for cutting arm (A) and free body diagram (B). The arm's equation of motion is given by Equation (2). Note that the force of gravity acts on the arm's center of mass (Ruina and Pratap 2012).

Figure 22 depicts the experiment used to record the natural pendulum-like response of the arm. Here the cutter's axis of rotation is oriented horizontally, to allow it to swing freely due to gravity. Figure 22 (B) illustrates the forces acting on the pendulum in this configuration. Taking the sum of the moments about the pendulum's fixed axis of rotation, the following equation was derived:

$$\ddot{\theta} + \frac{b}{I}\dot{\theta} + \frac{mgL_e}{I}\sin(\theta) = 0 \quad (12)$$

where: $\theta, \dot{\theta}, \ddot{\theta}$ = angular position, velocity, and acceleration of the arm, rad, rad/s, rad/s²

b = viscous damping coefficient, kgm²/s

The coefficients in Equation (12) ($\frac{b}{I}, \frac{mgL_e}{I}$) and the initial angle of the pendulum (θ_0) were adjusted until the recorded response of the pendulum matched the solution to this ideal model. The initial velocity of the pendulum $\dot{\theta}_0$ was held at zero. This optimization was performed by solving the arm's equation of motion using the ode45 function for several different iterations of parameters, which were supplied by the nonlinear least squares optimization function, lsnonlin.

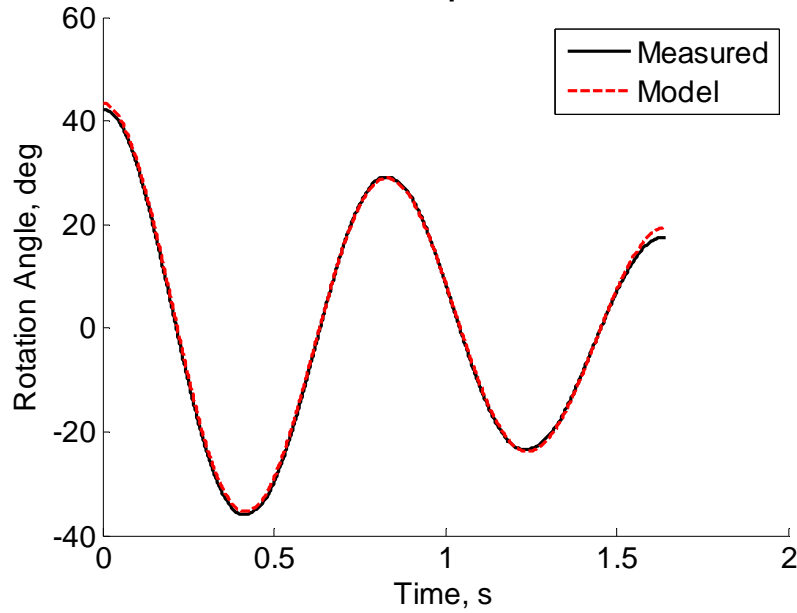


Figure 23 Recorded response and fitted model of pendulum-like motion of cutting arm, used to determine moment of inertia ($R^2 > 0.99$).

The recorded and modeled response of the arm's pendulum-like response is depicted in Figure 23. Resulting location of center of gravity, model parameters, and moments of inertia are given in Table 1.

Table 1 Calculation of moment of inertia of single stem cutter for each blade configuration.

Blade Configuration	Mass, m (kg)	Location of COM, L_e (cm)	Coefficient of Dynamic Model, mgL_e/I (s^{-2})	Model R^2	Moment of Inertia, I (kgm^2)
0°, Impact Cut	2.59	4.41	65.6	0.991	0.0171
30°, Intermediate	2.58	4.48	64.2	0.996	0.0177
60°, Slicing Cut	2.59	4.43	66.3	0.991	0.0170

4.2.2 Determination of Cutting Speed

As Equation (10) indicates, angular velocity of the cutter is required to determine cutting energy. Angular speed was determined by fitting a straight line to the motion of the cutter before and after cutting (see process_cannon_data.m in Appendix C.1). This approach assumes that the cutter travels at a constant velocity while not cutting and is accelerated very quickly by the cannon.

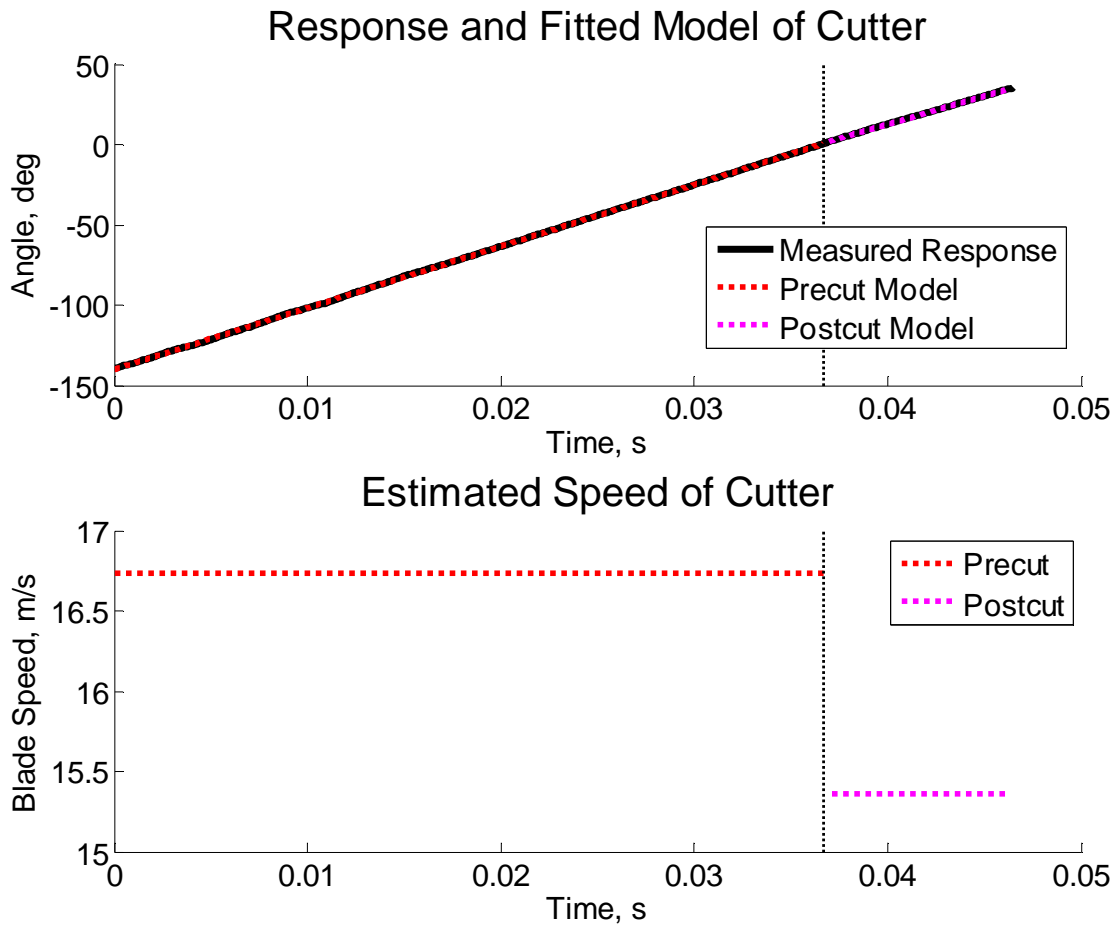


Figure 24 Estimation of blade speed before and after the cutting.

The change in cutter speed depicted in Figure 24 was sensitive to the manner in which experimental data was delineated into pre-cutting, cutting, and post-cutting regions. The start of each trial was detected automatically when the cutting arm’s instantaneous speed exceeded 3000 deg/s for three sampling periods. Here the cannon’s speed was approximated using numerical differentiation. The start of cutting was determined by zeroing the encoder’s output with the blade touching the stem. The end of cutting was estimated by measuring the diameter of the stem. The end of the trial was fixed as the point at which the cutter reached 38 degrees, a point near the edge of its range of motion. Each cutting trial occurred as depicted in Figure 25. First, the cutting arm is accelerated by an impact from the tennis ball (1). Second, the cutter severs the

miscanthus stalk (2). The cutter then contacts a stop on the device (3), and rebounds a second time against the muzzle of the cannon (4).

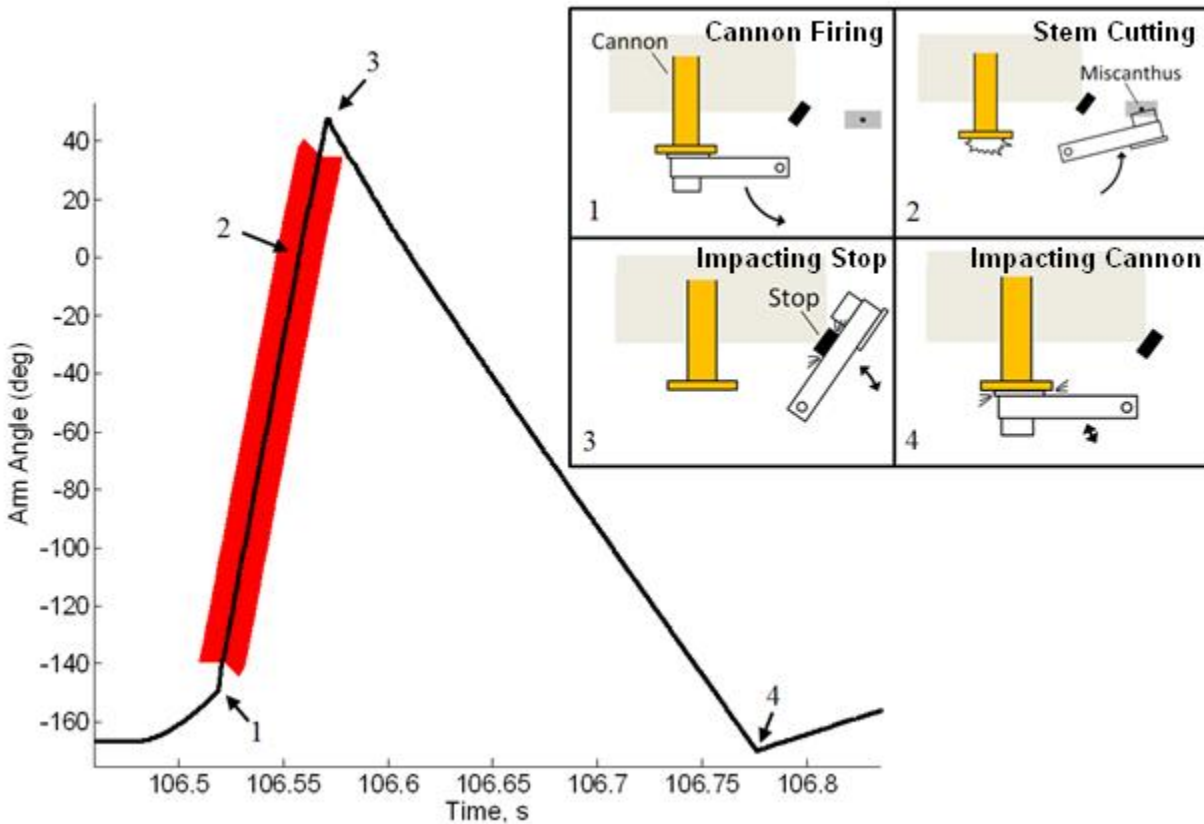


Figure 25 Firing sequence of cannon cutter and recorded output of encoder. The red portion of the plot indicates the portion of the response used by to determine the speed of the cutter before and after the stem is cut.

The pre-cutting region was identified as the area on the between points 1 and 2. The cutting region was from point 2 to a fixed number of degrees, based on the diameter of the stem being cut. This method was likely an approximation, since the stem would undoubtedly bend during cutting, as shown in Figure 19. The post-cut region began at the end of the calculated stem width and ended at 38°.

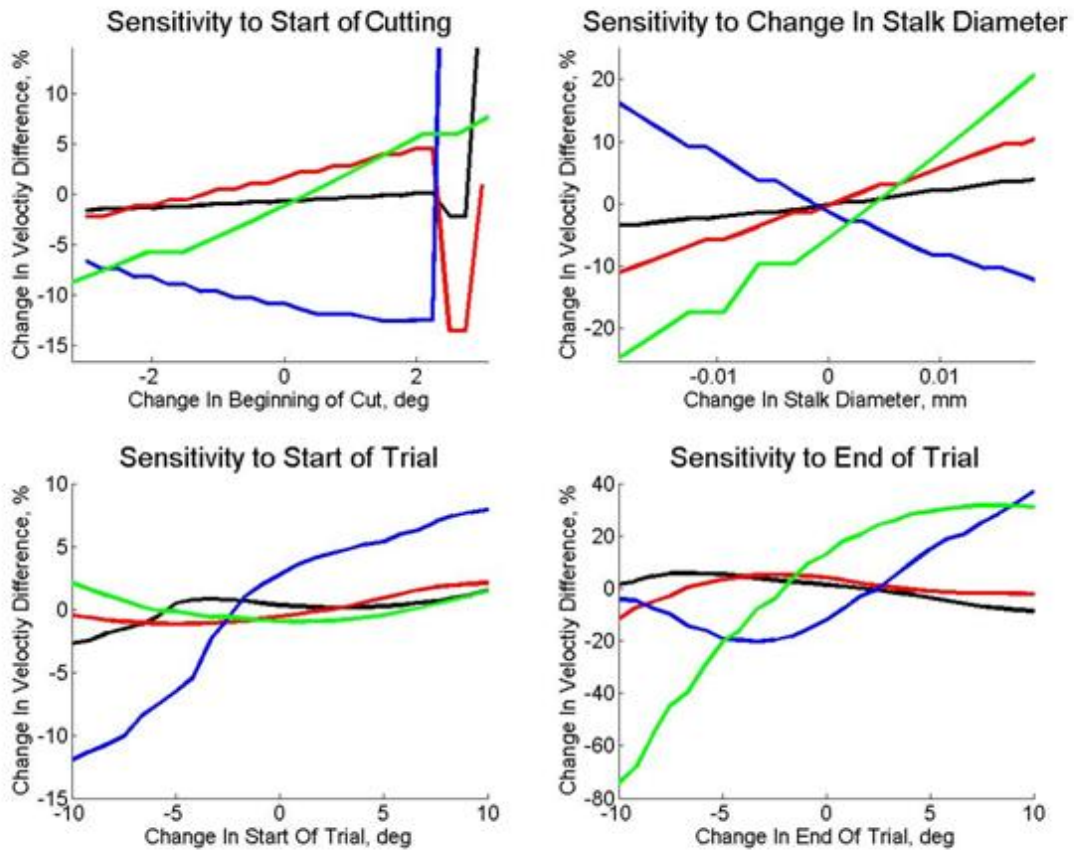


Figure 26 Sensitivity of calculated speed to division of pre-cut, cutting, and post-cut regions of the cutterhead’s motion. Each line is represents a different cutting trial.

Cutting speed was insensitive to the manner in which each region was defined, as indicated in Figure 26.

4.2.3 Characterization of Miscanthus Used In Cutting Trials

The miscanthus used in cutting trials was from a mature second year planting and was collected after overwintering on March 2, 2011. Samples were cut as close to the ground as possible at an approximate height of 1-4 cm. Harvested miscanthus stalks were placed in cold storage for several weeks prior to experimentation, which took place on March 16 and April 27, 2011. This freezing technique is supported by previous research, albeit in different crops.

O'Dogherty et al. (1986) observed no difference in cutting forces or energies when conducting

experiments with fresh and frozen stems of ryegrass. Tuck et al. (1991) employed similar cold storage techniques. Moisture tests were conducted on April 27, 2011. The diameter of the miscanthus stem was recorded prior to each cutting trial. This measurement was taken perpendicular to the direction of travel of the cutting blade and therefore represented the distance the blade had to traverse in order to sever the stalk. Measurements of stalk height and weight were also recorded for subset of the experimental trials with a 45° oblique angle.

4.2.4 Design Iterations of Single Stem Cutter

The cutting blade and sensing architecture were both modified to improve accuracy. The moment of inertia of the initial cutting blade was reduced significantly by using lighter components. This increased the blade's change in velocity per unit of energy lost. The blade was also modified to protrude from the end of the cutting arm, so the blunt portion of the arm did not contact the stalk. Initially, the velocity of the blade was determined using time of flight sensors. These sensors consisted of a laser emitter paired with two receivers. A Fresnel lens was used to refract and project the light emitted by a single laser into a linear pattern intercepted by two receivers. As it travelled, the cutting arm interrupted the path from emitter to receiver resulting in a logic change. The time of flight sensors provided inaccurate speed measurements. Errors were likely caused by vibration in the apparatus after firing and bounce (fast, unpredictable logic changes) in the output of the receivers. Encoder speed measurements were found to be more accurate than the time of flight sensors, since the measurement principle was the same and roughly one hundred times more data points were recorded during each trial.

4.2.5 Safety Considerations

The cutting apparatus developed was equipped with safety devices to isolate users from its fast moving parts and prevent accidental pressurization or firing. As depicted in Figure 18,

the muzzle of the cannon was surrounded on each side by a hinged enclosure, which was equipped with an electronic safety latch that prevented pressurization when the cage was open. Pressurization also required constant manual pressure on a safety switch on the cannon's instrumentation panel. An electronic valve was used to vent cannon pressure through a muffler if the switch was released or the cage was opened. This valve was open when the cannons electronics were unpowered, so that it was impossible to pressurize. Finally, the cannon's control system could be locked out to prevent unauthorized use.

CHAPTER 5: RESULTS AND DISCUSSION

The following sections present energy measurements from laboratory based cutting experiments and in-field harvesting trials. In-field energy measurements were affected by crop conditions, operator preferences, and machinery settings. Sections 5.1-5.1.3 summarize the areas harvested and provide average results for harvest energy, crop yield, and harvester throughput. Sections 5.1.4-5.1.5 explore the relationship between crop yield and groundspeed which is mathematically expressed in 5.1.6. Average measurements of single stem cutting energy are presented in section 5.2. Sections 5.2.1-5.2.2 discuss the effects of nodal cutting and miscanthus diameter. The effects of all parameters are summarized and statistically analyzed in section 5.2.3. Combining results from in-field and laboratory experiments provides an estimate of the portion of total harvest energy devoted to stem cutting, which is given in the conclusion.

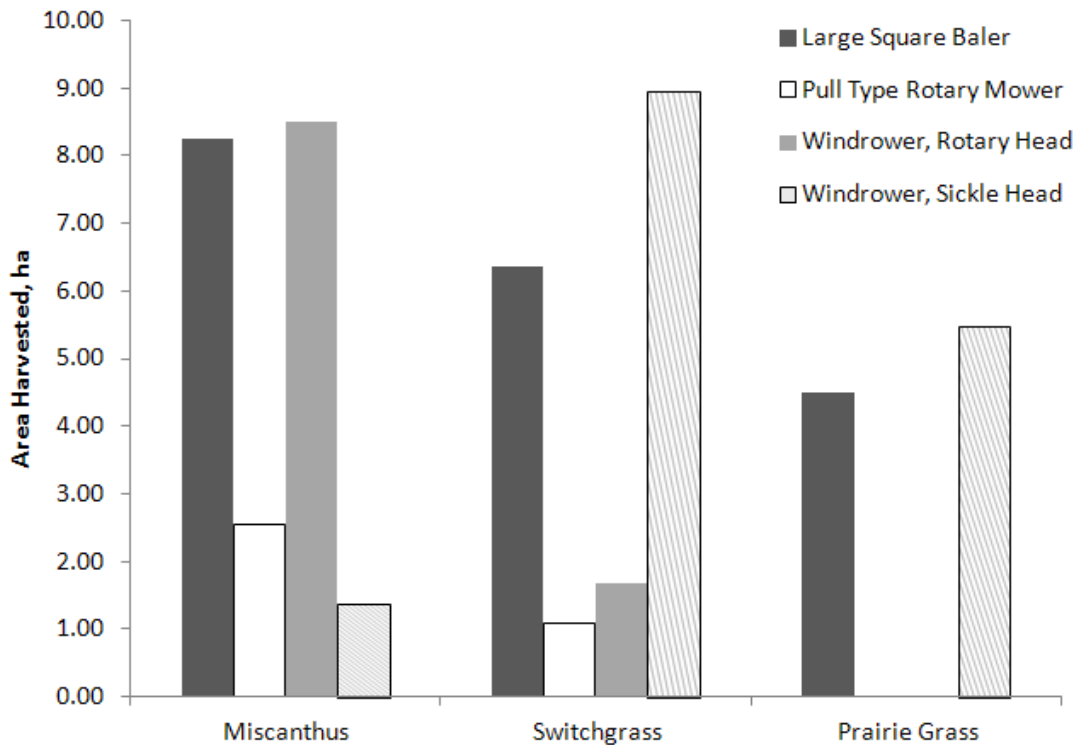


Figure 27 Area harvested by each machine, based on number of recorded data points, machine speed, and working width. Nonproductive time (turning and idling) was excluded.

5.1 In-Field Performance Monitoring

The total area harvested during in-field performance monitoring was approximately 50 ha (120 acres). Overall, field data logging was successful in estimating the power requirements of each machine. Disadvantages of the system were its slow sample rate, vulnerability to field conditions such as vibration and dust, and uncertainties introduced by unmonitored field conditions and operator settings. Figure 27 depicts crop acreages harvested by each machine. These areas were computed based on machine velocity during each sample period. The acreages presented provide an informal measure of the weight or confidence that can be associated with each set of results. The following sections present results for engine load variation, throughput, yield, and the combined effect of yield and groundspeed on power consumption.

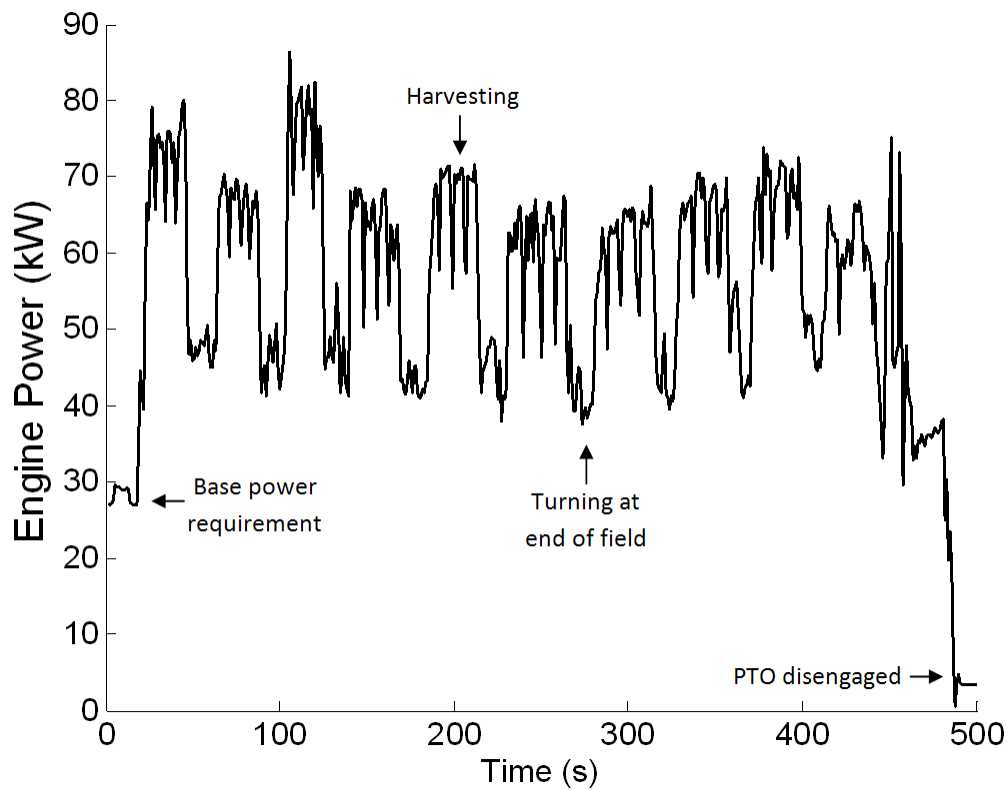


Figure 28 Variation in power usage of tractor pulling Case DC132 rotary mower-conditioner in miscanthus, based on percent engine torque CAN data.

5.1.1 Variation in Engine Load

Engine load changed throughout the field, reaching a minimum when equipment was turning at the boundaries. This variation was removed in the final results by filtering recorded data as described in section 4.1. Figure 28 depicts tractor engine load while mowing miscanthus with the DC 132 mower-conditioner. A significant amount of energy was required to overcome parasitic losses in the machine, even with no crop input. These losses are believed to be caused by driveline friction, inertial loads, air pumping, and stubble interference (McCrandal and McNulty 1978b). In an effort to better separate legitimate harvesting requirements from energy losses, the base energy requirements of each machine with no crop input were determined and are reported in Table 2.

Table 2: Baseline energy requirements of harvesting machinery. Numbers in parenthesis represent standard deviation.

Machine	Measured Baseline Power (kW)	Recommended PTO Power , Minimum (kW)
Self-Propelled Rotary Mower	63.4 (9.0)	-
Self-Propelled Sickle Mower	58.2 (5.5)	-
Pull-Type Disc Mower	29.1 (2.1)	67.1
Large Square Baler	25.9 (2.3)	74.5-89.5

Parasitic energy losses represent a large fraction of overall energy requirements. Energy efficient harvesting is therefore favored by high groundspeeds, as the machine accomplishes more useful work per unit of parasitic lost. The relationship between base energy and total power requirements is discussed further in section 5.4.

5.1.2 Aggregate Results

Average results across all crops and machines are given in the following sections. Some caution is advised when considering these aggregate results, as local effects such as yield, operator speed and moisture may have biased performance under some circumstances. Previous

studies have shown that harvesting power is greatly affected by yield and groundspeed, which combine to determine throughput (McCrandal and McNulty 1978b). An increase in groundspeed therefore influences power use for two reasons:

- It increases the crop load being processed (throughput).
- Additional power is required to propel the machine forward especially for the hydrostatically driven windrowers.

Field conditions are also important. In previous work, crop density and stem shear strength were the most important factors in determining rotary mower power requirements. The following sections describe average harvest conditions and power usage. The relationship between crop yield, harvester groundspeed, and power use is more carefully developed in section 5.1.5.

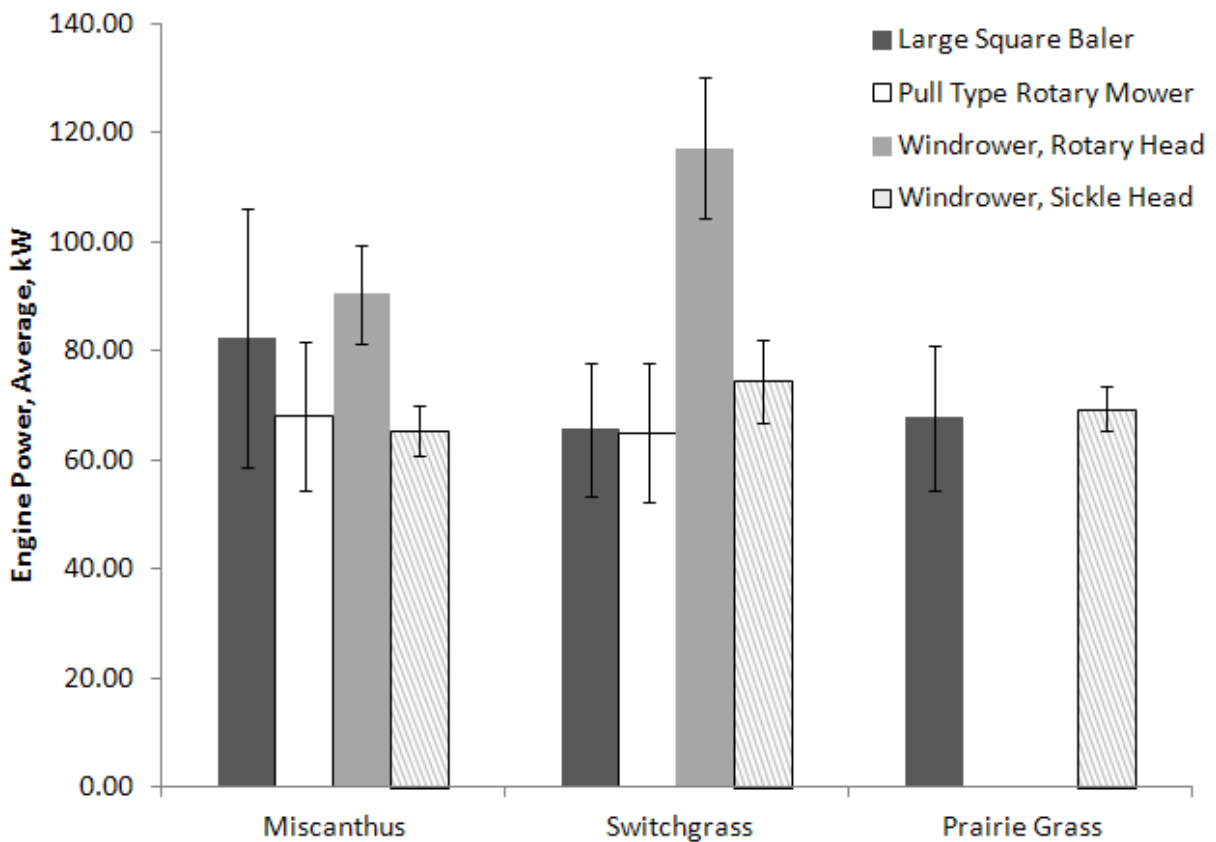


Figure 29 Average engine power demand for harvesting machines in each crop, based on percent engine torque CAN messages. Error bars represent one standard deviation.

5.1.2.1 Machine Power Usage

Average power consumption for each crop and machine is given in Figure 29. The most power intensive activity was rotary mowing with the self-propelled machine, which required 120 kW in switchgrass and 90 kW in miscanthus. The self-propelled sickle mower used less energy with the sickle head, requiring approximately 70 kW in switchgrass and miscanthus on average. Likewise, the pull-type rotary mower had lesser power demands than the self-propelled unit, requiring an average of approximately 65 kW in switchgrass and miscanthus. Average power demands of baling ranged from 65.6-82.3 kW, with dense miscanthus stands requiring more power.

Power recorded during this study was greater than reported values for similar machines in traditional crops such as alfalfa and timothy. This discrepancy is likely to be due to the heavy nature of herbaceous energy crops and inclusion of drawbar power in this study. ASAE D497.7 (2011) predicts power requirements of 18, 32, and 37 kW for the self-propelled sickle, pull-type rotary, and self-propelled rotary mowers respectively. Estimates vary, however, and power ranges as high as 51-75 kW have been reported for rotary mowers (McCrandal and McNulty 1978b). ASAE D497.7 links baling power consumption to throughput, and predicts baling power requirements of 60, 82, and 97 kW for the average switchgrass, prairie, and miscanthus throughputs observed. The significant variability of baling power in miscanthus is likely due to large yield variations in this crop, as illustrated in section 5.1.2.3.

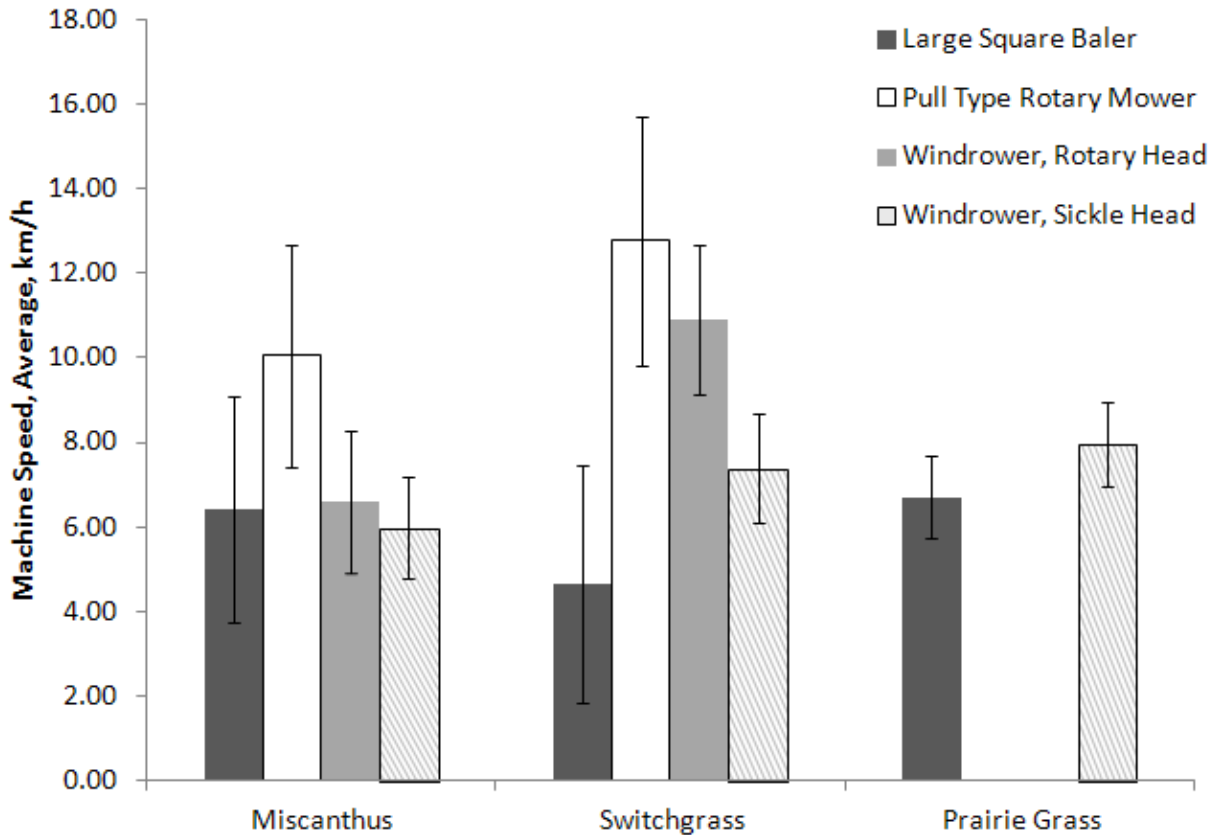


Figure 30 Average speed of harvesting machines in each crop based on GPS speed measurement. Error bars represent one standard deviation. Operators were advised to travel at maximum speed allowed by crop and field conditions.

5.1.2.2 Average Machine Speed

Average machine speeds are presented in Figure 30. Speeds ranged from 4.6-10.9 km/h, with baling requiring slower groundspeeds. Throughout testing, machine speed was largely determined from operator preference, as some operators challenged themselves to travel faster than others. Square baling required the lowest groundspeeds, 4-7 km/h. Mowing groundspeeds were greatest with the pull type rotary mower, which achieved an average speed of 12.8 km/h in switchgrass. In miscanthus, there was little difference in speed between the rotary and sickle mowers, possibly due to operator preference. Groundspeed tended to be less variable with the sickle mower, likely due to limitations in effective cutting speed.

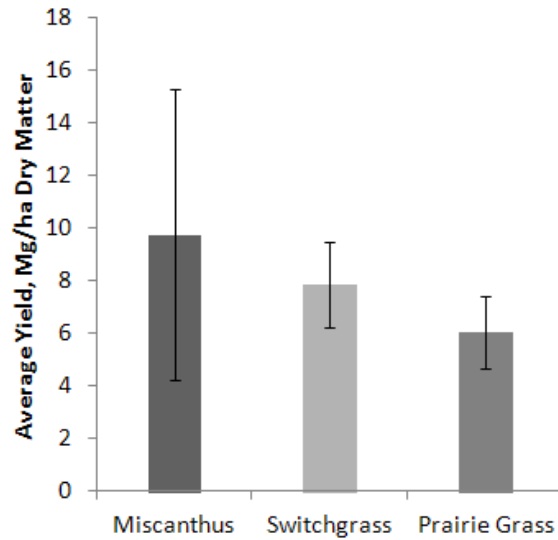


Figure 31 Average yield and variation for miscanthus, switchgrass, and tallgrass prairie. Average plot yields were weighted based on the acreage harvested from each plot (see Figure 27).

5.1.2.3 Crop Conditions

Average yield information is given in Figure 31. Miscanthus produced the highest average, 9.75 Mg/ha, but also the greatest variation, ranging from 2.3 to 19.1 Mg/ha. This variation was due to differences in maturity of the miscanthus stands that were harvested, as some stands were immature and therefore sparse. Switch and prairie grass stands were lower yielding but more consistent, with average yields of 7.82 and 6.06 Mg/ha, respectively. Average moisture contents for miscanthus, switchgrass, and prairie were 84, 76, and 86 % dry matter. Given the average speeds presented in section 5.2.2, average machine throughputs were calculated. Baling throughputs ranged from 12-20 Mg/h. Mowing equipment experienced slightly higher throughputs of 18-29 Mg/h.

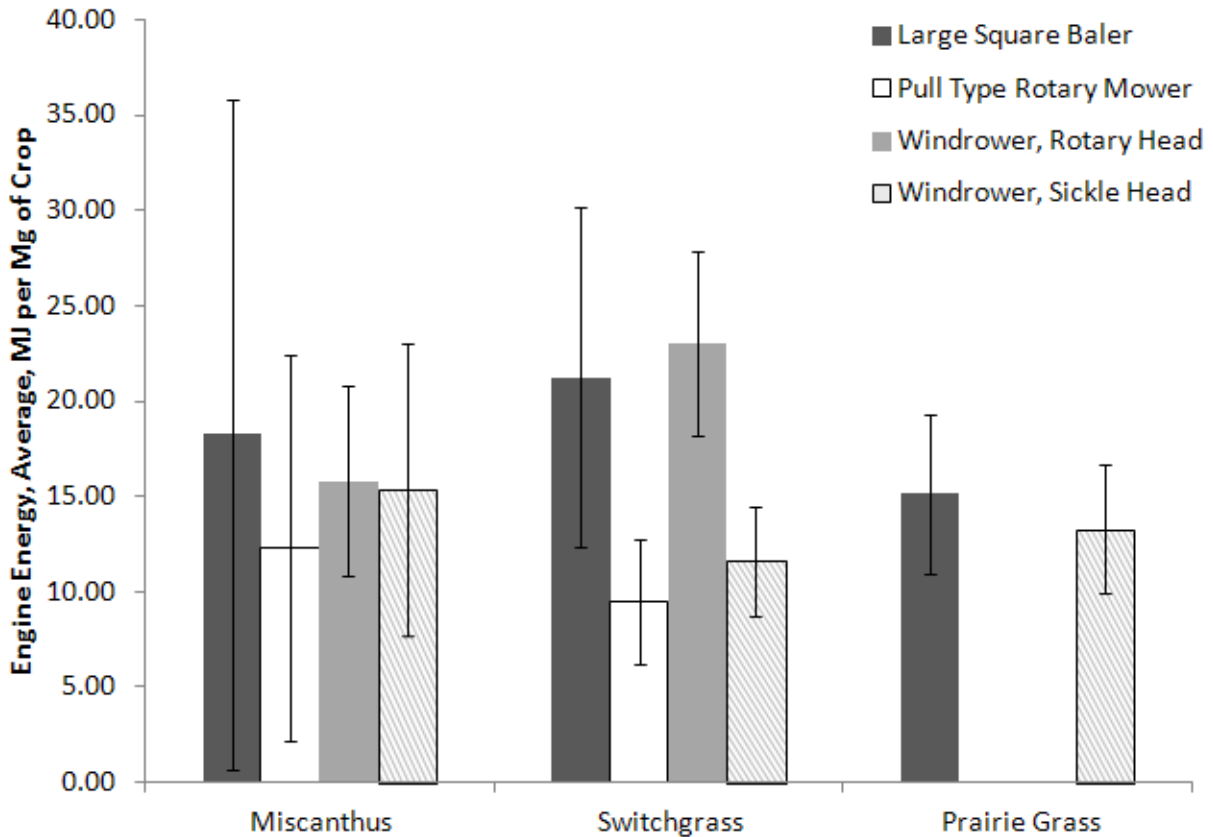


Figure 32 Average energy requirement of harvesting machines in each crop based on machine power, speed, and crop yield. Error bars represent one standard deviation.

5.1.2.4 Average Harvest Energy

Harvest energy is a complex metric to consider, as it combines groundspeed, crop yield, and engine power. The average energy required to harvest one Mg of crop is given in Figure 32. Mowing and baling required approximately equal amounts of energy, with baling ranging from 15.2-21.2 MJ/Mg, and mowing 11.6-23 MJ/Mg. The pull-type mower-conditioner was the most energy efficient across all crop conditions. This was likely due to the efficiency of its mechanical drive, relative to the hydrostatically driven self propelled machines. As expected, the self-propelled sickle mower was more energy efficient in light switchgrass, but did not differ significantly from the rotary mower in miscanthus, which was more difficult to cut. Comparing the pull-type and self-propelled rotary mowers, one can estimate a hydrostatic loss of

approximately 3.55 MJ/Mg in switchgrass, and 13.5 MJ/mg in miscanthus. Energy requirements of the large square baler varied significantly due to power fluctuations throughout the cyclic motion of its plunger.

5.1.3 Effect of Yield on Engine Power

As described in section 5.1.2, crop yield and groundspeed are believed to have a significant effect on power requirements.

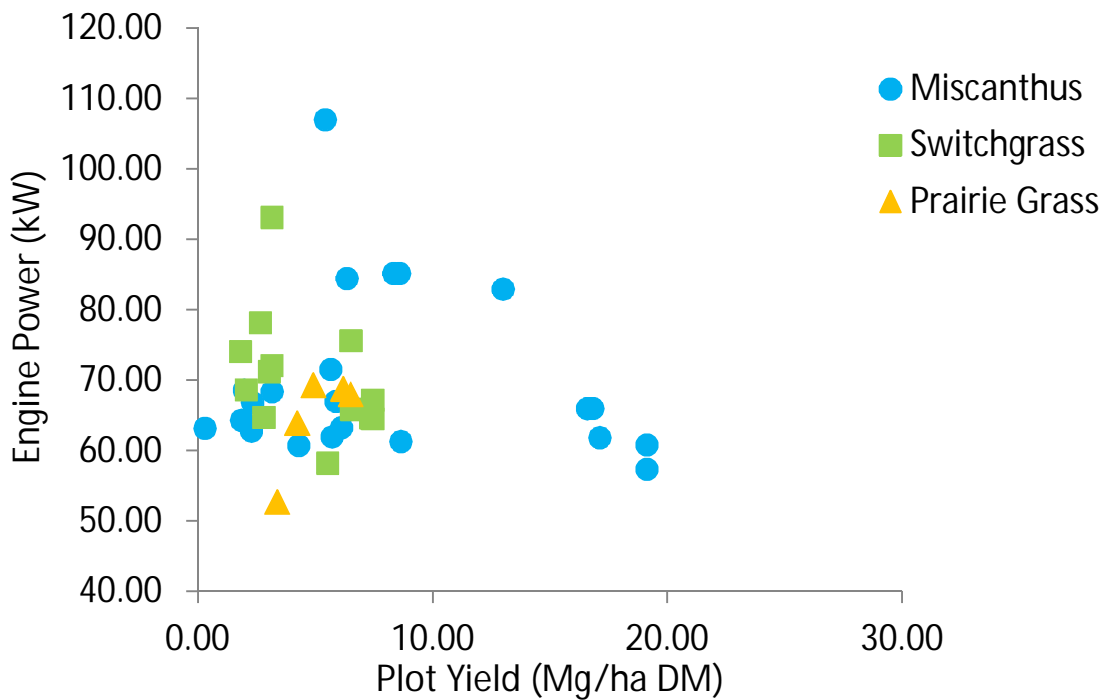


Figure 33 Engine power versus crop yield for large square baler.

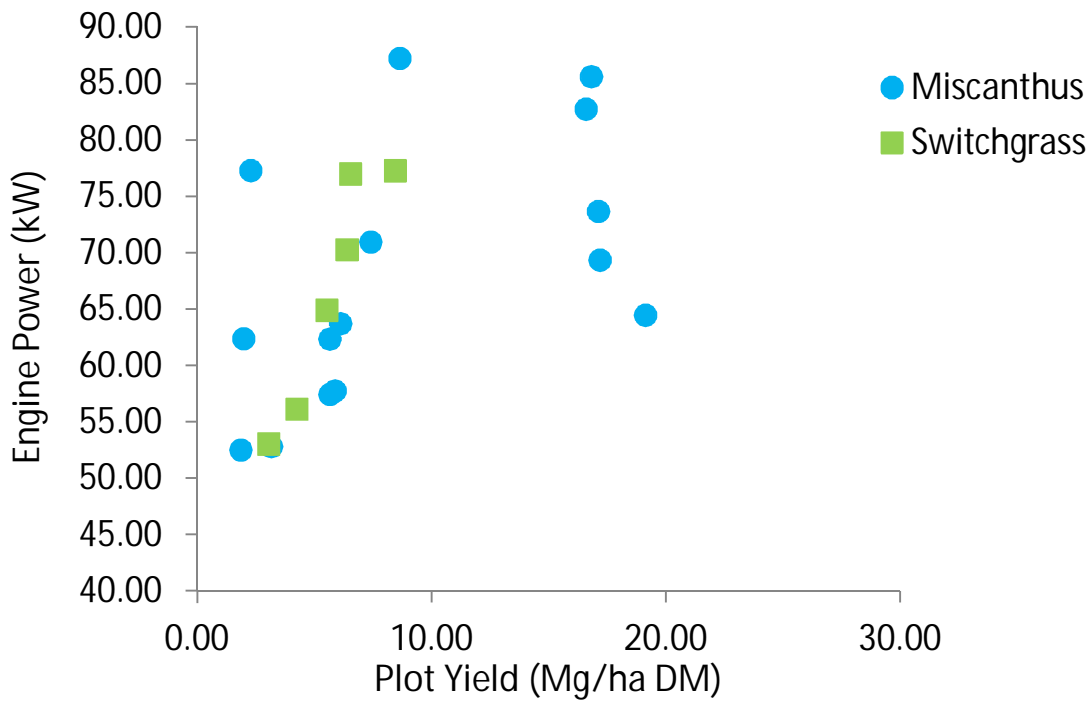


Figure 34 Engine power versus crop yield for pull-type rotary mower.

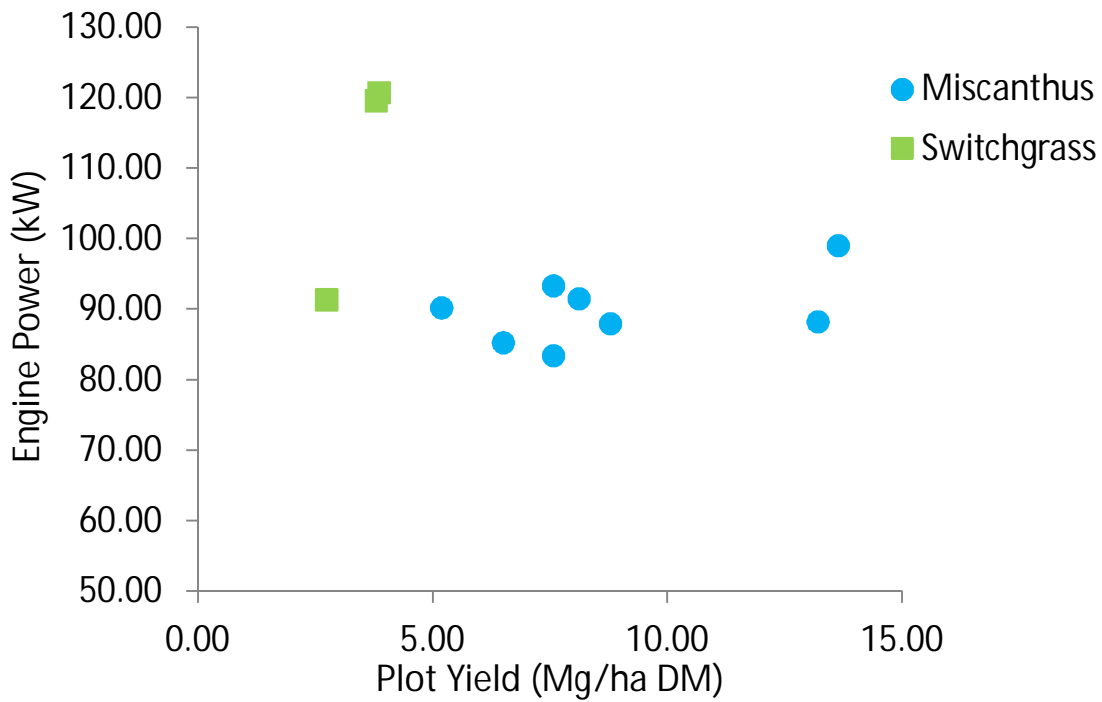


Figure 35 Engine power versus plot yield for self-propelled rotary mower.

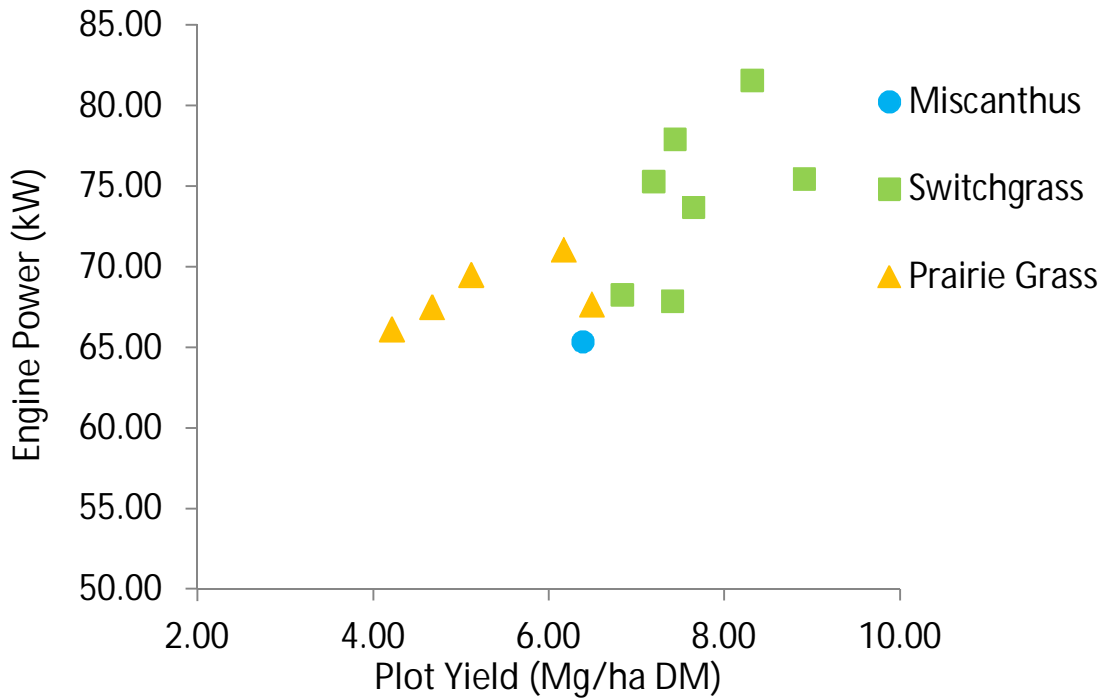


Figure 36 Engine power versus plot yield for self-propelled sickle mower.

Figures 33 through 36 illustrate the effect of crop yield on required engine power. Each data point in these Figures represents the conglomeration (averaging) of several hundred seconds of 1 Hz logging. The effect of groundspeed on power is given in section 5.1.4.

Energy requirements of the large square baler were not strongly correlated with engine power as depicted in Figure 33. Even in high yielding miscanthus plots (15-18 Mg/ha DM), engine power did not increase substantially with yield. This may have been due to the need to observe a slower operating speed in denser crops. Yield correlated well with engine power for the pull-type rotary mower (Figure 34). For the self-propelled rotary mower, crop yield had little effect on engine power (Figure 35). In contrast, the self-propelled sickle mower experienced a very clear increase in engine power with additional crop yield, as depicted in Figure 36.

5.1.4 Effect of Ground Speed on Engine Power

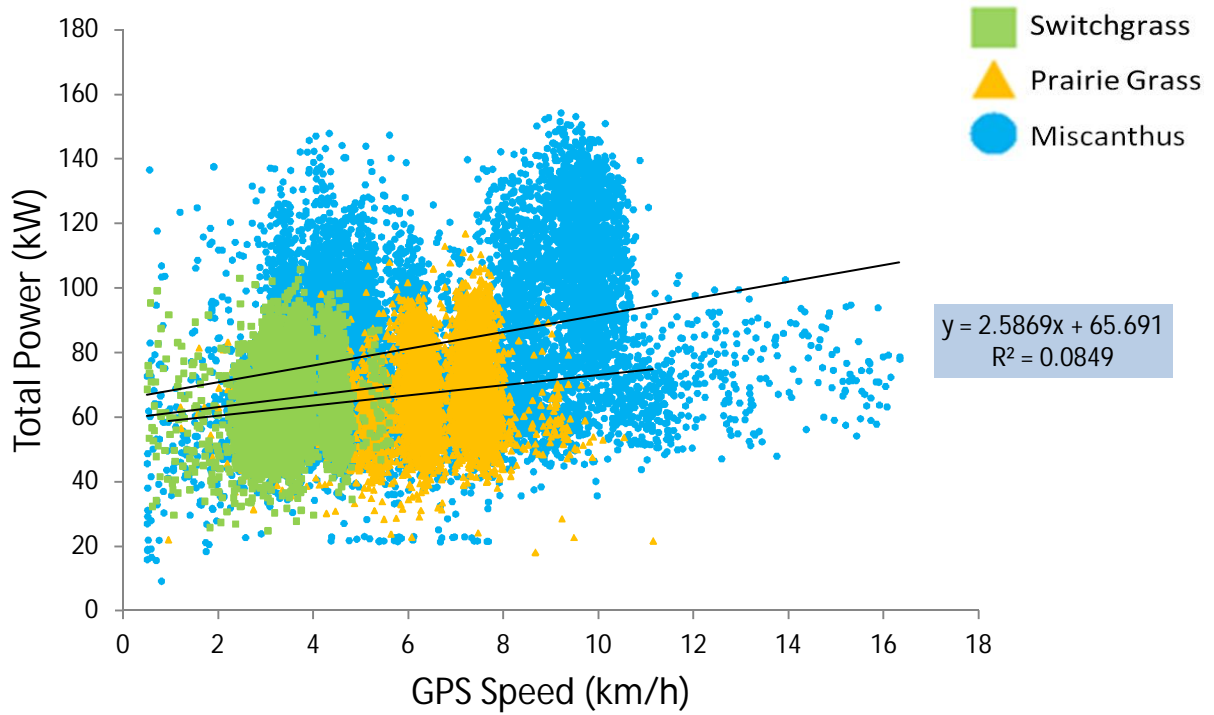


Figure 37 Engine power versus groundspeed for large square baler.

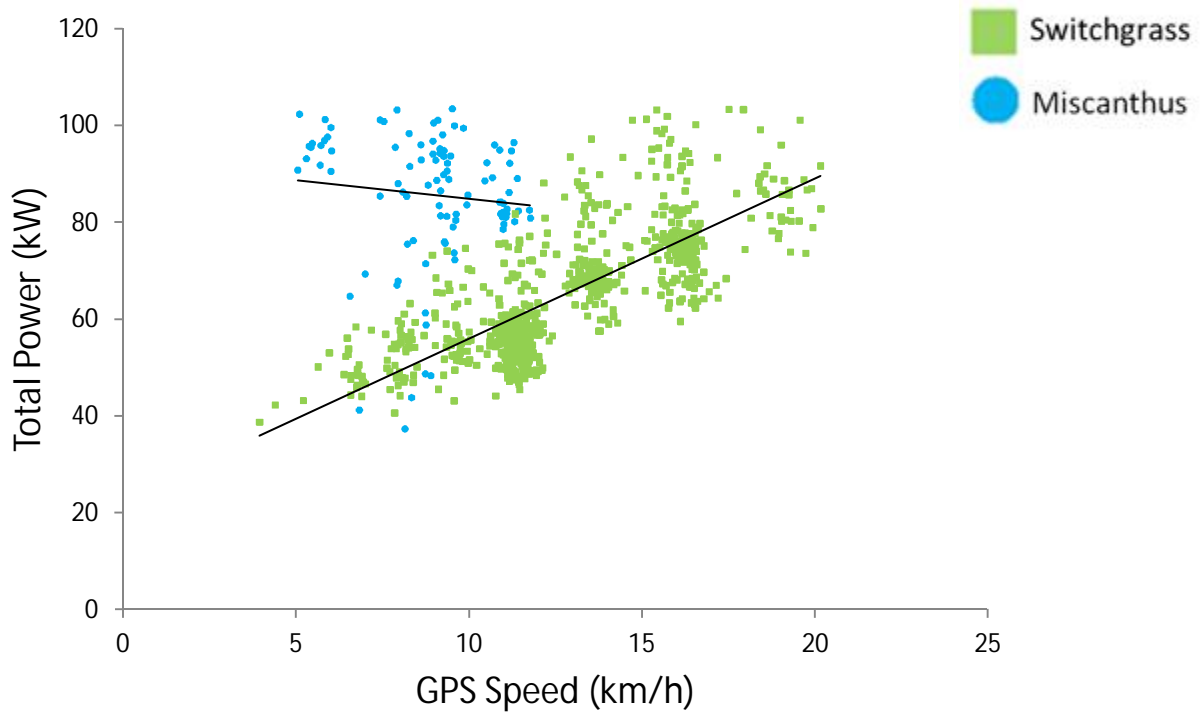


Figure 38 Power use versus speed for pull-type rotary mower.

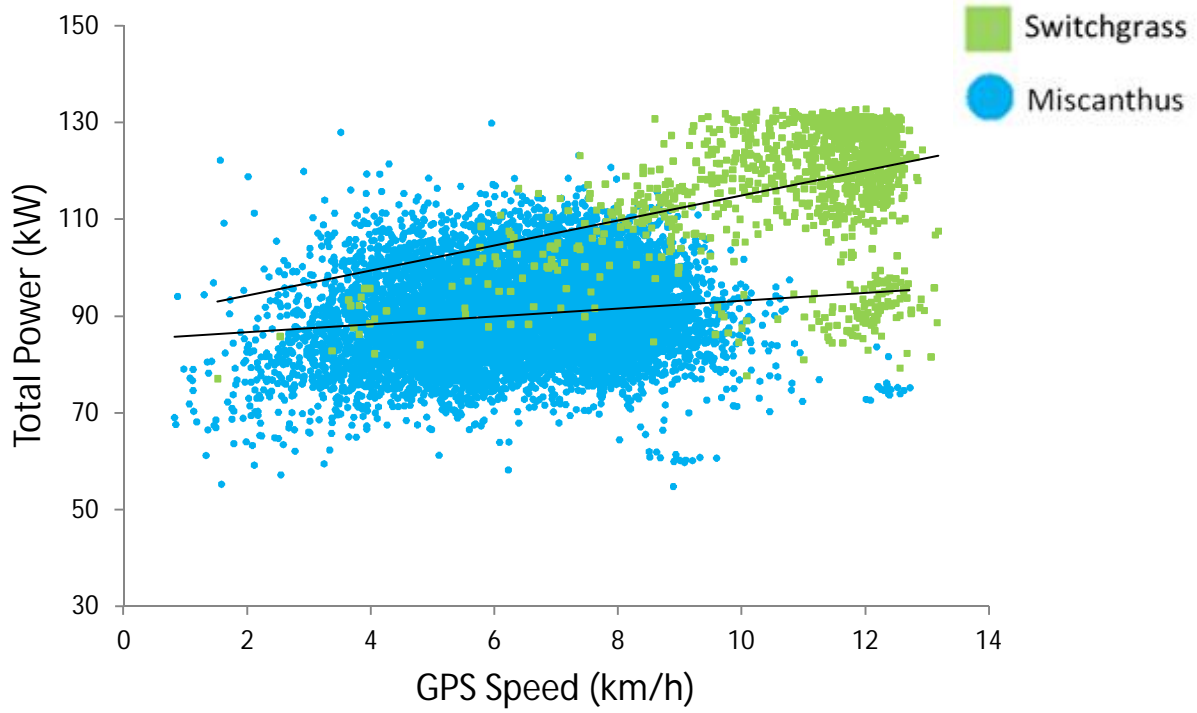


Figure 39 Total power versus groundspeed for self-propelled rotary mower.

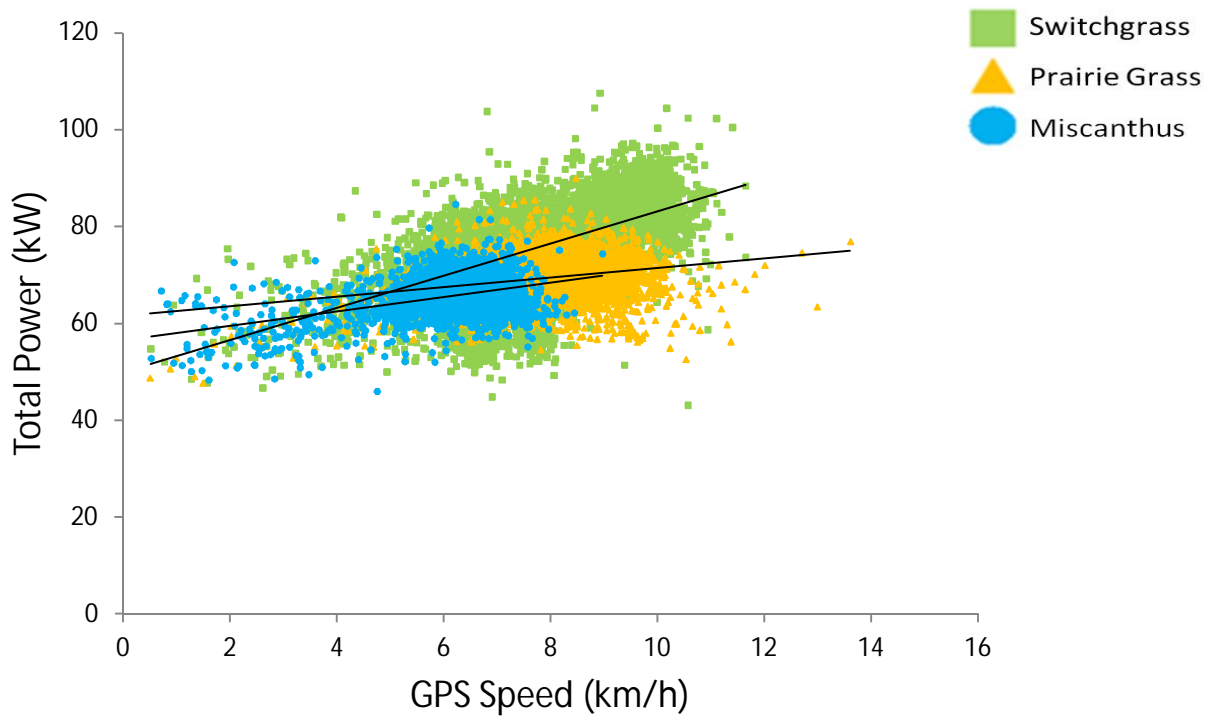


Figure 40 Engine power versus groundspeed for self-propelled sickle mower.

Figures 37 through 40 illustrate the relationship between harvester speed and engine power. Note that groundspeed has a much higher resolution (once per second) than crop yield (once per plot). Engine power was highly variable for the large square baler (Figure 37), and increased only slightly with groundspeed. The effect of yield on engine power was also small for this machine, indicating that average power requirements of large square balers are relatively insensitive to throughput but vulnerable to short term spikes in demand. This variability in required power justifies the use of flywheels on reciprocating balers. The effect of groundspeed on power use was mixed for the pull-type rotary mower (Figure 38). While higher groundspeed increased engine power in switchgrass ($R^2 = 0.58$), it had no effect in miscanthus. This mixed behavior may have been due to operator preference to slow down when miscanthus stands became thick, and maintain speed in dense switchgrass, which flowed better through the machine.

Groundspeeds were discrete for the pull-type mower and large square baler, and continuous for the hydrostatically driven windrowers. The self-propelled rotary mower experienced a weak relationship between groundspeed and engine power (Figure 39). Recalling that the effect was also small for yield, one may conclude that the rotary mower is also insensitive to crop conditions and groundspeed. Engine power of the self-propelled sickle mower was most affected by groundspeed when mowing switchgrass, while groundspeed was less influential in miscanthus and tallgrass prairie (Figure 40).

5.1.5 Relationship Between Engine Power, Yield, and Harvest Speed

The yield and groundspeed measurements considered in the previous two sections were combined to evaluate engine load in terms of harvester throughput. As noted in Tuck et al. (1991), groundspeed and throughput are the two most influential factors in determining power

requirements. ASAE standard 497.7 notes that power requirements of large square balers can be described in terms of the following,

$$P = P_s + CT \tag{13}$$

where: P = engine power, kW

P_s = the static power requirement, kW

C = processing energy, kWh/Mg

T = throughput, Mg/h

This throughput relationship was applied to each of the machines considered in this trial.

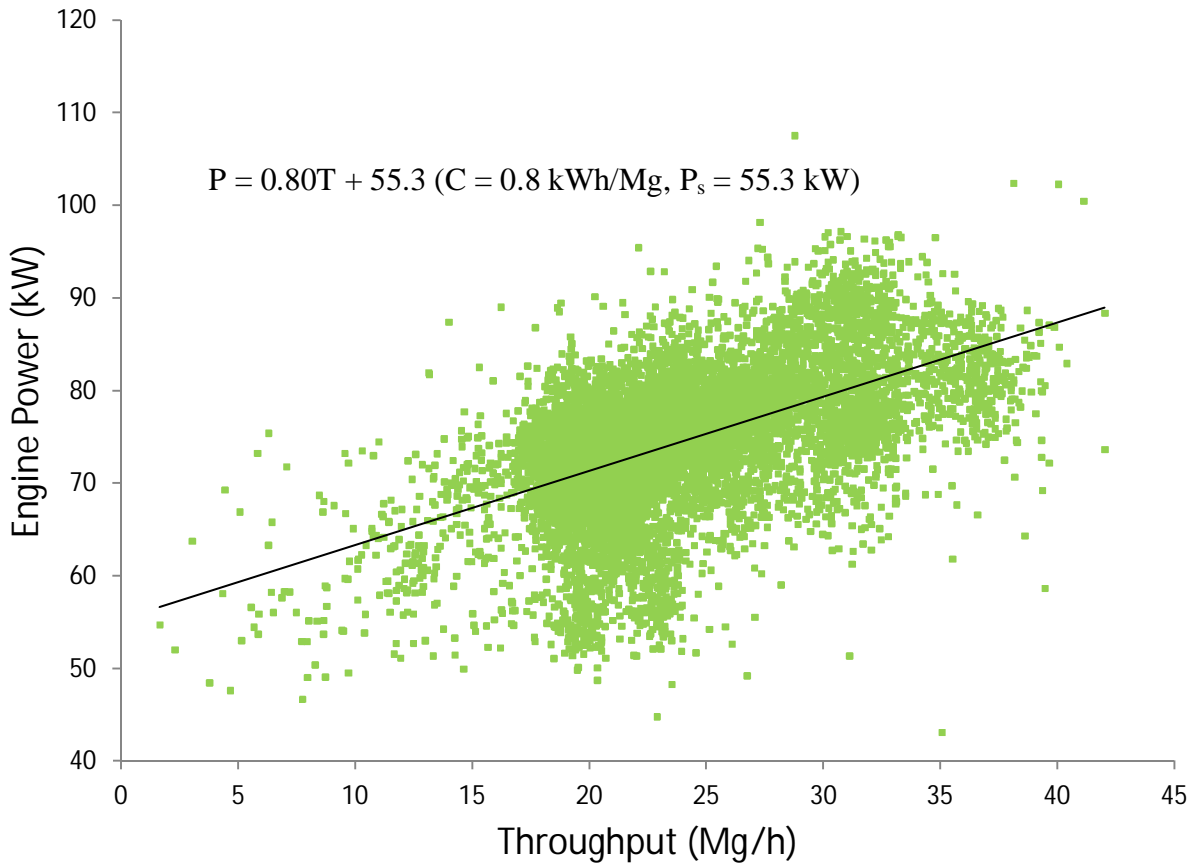


Figure 41 Application of linear throughput relationship, Equation (13), to mowing of switchgrass with the self-propelled sickle mower.

Figure 41 illustrates the application of equation (13) to switchgrass harvesting with the self-propelled sickle mower.

Table 3: Fitted parameters of throughput versus energy model, Equation (13), for each machine and crop.

Machine	Crop	Model Parameters		Number of Samples
		Ps (kW)	C (kWs/Mg)	
Large Square Baler	Miscanthus	74.0	1500	10476
	Switchgrass	60.3	1591	11770
	Prairie Grass	52.6	3285	5567
Pull-Type Rotary Mower	Miscanthus	59.3	918	2287
	Switchgrass	43.9	2621	773
Self-Propelled Rotary Mower	Miscanthus	86.8	593	9908
	Switchgrass	65.0	9985	1189
Self-Propelled Sickle Mower	Miscanthus	56.5	1930	1921
	Switchgrass	55.3	2886	10047
	Prairie Grass	60.8	1589	5727

Table 3 presents fitted values for static power (P_s) and throughput sensitivity (C) for each machine and crop. Static power requirements ranged from 43.9 to 86.8 kW. The increase in engine power with additional throughput varied considerably, from 593 to 9985 kWs/Mg. In many cases, R^2 was small, indicating that a large portion of recorded variation was not explained by throughput measurements. This result is not unreasonable due to the low resolution of yield measurements and general complexity of harvesting machinery relative to the limited CAN information collected.

Static power requirements in Table 3 can be compared to actual power measurements in Table 2. Recall that values given in Table 2 were for a stationary machine, running at rated speed, with no crop input. Values given in Table 3 represent the theoretical power required

when the machine is moving with zero throughput. Static energies in Table 3 are greater because they account for draft power requirements.

5.2 Laboratory Based Cutting of Miscanthus

The energy requirements for cutting miscanthus with varying speed (10-20 m/s), oblique angle (0°, 30°, and 60°), and location (node or internode) are provided in sections 5.2.1 and 5.2.2. Average energy requirements were 9.30 ± 2.60 J per stem, or 1.02 ± 0.25 J per mm of stem thickness. These results agree with cutting energies of 7.5 – 18 J reported by Kroes et al. (1996) for several varieties of sugarcane stalks at 20 m/s. Generally accepted values for single stem cutting of timothy and alfalfa are much lower, at 10-1000 mJ per stem (Tuck et al. 1991b). Average stand density of miscanthus is 50-100 stems per m² (Pyter et al. 2007). Assuming each stem is cut only once, this leads to an energy consumption of approximately 4.65-9.30 MJ/ha. Given a plot yield of 13.5 Mg/ha (Lewandowski and Heinz 2003), the energy consumption required for cutting would be 0.39-0.78 MJ/Mg. This represents 2.1% of the average harvesting energy reported for Miscanthus, which is in agreement with Kroes et al. (1996), who estimated that energy required for cutting would comprise approximately 3% of overall power requirements. Miscanthus diameter ranged from 7.4 to 11.0 mm and averaged 9.02 ± 1.08 mm. The average moisture content of miscanthus was 17.0% (dry basis) with a standard deviation of 0.3%, determined using ASAE S358.2. Cutting energy tended to increase linearly with speed, in a manner supported by Prasad (1975) and Taghijarah et al. (2011) but contrary to the findings of previous studies with grass-like stems (Chancellor 1958, O'Dogherty and Gale 1986, Persson 1987). This implies that miscanthus cutting was taking place below the critical speed, or that a different mode of cutting was occurring due to the high structural rigidity of miscanthus relative to smaller stemmed plants.

5.2.1 Effect of Cutting at Node and Internode

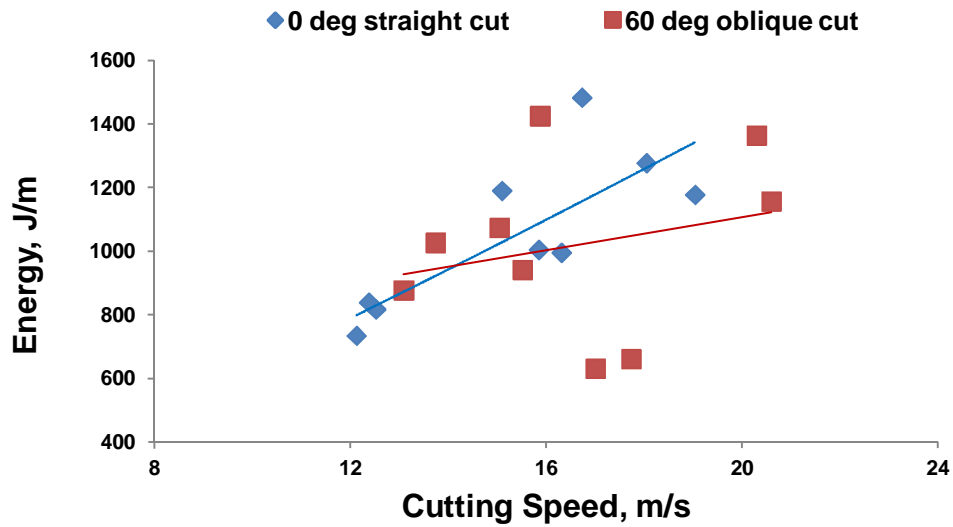


Figure 42: Energy required for nodal cutting of miscanthus, with varying blade speed and oblique angle.

Figure 42 illustrates the specific cutting energy for miscanthus stems at the node with each oblique angle. Cutting energy was affected by the oblique angle of the blade, with interaction between oblique angle and cutting speed. Speed had a much greater effect on energy for an oblique angle of 60° ($R^2 = 0.70$), whereas a straight cut (oblique angle of 0°) resulted in no relationship. The average cutting energy was 1057.3 ± 244.3 J/m for the straight cut and 1017.2 ± 276.3 J/m for the 60° oblique cut.

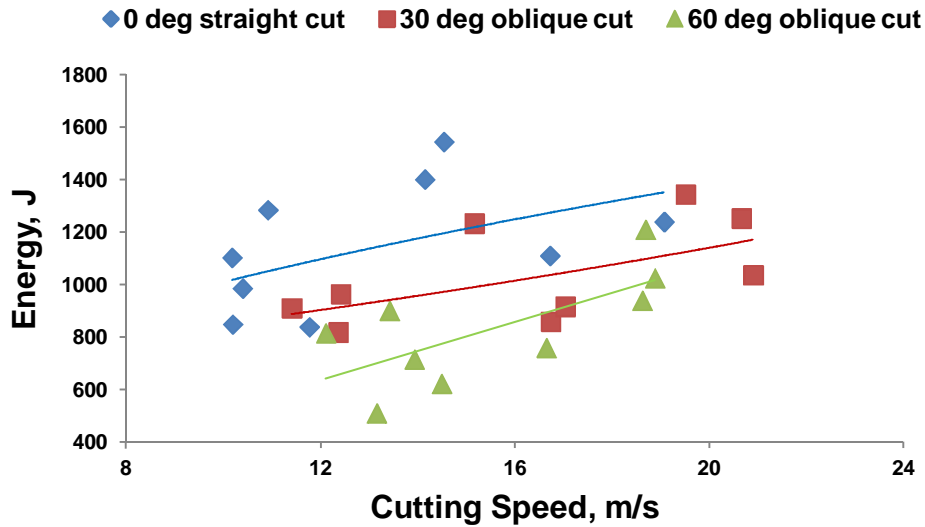


Figure 43: Energy as a function of cutting speed for miscanthus stems between nodes.

Figure 43 depicts the specific cutting energy required for miscanthus stems at the internode, a point equidistant between nodes. Once again, cutting energy was proportional to cutting speed for each oblique angle. Average specific energy was 1151.3 ± 240.6 J/m, 1037.9 ± 191.7 J/m, and 833.3 ± 212.9 J/m for oblique angles of 0° , 30° , and 60° , respectively. Again there was no relationship between cutting energy and speed for an oblique angle of 0° . The blade required the least cutting energy, and exhibited a weak correlation with speed ($R^2 = 0.5$).

Optimal cutting occurred with an oblique angle of 60° and blade speed of 13 m/s. This resulted in an average specific energy of 741.9 J/m. Cutting energy with the 60° blade increased to 1058.3 J/m at a cutting speed of 18.7 m/s. This trend agrees with Dobler et al. (1972), who reported larger energy requirements as blade speed increased in quasi-static experiments and recommended lower cutting speeds. Prasad et al. (1975) reported that cutting energy also increased with speed in maize stems. These findings stand in contradiction to the vast amount of

cutting work done with small diameter grass stems, which implies lower energy requirements at higher cutting speeds.

5.2.2 Effect of Miscanthus Diameter

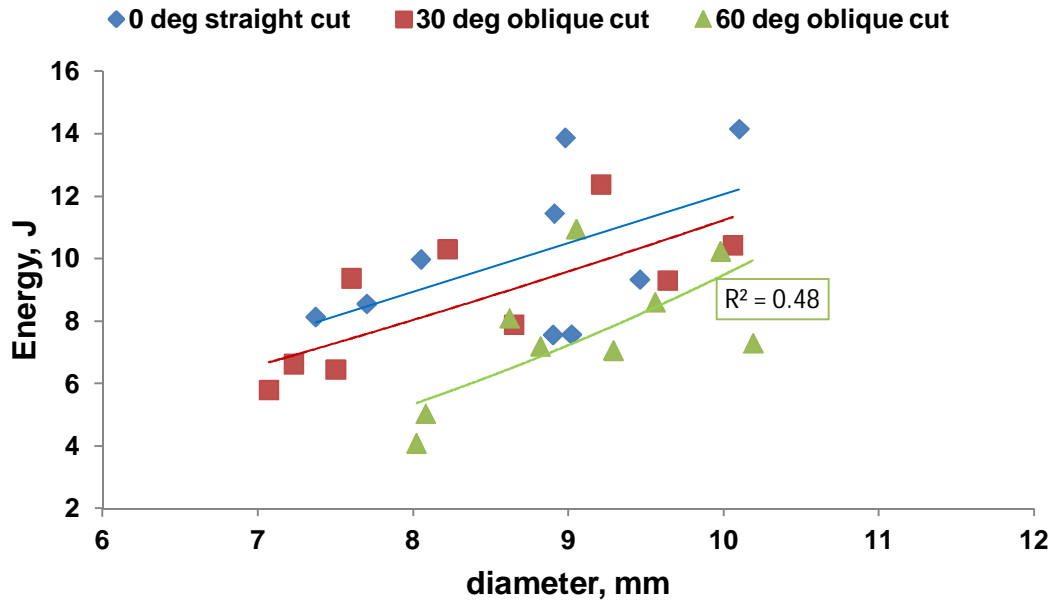


Figure 44: The effect of stem diameter on cutting energy, with varying oblique angle.

Figure 44 illustrates the relationship between cutting energy and stem diameter with each oblique angle. Again, impact cutting required the greatest energy. For all oblique angles, cutting energy increased with stem diameter. For a straight cut, the average cutting energy was 10.07 ± 2.56 J, and the average diameter was 8.72 ± 0.86 mm. Similarly, for the 30° cut, the average cutting energy was 8.73 ± 2.19 J, and average diameter was 9.25 ± 0.97 mm. The 60° oblique cut required 7.62 ± 2.20 J with an average diameter of 9.07 ± 0.77 mm.

5.2.3 Statistical Interpretation of Results

The significance of experimental factors in high speed cutting was quantified using analysis of variance (ANOVA). Since the 30° blade was only used only in internode cutting, two tests were used. As in section 5.2.1, cutting energy was normalized by stem diameter to

produce specific cutting energy (J/m). The first test considered cut location (node vs internode), oblique angle (0° and 60°), and cutting speed, while omitting the 30° blade. All three factors were significant. Oblique angle and cut location interacted ($p = 0.03$), and blade speed was significant ($p = 0.005$). A linear regression was developed to estimate cutting energy in terms of cut location, oblique angle, and cutting speed for blade angles of 0° and 60°,

$$E_{sc} = 264 - 23.1 p_{location} + 256 p_{oblique} + 41.9 v_{blade} \quad (14)$$

where: E_{sc} = specific cutting energy, J/m

$$p_{location} = \{1 \text{ for nodal cutting, } 0 \text{ for internode cutting}\}$$

$$p_{oblique} = \{1 \text{ for } 0^\circ \text{ oblique angle, } 0 \text{ for } 60^\circ \text{ oblique angle}\}$$

$$v_{blade} = \text{cutting speed of blade, m/s}$$

This regression above produced a multiple R^2 of 0.31. Cutting speed was directly related to cutting energy, with each unit increase in speed requiring an additional 42 J/m ($p = 0.006$). Oblique angle was also significant, with the 0° blade consuming an additional 256 J/m ($p = 0.003$). Relative to the other two factors, cutting location was not significant ($p = 0.77$).

A second ANOVA test considered internode cutting with all three oblique angles (0°, 30°, 60°) at varying speed. Here the oblique angle used was significant ($p = 0.01$) and cutting speed was not ($p = 0.15$). A linear regression of these factors yielded,

$$E_{sc} = 671 - 707 p_{blade30} + 343 p_{blade0} + 10.4 v_{blade} \quad (15)$$

where: $p_{blade30} = \{1 \text{ for oblique angle of } 30^\circ, 0 \text{ otherwise}\}$

$$p_{blade0} = \{1 \text{ for oblique angle of } 0^\circ, 0 \text{ otherwise}\}$$

This regression had a multiple R^2 of 0.35. Cutting with a 0° oblique angle increased energy requirements by approximately 343 J/m ($p = 0.003$). The 30° and 60° oblique angles were indistinguishable ($p = 0.3$). The effect of velocity was also nonexistent ($p = 0.17$).

CHAPTER 6: SUMMARY AND CONCLUSIONS

Harvest energy of three herbaceous energy crops was measured in both field and laboratory settings. In-field performance monitoring was an effective means of estimating power requirements. Average mowing productivity was 23.6 Mg/h, and was considerably higher for the pull-type mower (32 Mg/h), likely due to operator preference. Baling productivity was 20, 16.6, and 12 Mg/h, in miscanthus, tallgrass prairie, and switchgrass respectively. Average power demands for mowing ranged from 65 to 117 kW, with the mechanically driven pull-type rotary mower requiring the least power. When driven by identical machines, sickle mowing required less power than rotary (70 vs 103 kW), and was capable of maintaining throughput in miscanthus. Miscanthus was the most energy intensive crop to harvest, requiring 32.8 MJ/Mg for mowing and baling. Average harvest energies for each machine in miscanthus were 18.2, 10.9, 19.4, and 13.4 MJ/Mg for the large square baler, pull-type rotary mower, self-propelled rotary, and sickle, respectively. Parasitic energy losses in harvest machinery were high by multiple metrics (Tables 2 and 3), averaging 56% of total power demand. Total, harvest energy decreased with groundspeed as the machine accomplished more useful work per unit of parasitic energy lost to friction.

The high energies recorded during in-field performance monitoring contrasted with the low energy requirements of single stem cutting. Cutting a single miscanthus stem required 9.30 ± 2.60 J per stem. Angled blades improved cutting efficiency, and impact-like cutting (0°) required an additional 343 J per meter of cut miscanthus. Surprisingly, cutting energy increased with blade velocity. This contrasted earlier research (Chancellor 1958, Mcrandal and McNulty 1978a, O'Dogherty and Gale 1986, Persson 1987, Tuck et al. 1991b) in which cutting was more efficient as speed increased for small-stemmed crops. The results presented here therefore

contradict the prediction of Persson (1987) who argued for a critical speed beyond which cutting energy remains constant. This discrepancy may indicate that high speed cutting is fundamentally different in miscanthus than small-stemmed crops, or that the critical speed is greater than the range considered in this experiment (10-20 m/s).

Assuming a miscanthus stand density of 50-100 stems per m² (Pyter et al. 2007), stem cutting should require 4.65-9.30 MJ/ha. Given a plot yield of 13.5 Mg/ha (Lewandowski and Heinz 2003), the energy consumption required for cutting would be 0.39-0.78 MJ/Mg. This represents 2.1% of the average mowing energy reported for Miscanthus. Stem cutting therefore represents a small portion of overall energy requirements, as has been reported for traditional hay and forage crops (Chancellor 1958).

CHAPTER 7: RECOMMENDATIONS FOR FUTURE WORK

Both in-field performance monitoring and laboratory based cutting experiments present opportunities for future work. In-field machinery monitoring may be improved with higher resolution measurements of yield, by scanning standing crop before it is cut or processing images of crop stubble. The accuracy of harvesting power measurements may be improved by mapping each machine's draft power requirements relative to speed and excluding draft power from harvest energy measurements. Improvements in real-time yield measurement may facilitate the development of throughput controllers in which machine speed is automatically adjusted to maintain optimum crop load.

Laboratory based cutting experiments would benefit from an evaluation of miscanthus cutting at higher blade velocities. Experimentation at higher cutting speeds may lead to the discovery of a critical cutting speed which minimizes cut energy, as demonstrated by previous research in smaller forages. The discovery of a critical cutting speed for miscanthus may influence the design of size reduction equipment such as tub grinders, which may be more sensitive to stem cutting energy as they perform size reduction. Cutting experiments may also benefit from the measurement of cutting force as performed by Kroes et al. (1996), since this affects both blade wear and machine design. Future experiments may also consider variations in cutting geometry. Experimental results from this report indicate that cutting energy is reduced when the cutting edge of the blade forms an oblique angle of 60° . Further iteration in blade and stem angle may reduce energy needs, resulting in more efficient harvesting and size reduction.

REFERENCES

Adler, P. R., M. A. Sanderson, A. A. Boateng, P. J. Weimer and H. G. Jung. 2006. Biomass yield and biofuel quality of switchgrass harvested in fall or spring. *Agronomy Journal* 98(6): 1518-1525.

Anderson, E., R. Arundale, M. Maughan and A. Oladeinde. 2011. Growth and agronomy of *Miscanthus x giganteus* for biomass production. *Biofuels* 167(183): 167.

ASABE D497.7. 2011. Agricultural Machinery Management Data. *ASABE D497.7*.

Case New Holland Agriculture. 2006. Heavy Duty and Economy Disk Mowers. Available at: http://www.caseih.com/en_us/Products/HayForage/Documents/Cutting_Tools/Mower_Conditioners_Rotary_Disc_and_Sicklebar_Brochure.pdf. Accessed July 14 2011.

Case New Holland Agriculture. 2008. New Holland H8000 Series Speedrower® Self-Propelled Windrowers. Available at: <http://agriculture.newholland.com/us/en/Products/Hay-and-Forage-Equipment/Self-Propelled-Windrowers/Documents/NH7030802.pdf>. Accessed July 15 2011.

Chancellor, W. J. 1958. Energy Requirements of Cutting Forage. *Agricultural Engineering* 39(October): 633.

Chattopadhyay, P. and K. Pandey. 2001. Impact Cutting behavior of sorghum stalks using a flail-cutter - a mathematical model and its experimental verification. *Journal of Agricultural Engineering Research* 78(4): 369-376.

Christian, D. G., A. B. Riche and N. E. Yates. 2008. Growth, yield and mineral content of *Miscanthus × giganteus* grown as a biofuel for 14 successive harvests. *Industrial Crops and Products* 28(3): 320-327.

Coates, W. and J. Porterfield. 1975. Compound Helical Cutterbar - Design and Field Testing. *Transactions of the ASAE* 18(1): 17-19.

DeHaan, L. R., S. Weisberg, D. Tilman and D. Fornara. 2010. Agricultural and biofuel implications of a species diversity experiment with native perennial grassland plants. *Agriculture, Ecosystems and Environment* 137(1-2): 33-38.

Dobler, K. 1972. Der friei Schnitt Beim Mahen von Iialmgut (Impact cutting in mowing forage crops). *Hohenheimer Arbeiten* 62.

Dyson, F. J. 1989. *Infinite In All Directions*. VIII ed. Gretna, Louisiana: Pelican.

Fike, J. H., D. J. Parrish, D. D. Wolf, J. A. Balasko, J. T. Green Jr., M. Rasnake and J. H. Reynolds. 2006. Switchgrass production for the upper southeastern USA: Influence of cultivar and cutting frequency on biomass yields. *Biomass and Bioenergy* 30(3): 207-213.

Giampietro, M., S. Ulgiati and D. Pimentel. 1997. Feasibility of large-scale biofuel production. *Bioscience* 47(9): 587-600.

Greenlees, W., H. Hanna, K. Shinnars, S. Marley and T. Bailey. 2000. A comparison of four mower conditioners on drying rate and leaf loss in alfalfa and grass. *Applied Engineering in Agriculture* 16(1): 15-21.

Guarnieri, A., C. Maglioni and G. Molari. 2007. Dynamic analysis of reciprocating single-blade cutter bars. *Transactions of the ASABE* 50(3): 755-764.

Harbage, R. P. and R. V. Morr. 1962. Development and Design of a Ten-Foot Mower. *Agricultural Engineering* 43(April): 208.

Heaton, E. A., J. Clifton-Brown, T. B. Voigt, M. B. Jones and S. P. Long. 2004. Miscanthus for renewable energy generation: European Union experience and projections for Illinois. *Mitigation and Adaptation Strategies for Global Change* 9(4): 433-451.

Hohenstein, W. G. and L. L. Wright. 1994. Biomass energy production in the United States: an overview. *Biomass and Bioenergy* 6(3): 161-173.

Hoy, R. M., M. F. Kocher, V. I. Adamchuk and J. A. Smith. 2007.

Nebraska Summary 563 John Deere 7930 Autoquad-Plus Diesel. 1896(July 10): .

Igathinathane, C., A. R. Womac and S. Sokhansanj. 2010. Corn stalk orientation effect on mechanical cutting. *Biosystems Engineering* 107(2): 97-106.

Karpenko, A. N. 1968. Cutters. In *Agricultural machines (Sel'skokhozyaistvennyye mashiny)*, Chapter 21. ed. L. M. Hugues, Jerusalem: Israel Program for Scientific Translations.

Kepner, R. A. 1952. Analysis of the Cutting Action of a Mower. *Agricultural Engineering* 33(11): 693.

Kristensen, E. F. 2003. Harvesting and handling of miscanthus - Danish experiences. In *IEA-Bioenergy Task 30*, 41.

Kroes, S. and H. Harris. 1996. *Cutting forces and energy during an impact cut of sugarcane stalks*. In *Paper 96A-035*, Madrid: European Agricultural Engineering.

Lewandowski, I. and A. Heinz. 2003. Delayed harvest of miscanthus - Influences on biomass quantity and quality and environmental impacts of energy production. *European Journal of Agronomy* 19(1): 45-63.

Lewandowski, I., J. M. O. Scurlock, E. Lindvall and M. Christou. 2003. The development and current status of perennial rhizomatous grasses as energy crops in the US and Europe. *Biomass and Bioenergy* 25(4): 335-361.

Lewandowski, I., J. C. Clifton-Brown, J. M. O. Scurlock and W. Huisman. 2000. Miscanthus: European experience with a novel energy crop. *Biomass and Bioenergy* 19(4): 209-227.

National Agriculture Compliance Assistance Center. 2012. Major Crops Grown in the United States. US Environmental Protection Agency. Available at:

<http://www.epa.gov/oecaagct/ag101/cropmajor.html>. Accessed June/3 2012.

McGechan, M. B. 1989. A review of losses arising during conservation of grass forage: Part 1, field losses. *Journal of Agricultural Engineering Research* 44(C): 1-21.

Mcrandal, D. M. and P. B. McNulty. 1978a. Impact Cutting Behavior of Forage Crops .1. Mathematical-Models and Laboratory Tests. *Journal of Agricultural Engineering Research* 23(3): 313-328.

Mcrandal, D. M. and P. B. McNulty. 1978b. Impact Cutting Behavior of Forage Crops .2. Field-Tests. *Journal of Agricultural Engineering Research* 23(3): 329-338.

Monroe, G. E. and D. L. Peterson. 1977. Oversize Mower Cutterbar for Pruning Trees. *Transactions of the American Society of Agricultural Engineers* 20(4): 606-609.

New Holland. 2009. *BB9080 Operator's Manual*. 1st ed. New Holland, PA: CNH.

O'dogherty, M. J. and G. E. Gale. 1991. Laboratory Studies of the Effect of Blade Parameters and Stem Configuration on the Dynamics of Cutting Grass. *Journal of Agricultural Engineering Research* 49(2): 99-111.

O'dogherty, M. J. and G. E. Gale. 1991. Laboratory Studies of the Dynamic Behaviour of Grass, Straw and Polystyrene Tube During High-speed Cutting. *Journal of Agricultural Engineering Research* 49(C): 33-57.

O'Dogherty, M. J. and G. E. Gale. 1986. Laboratory Studies of the Cutting of Grass Stems. *Journal of Agricultural Engineering Research* 35(2): 115-129.

Perlack, R. D., L. L. Wright, A. F. Turhollow, R. L. Graham, B. J. Stokes and D. C. Erbach. 2005. Biomass as Feedstock for a Bioenergy and Bioproducts Industry : The Technical Feasibility of a Billion-ton Annual Supply.

Persson, S. 1987. *Mechanics of cutting plant material*. St. Joseph, Michigan: American Society of Agricultural Engineers.

Plinius Gaius, S. AD 77-79. *Naturalis Historiæ*. In 26. ed.

Prasad, J. and C. P. Gupta. 1975. Mechanical Properties of Maize Stalk as Related to Harvesting. *Journal of Agricultural Engineering Research* 20(1): 79-87.

Pyter, R., T. Voigt, E. Heaton, F. Dohleman and S. Long. 2007. Growing Giant Miscanthus in Illinois .

Rees, D. V. H. 1982. A discussion of Sources of Dry Matter Loss During the Process of Haymaking. *Journal of Agricultural Engineering Research* 27(6): 469-479.

Richard, T. L. 2010. Challenges in Scaling Up Biofuels Infrastructure. *Science* 329(5993): 793-796.

Rotz, C. A. and D. J. Sprott. 1984. Drying Rates, Losses and Fuel Requirements for Mowing and Conditioning Alfalfa. *Transactions of the American Society of Agricultural Engineers* 27(3): 715-720.

Ruina, A. and R. Pratap. 2012. *Introduction to Statics and Dynamics*. Oxford University Press (Preprint).

Shinners, K. J., G. C. Boettcher, R. E. Muck, P. J. Weimer and M. D. Casler. 2010. Harvest and Storage of Two Perennial Grasses as Biomass Feedstocks. *Transactions of the Asabe* 53(2): 359-370.

Srivastava, A. K., C. E. Goering and R. P. Rohrbach. 2006. Hay and Forage Harvesting. In *Engineering principles of agricultural machines*, 325. ed. Anonymous , St. Joseph, Michigan: American Society of Agricultural Engineers.

Stone, A. A. 1977. Mowers. In *Machines for Power Farming*, 387. ed. Anonymous , New York: Wiley.

Taghijarah, H., H. Ahmadi, M. Ghahderijani and M. Tavakoli. 2011. Shearing Characteristics of Sugar Cane (*Saccharum officinarum* L.) Stalks as a Function of the Rate of the Applied Force.

Australian Journal of Crop Science 5(6): 630-634.

Thomason, W. E., W. R. Raun, G. V. Johnson, C. M. Taliaferro, K. W. Freeman, K. J. Wynn and R. W. Mullen. 2004. Switchgrass Response to Harvest Frequency and Time and Rate of Applied

Nitrogen. *Journal of Plant Nutrition* 27(7): 1199-1226.

Tilman, D., J. Hill and C. Lehman. 2006. Carbon-negative Biofuels from Low-Input High-Diversity Grassland Biomass. *Science* 314(5805): 1598-1600.

Tuck, C. R., M. J. O'Dogherty, D. E. Baker and G. E. Gale. 1991a. Field Experiments to Study the Performance of Toothed Disk Mowing Mechanisms. *Journal of Agricultural Engineering*

Research 50(2): 93-106.

Tuck, C. R., M. J. O'Dogherty, D. E. Baker and G. E. Gale. 1991b. Laboratory Studies of the Performance Characteristics of Mowing Mechanisms. *Journal of Agricultural Engineering*

Research 50(C): 61-80.

Venuto, B. C. and J. A. Daniel. 2010. Biomass feedstock harvest from conservation reserve program land in Northwestern Oklahoma. *Crop Science* 50(2): 737-743.

Vogel, K. P., G. Sarath, A. J. Saathoff and R. B. Mitchell. 2010. Switchgrass. In *Energy Crops*, 426. ed. N. G. Halford and Karp, A., Cambridge, MA: Royal Society of Chemistry.

Vogel, K. P. 1996. Energy production from forages (or American agriculture-Back to the future).

Journal of Soil and Water Conservation 51(2): 137-139.

Vogel, K. P., J. J. Brejda, D. T. Walters and D. R. Buxton. 2002. Switchgrass biomass production in the midwest USA: Harvest and nitrogen management. *Agronomy Journal* 94(3): 413-420.

Voigt, T., G. Bollero, D. K. Lee, S. Long, M. Dietze, T. Bratsch and G. Kling. 2010. Feedstock Production/Agronomy Program. Energy Biosciences Institute. Available at: http://www.energybiosciencesinstitute.org/index.php?option=com_content&task=view&id=129&Itemid=20. Accessed March 15 2011.

Yu, M., A. R. Womac, C. Igathinathane, P. D. Ayers and M. J. Buschermohle. 2006. Switchgrass Ultimate Stresses at Typical Biomass Conditions Available for Processing. *Biomass and Bioenergy* 30(3): 214-219.

APPENDIX A: MEASUREMENT RESULTS

A.1 Summarized Results of Harvesting Field Trials

Table 4 Yield, area, and groundspeed measured during in-field performance trials.

Task	Machine	Crop^A	Yield^B (Mg DM/ha)	Area^C (ha)	Harvester Speed (km/h)
Baling	BB9080R	mxg	9.18 (7.02)	8.26	6.43 (2.67)
Baling	BB9080R	pg	5.85 (1.60)	4.50	6.71 (0.96)
Baling	BB9080R	swg	5.89 (2.82)	6.36	4.63 (2.81)
Mowing	Disc Moco	mxg	10.65 (7.59)	2.55	10.04 (2.65)
Mowing	Disc Moco	swg	7.44 (2.48)	1.10	12.76 (2.95)
Mowing	SP Rotary	mxg	10.40 (3.51)	8.49	6.61 (1.68)
Mowing	SP Rotary	swg	4.53 (0.82)	1.68	10.91 (1.76)
Mowing	SP Sickle	mxg	7.55 NA ^D	1.39	5.99 (1.22)
Mowing	SP Sickle	pg	6.23 (1.19)	5.49	7.95 (1.00)
Mowing	SP Sickle	swg	9.87 (0.82)	8.95	7.39 (1.28)

^A Crop abbreviations: mxg – miscanthus, swg – switchgrass, and pg – tallgrass prairie.

^B Moisture content was not collected in every plot (some results are assumed from similar conditions).

^C Area covered by harvester during data acquisition (based on number of data points recorded at 1 Hz).

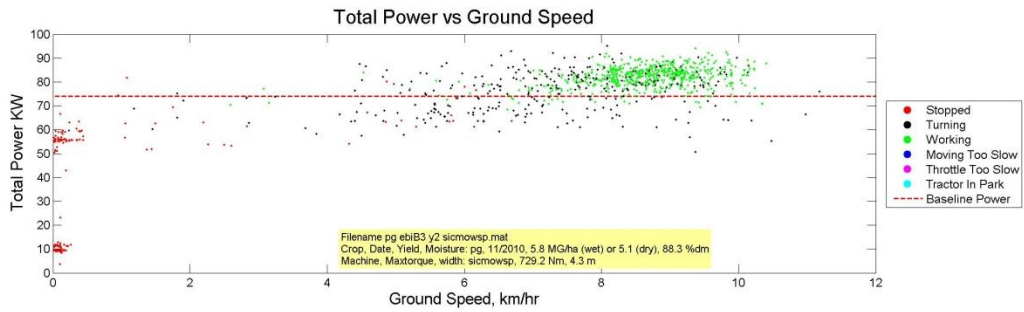
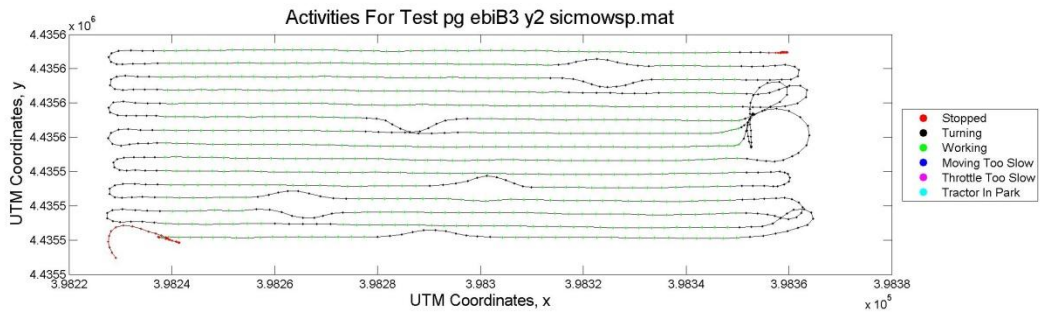
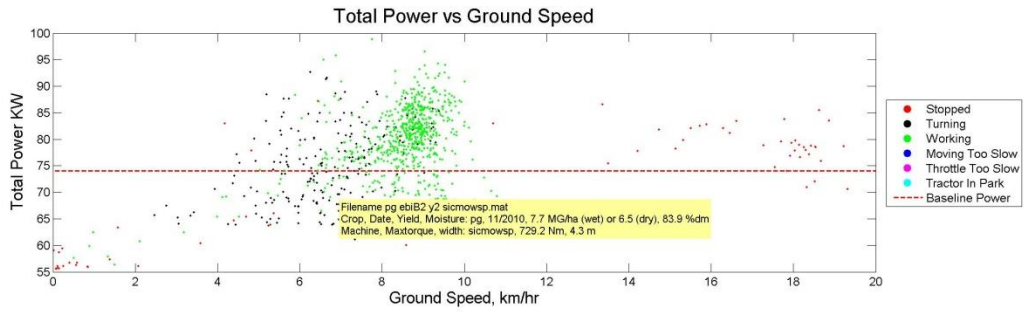
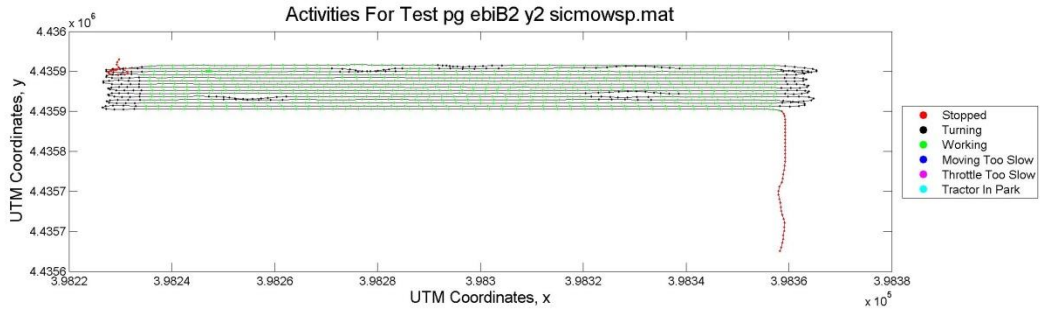
^D Only one plot was considered, so standard deviation is excluded.

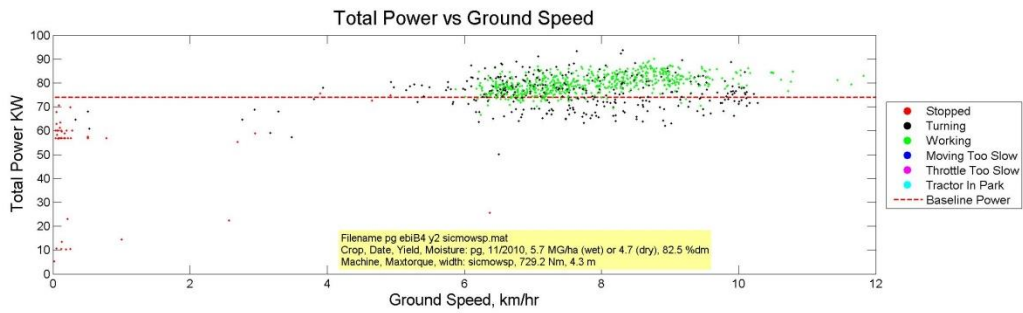
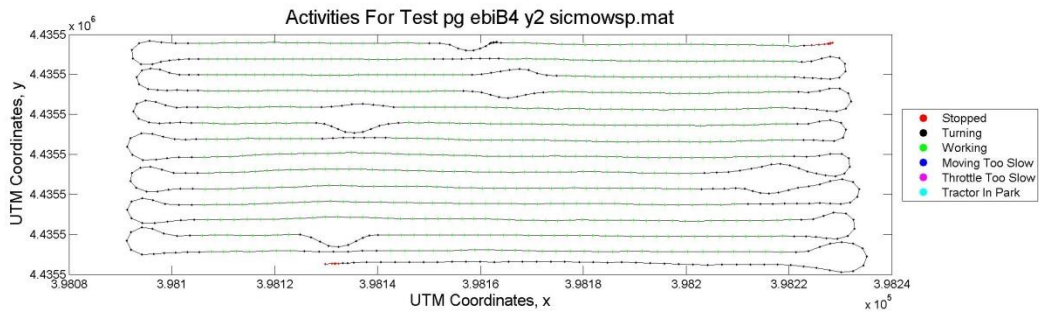
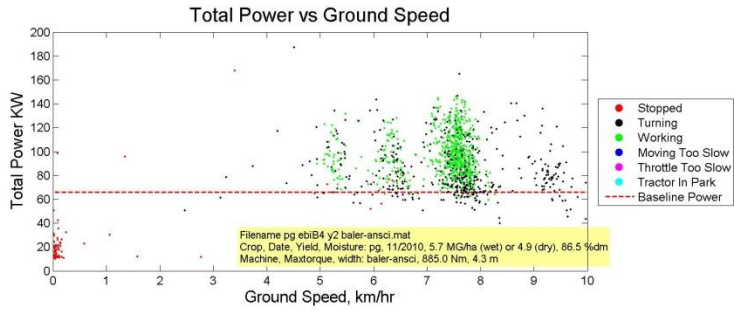
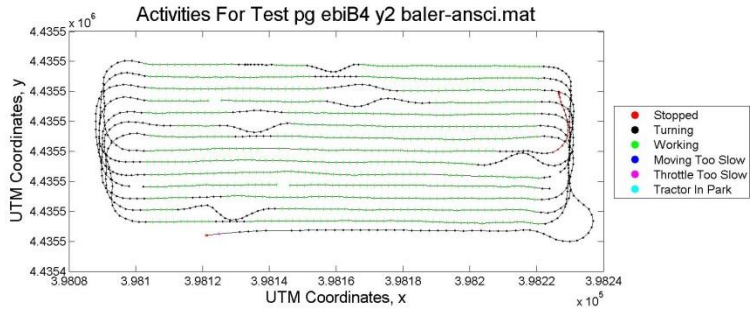
Table 5 Engine power and harvesting energy measured during in-field performance trials.

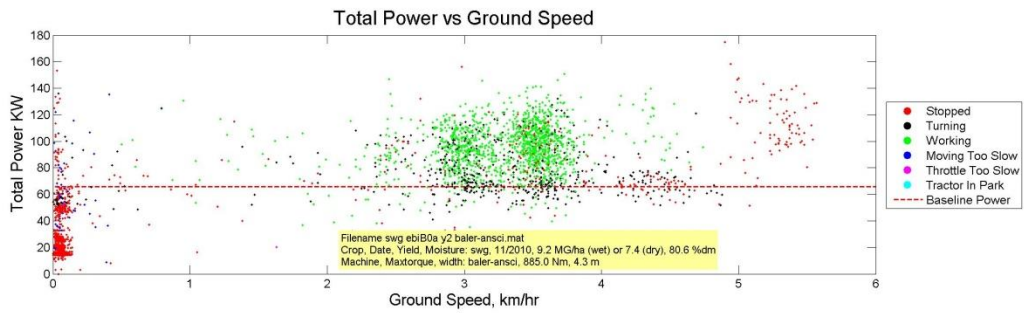
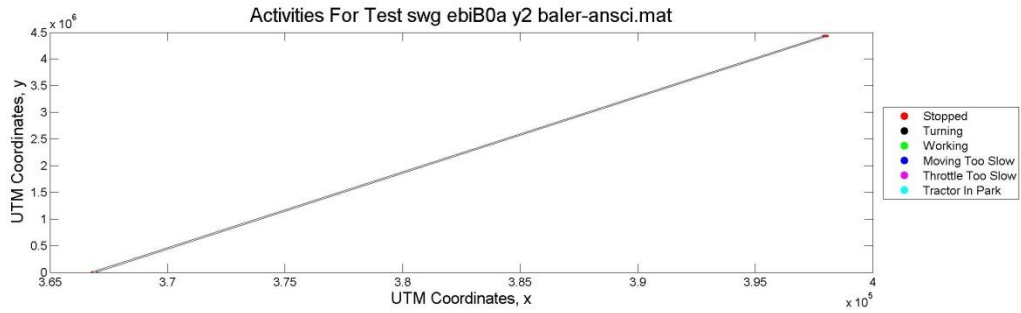
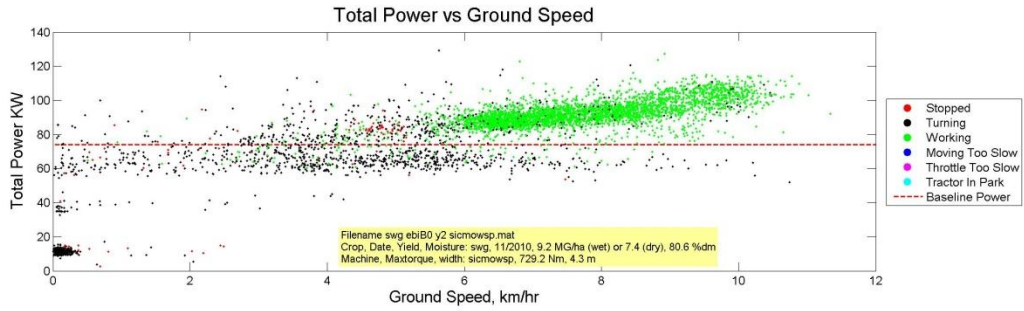
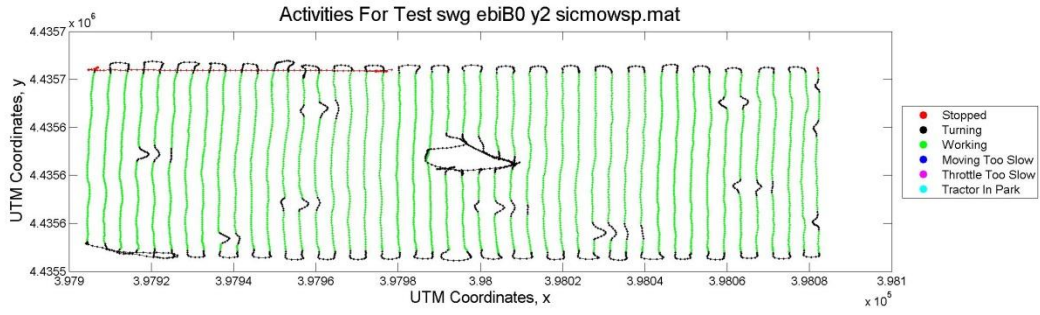
Task	Machine	Crop	Engine Power^A (kW)	Harvest Energy^A (MJ/Mg)
Baling	BB9080R	mxg	82.33 (23.70)	18.26 (17.56)
Baling	BB9080R	pg	67.83 (13.34)	15.15 (4.16)
Baling	BB9080R	swg	65.60 (12.15)	21.25 (8.93)
Mowing	Disc Moco	mxg	68.18 (13.69)	12.27 (10.10)
Mowing	Disc Moco	swg	65.04 (12.81)	9.51 (3.27)
Mowing	SP Rotary	mxg	90.42 (8.95)	15.82 (4.97)
Mowing	SP Rotary	swg	117.29 (12.92)	23.03 (4.86)
Mowing	SP Sickle	mxg	65.37 (4.50)	15.40 (7.65)
Mowing	SP Sickle	pg	69.43 (4.14)	13.30 (3.38)
Mowing	SP Sickle	swg	74.49 (7.51)	11.63 (2.85)

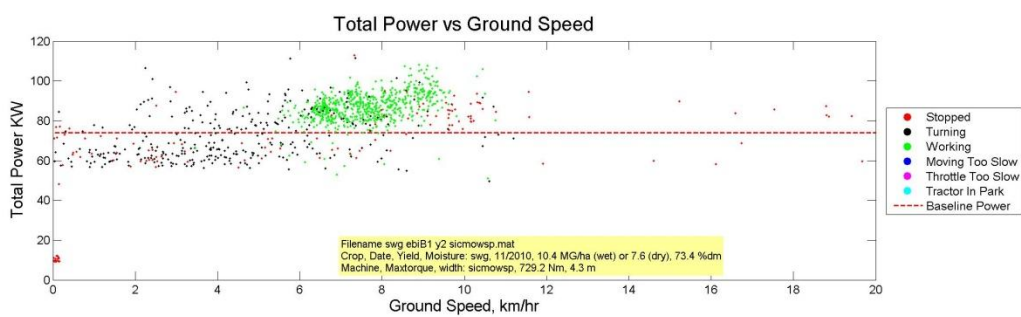
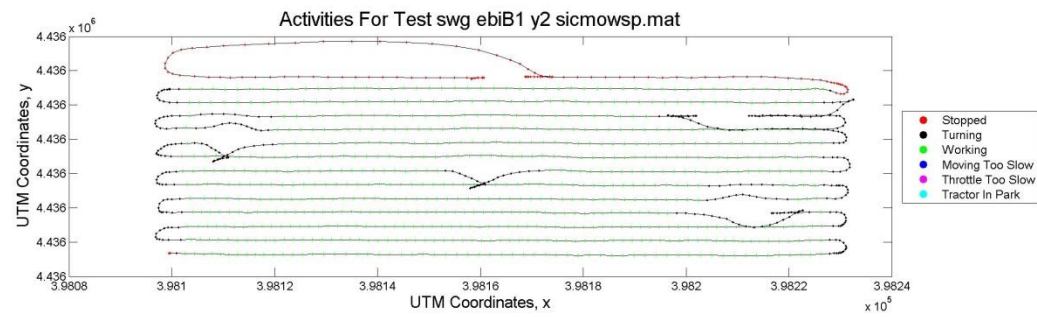
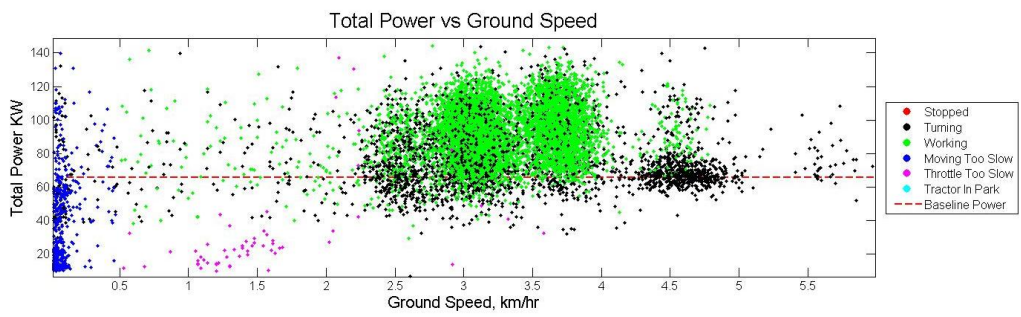
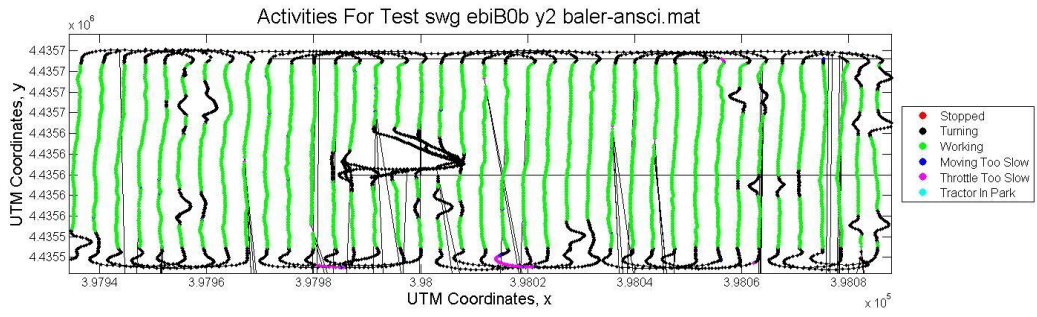
^ANumbers in parentheses indicate standard deviation.

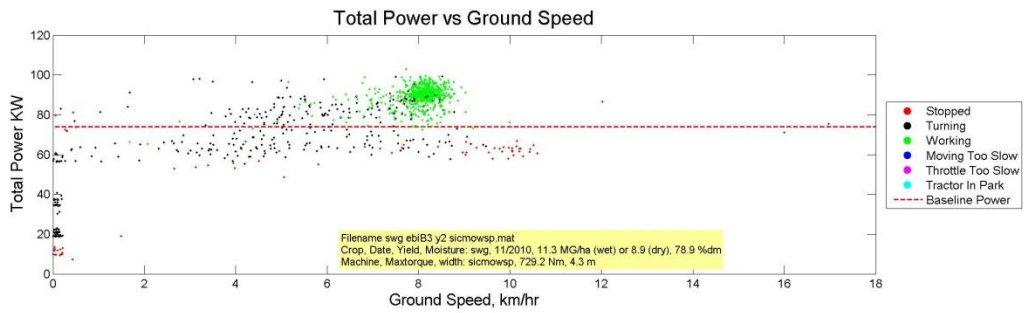
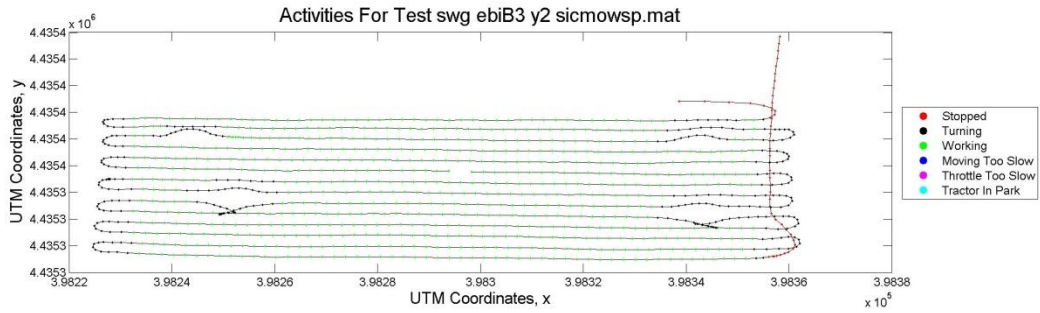
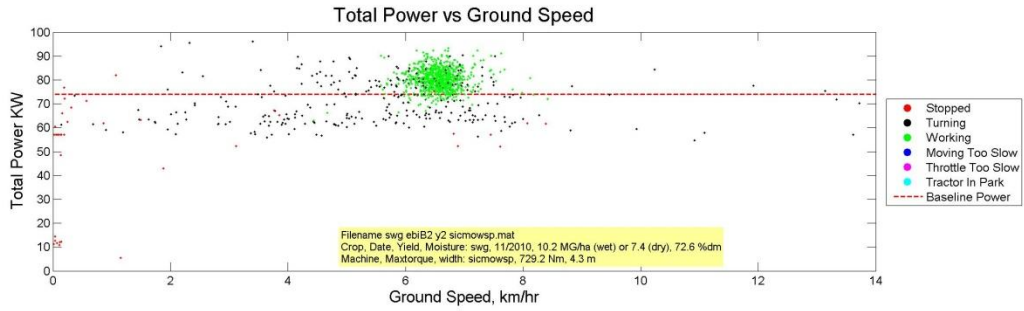
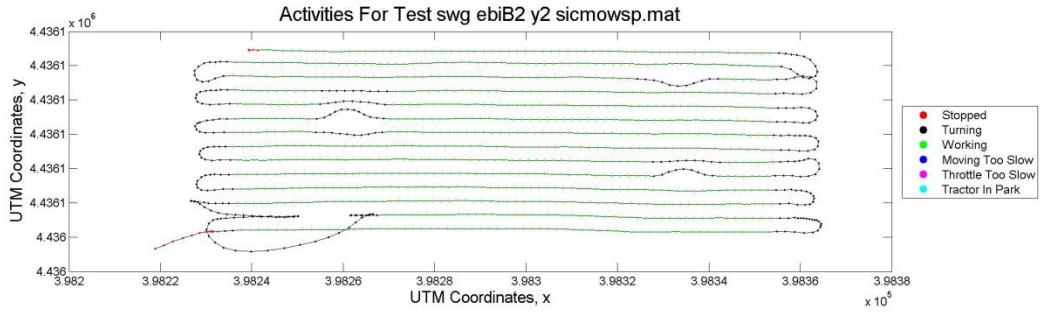
A.2 Data Files Recorded During Harvesting Field Trials

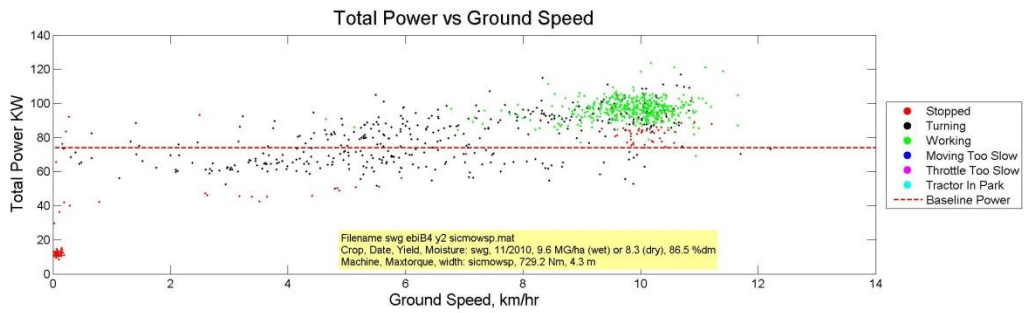
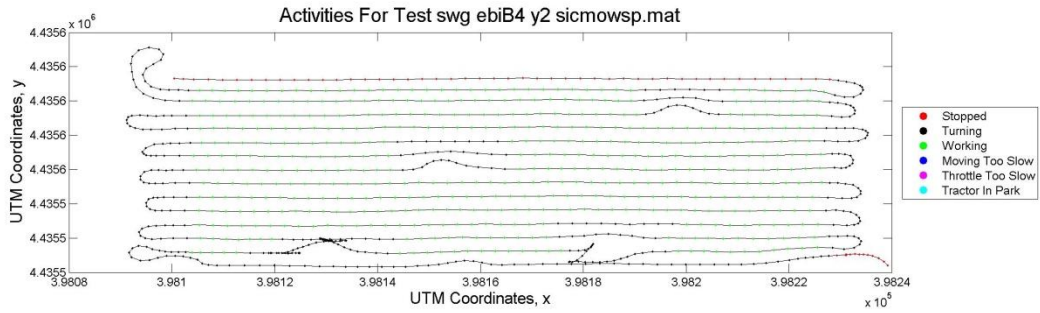
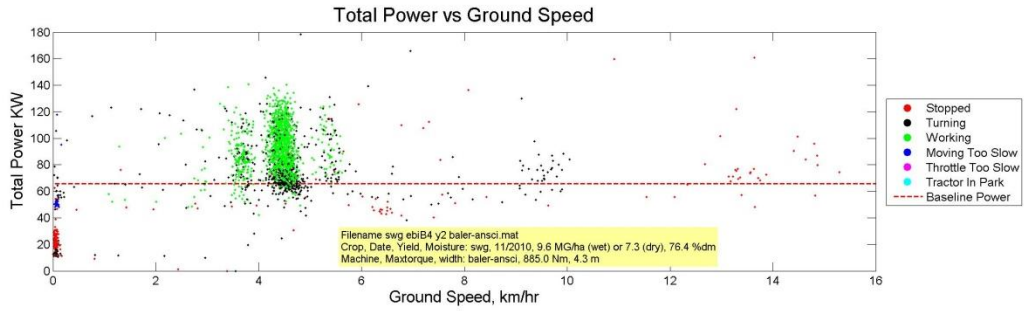
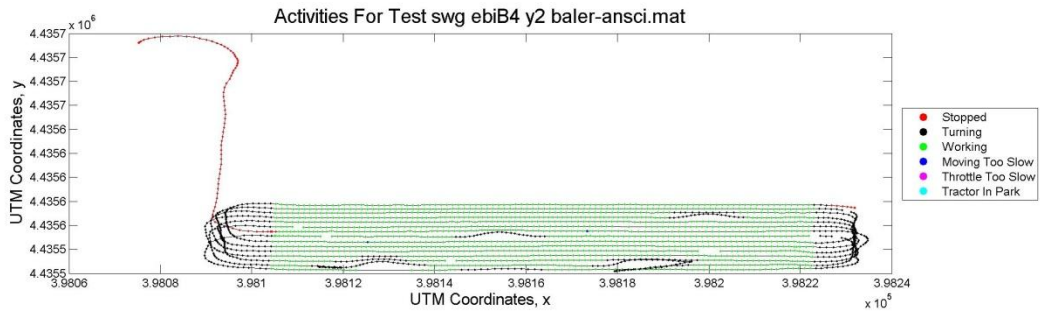


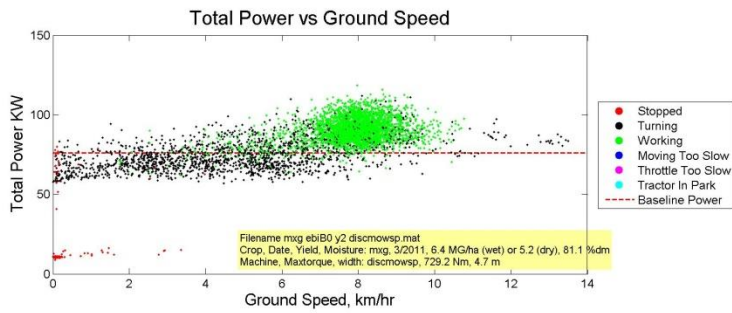
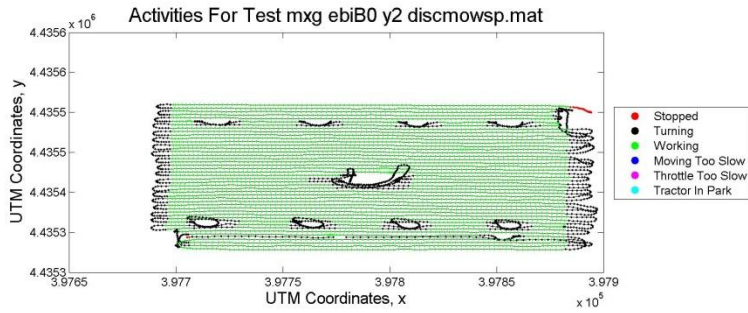
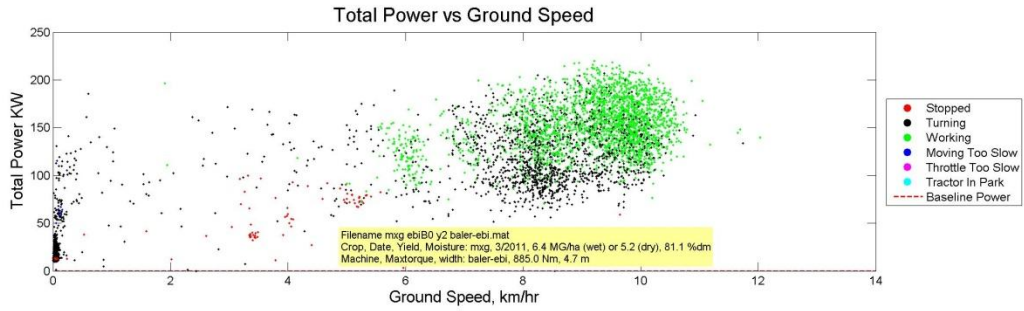
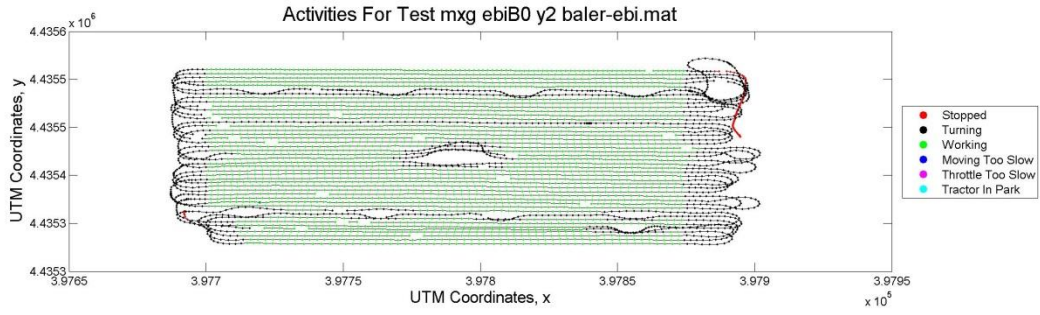


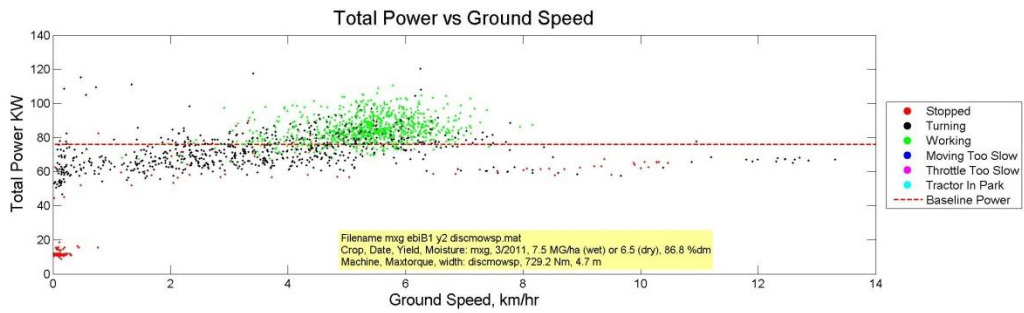
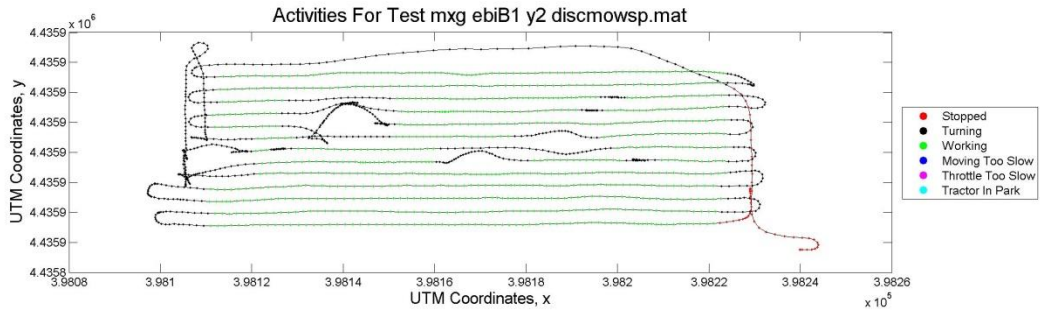
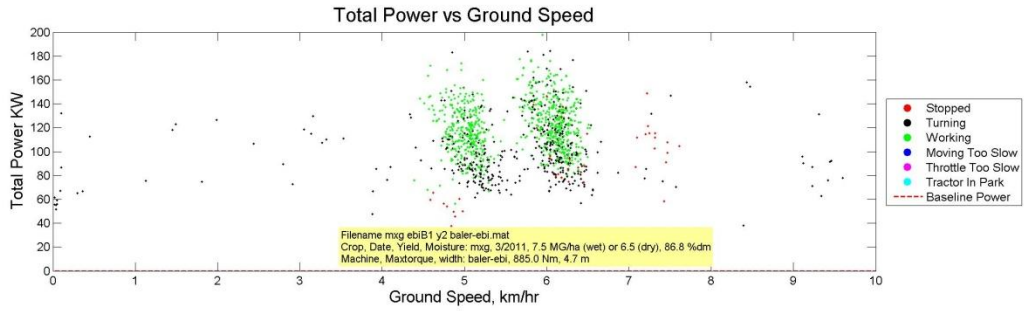
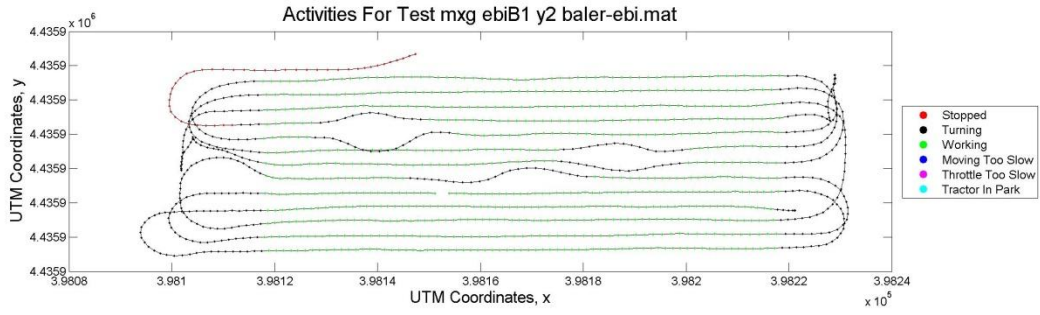


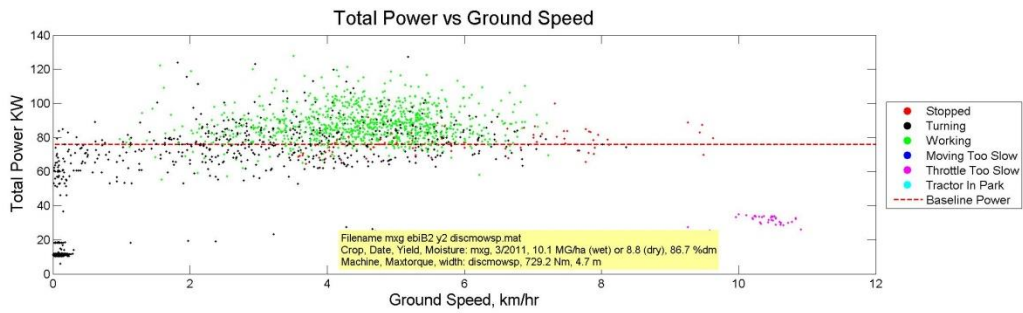
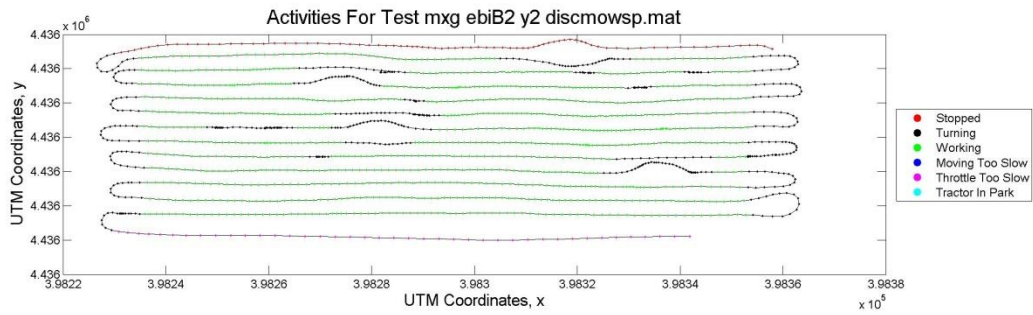
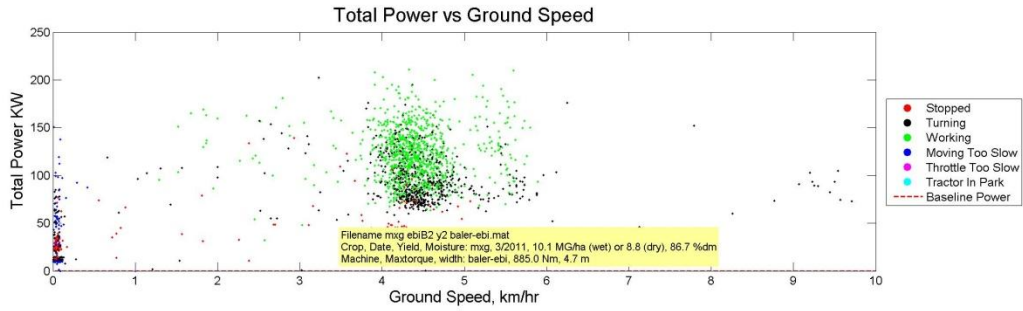
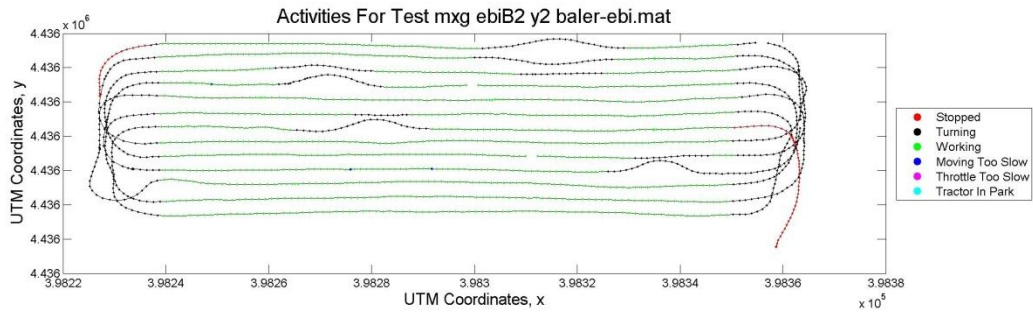


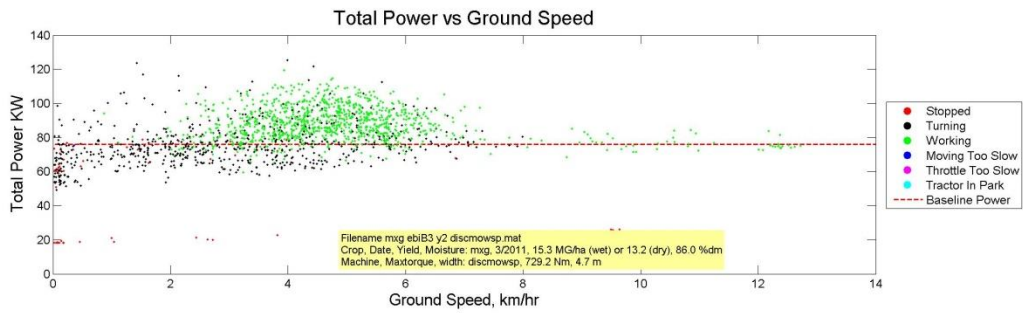
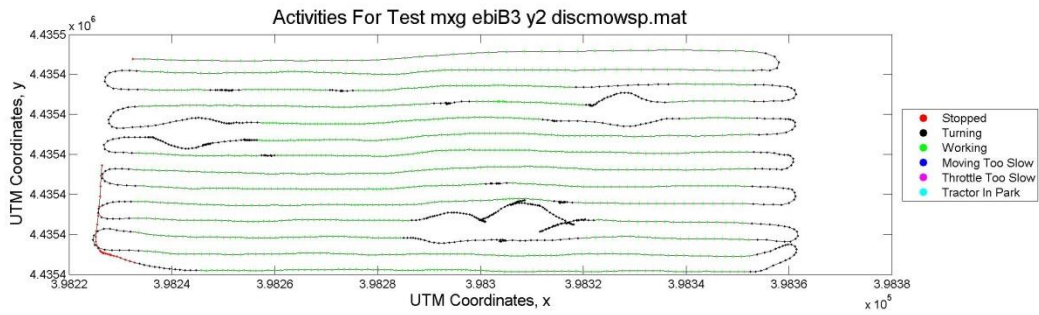
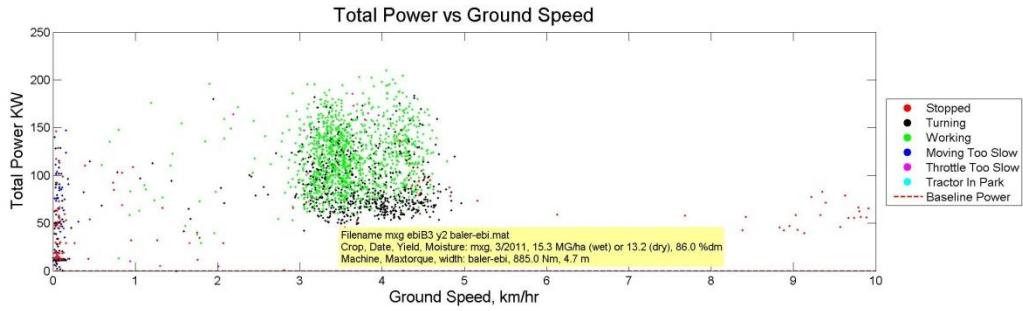
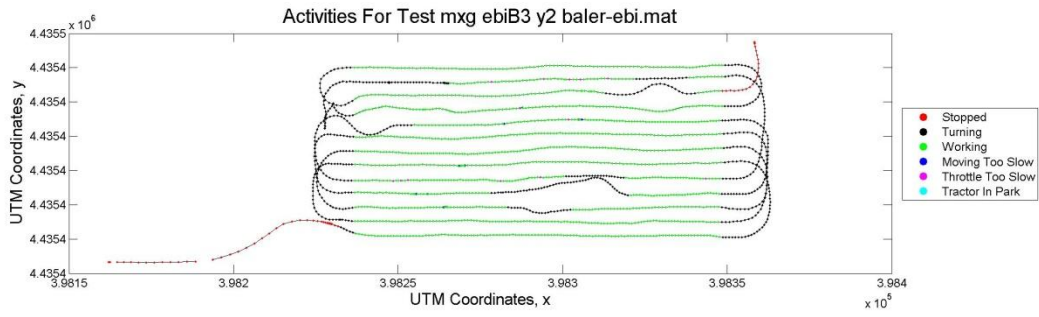


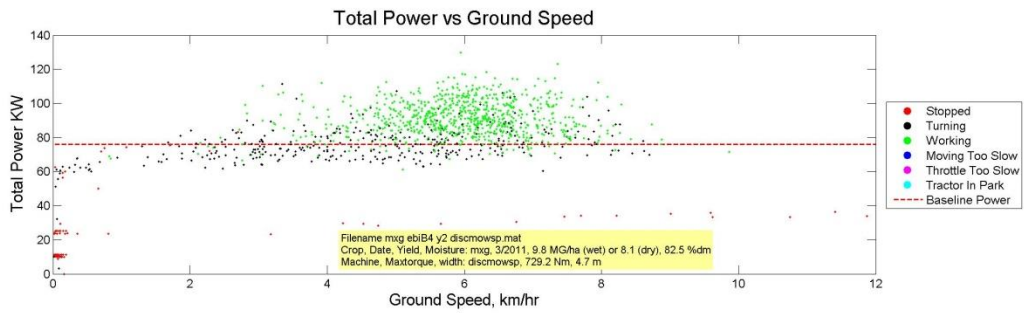
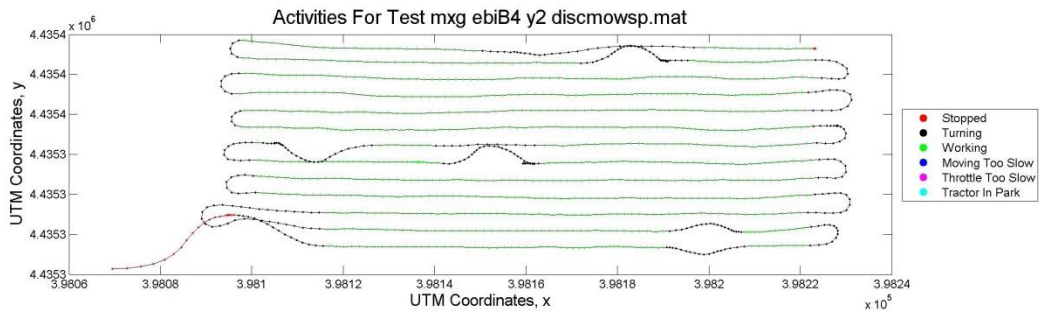
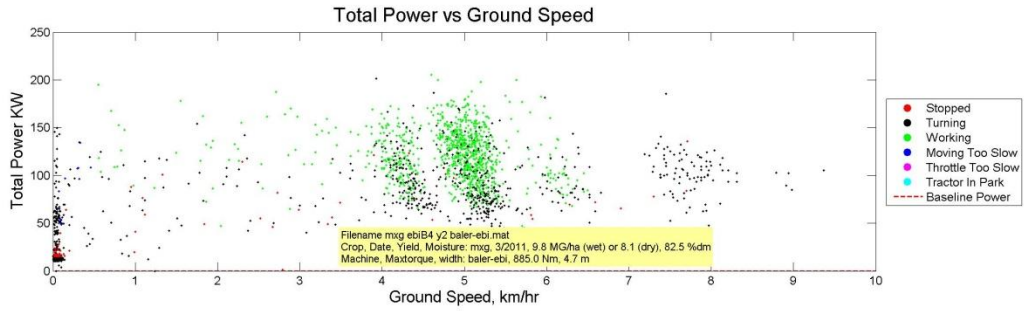
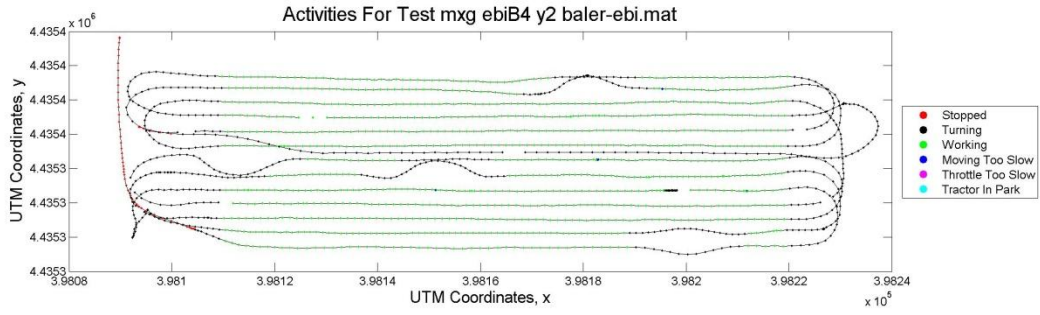


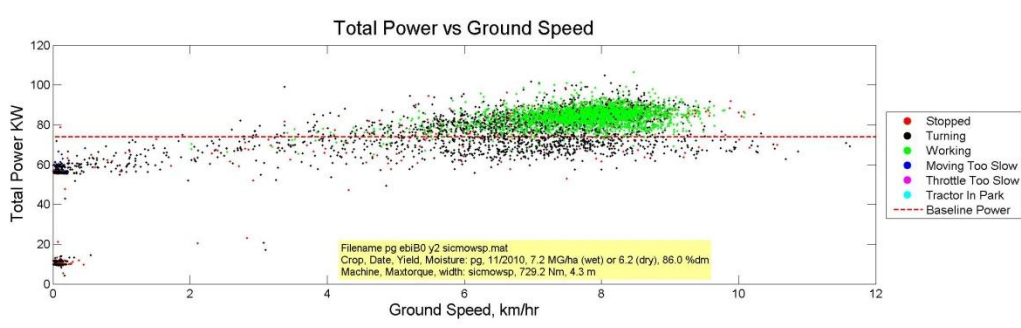
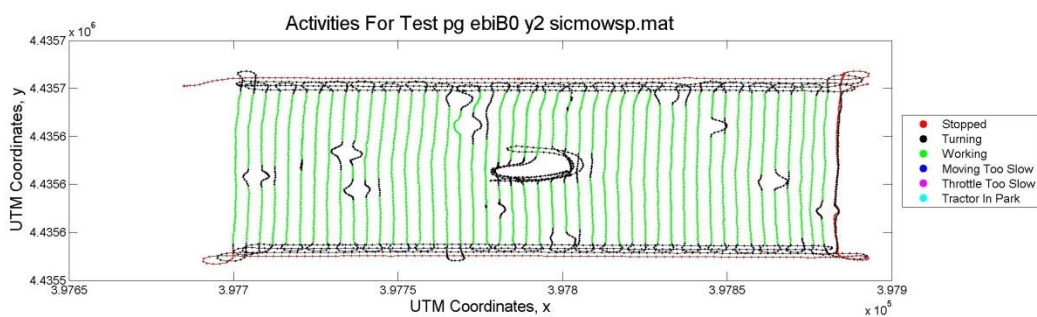
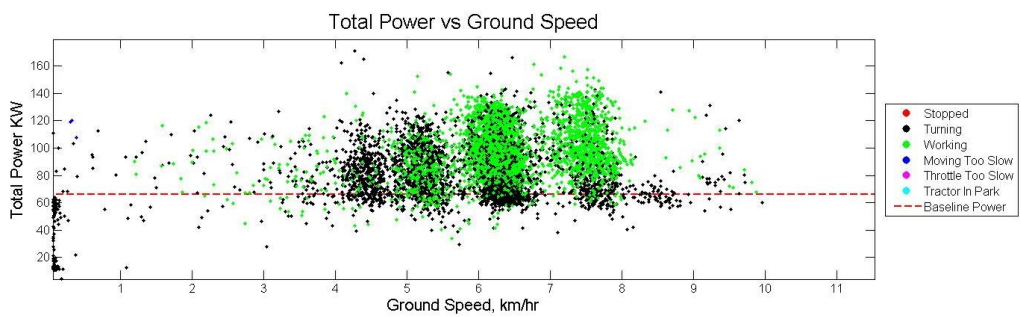
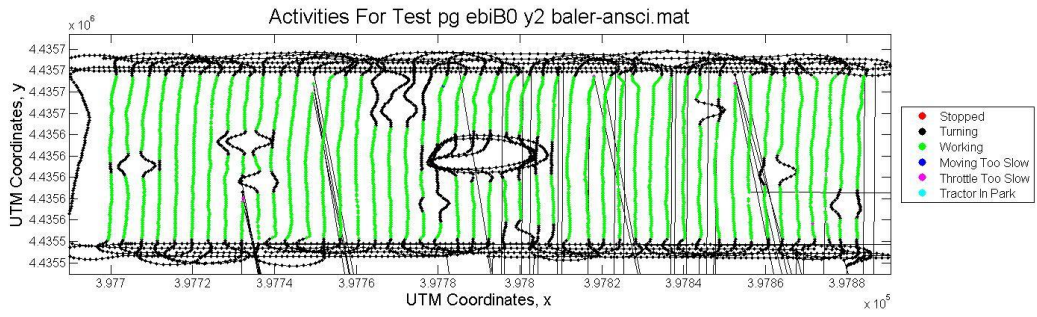


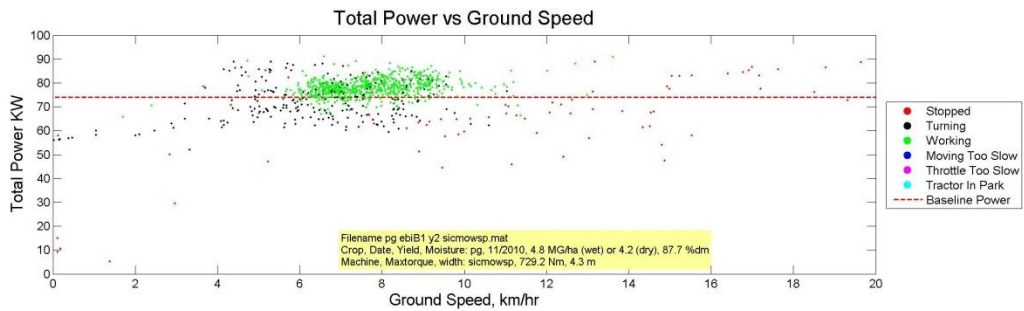
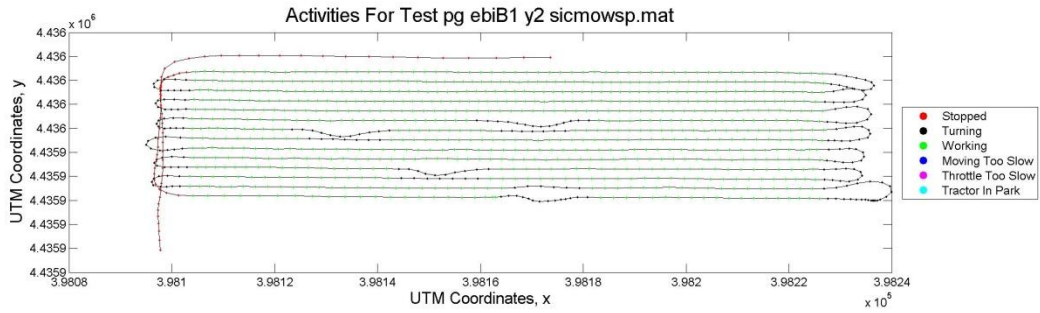
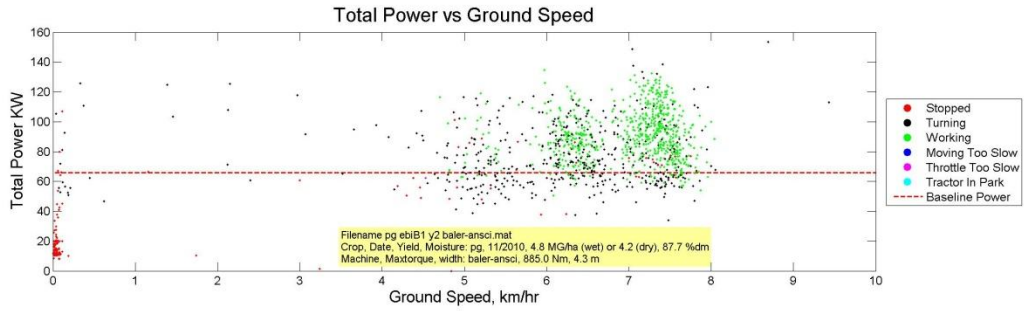
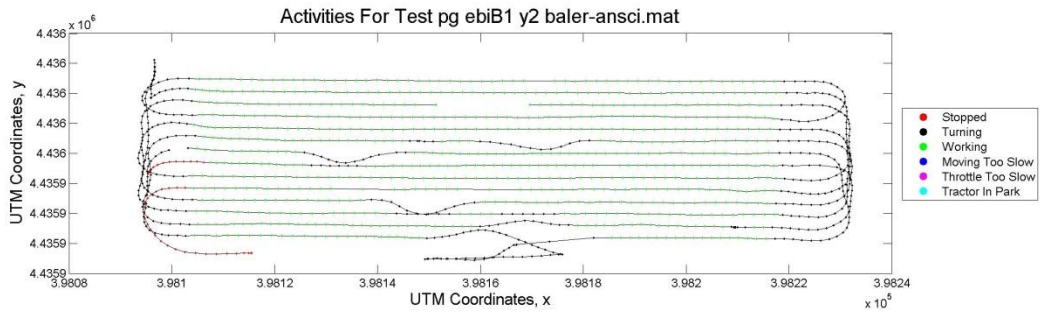


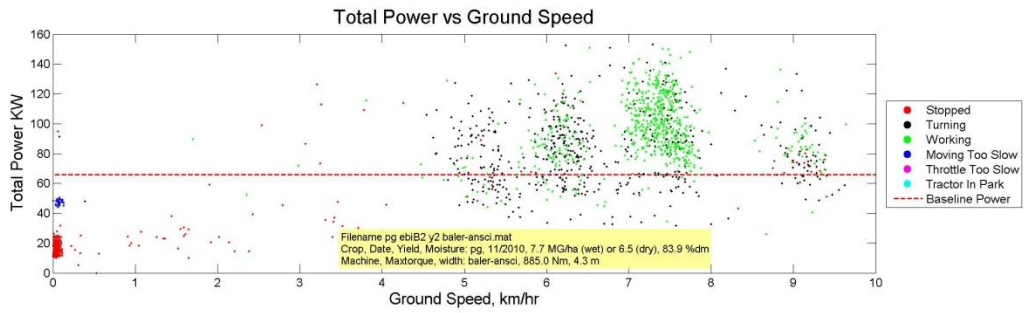
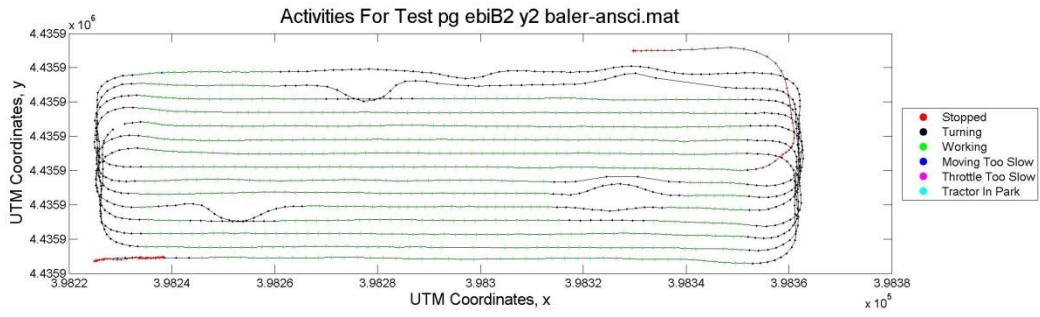













APPENDIX B: PROGRAMS USED IN DATA ACQUISITION

Evaluation
Harvest Monitor
C:\Users\pj18160\Desktop\Harvest Monitor 2010\Harvest Monitor.vi
Last modified on 11/13/2012 at 8:08 PM
Printed on 11/13/2012 at 8:13 PM

Page 1 


Connector Pane

Harvest Monitor



Use this template to build a producer/consumer design pattern. Use this template when you need to execute a proc such as data analysis, when a data source, such as a triggered acquisition, produces data at an uneven rate and you need to execute the process when the data becomes available.

Front Panel



Status and Control

Recording Start REC
Stop Recording

CAN Status GPS Status

GPS

Sample Time (ms) Port Settings

Local Time
Latitude
Longitude
Speed (km/hr)
Fix Type

Course (degrees)


CAN

CAN Settings

Engine Speed (RPM)	0
Actual Engine Torque (%)	0
Engine Torque Mode	0
Nominal Engine Frictional Torque	0
Instantaneous Fuel Economy	0
Average Fuel Economy	0
Fuel Rate (Determined by ECU)	0

Phil's Cell #

NATIONAL INSTRUMENTS
LabVIEW™ Evaluation Software

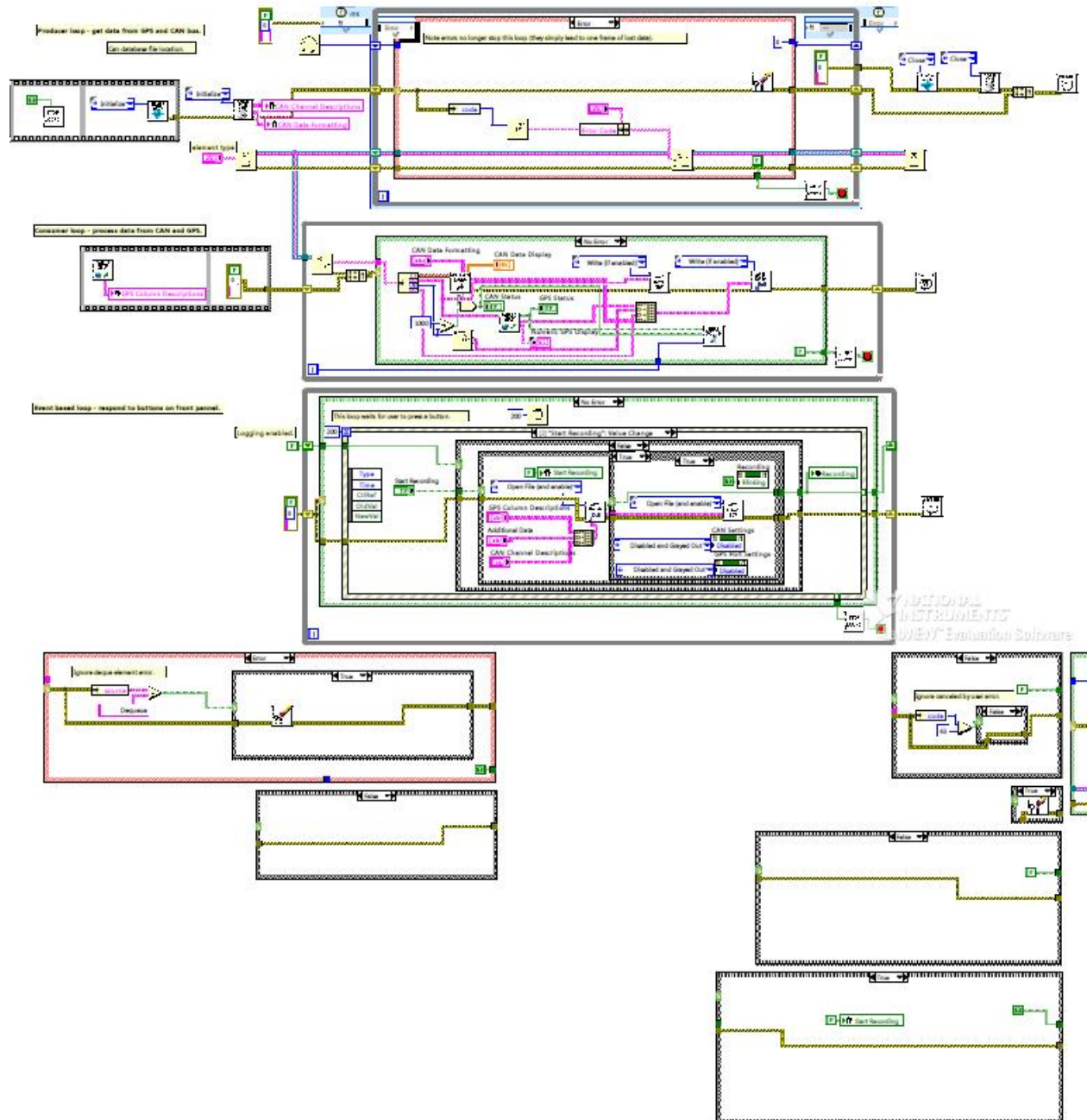
EXIT

C:\Users\pj18160\Desktop\Harvest Monitor 2010\Harvest Monitor.vi

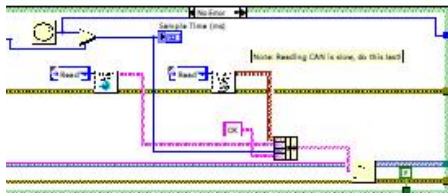
Last modified on 11/13/2012 at 8:08 PM

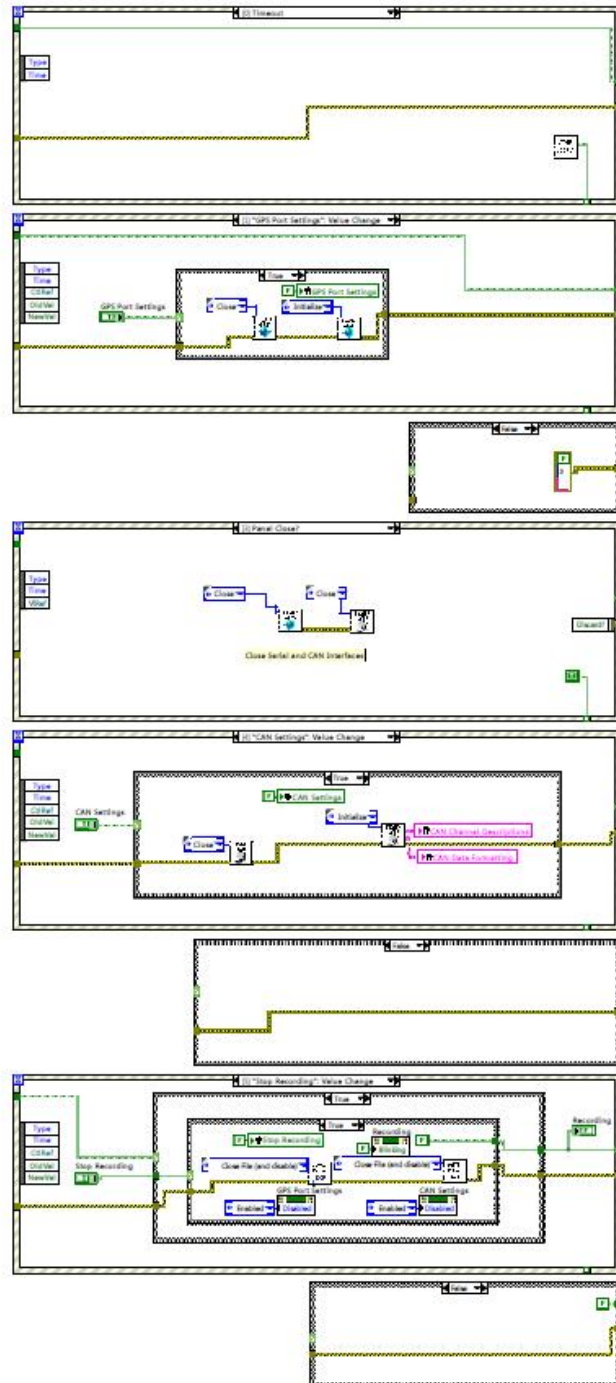
Printed on 11/13/2012 at 8:13 PM

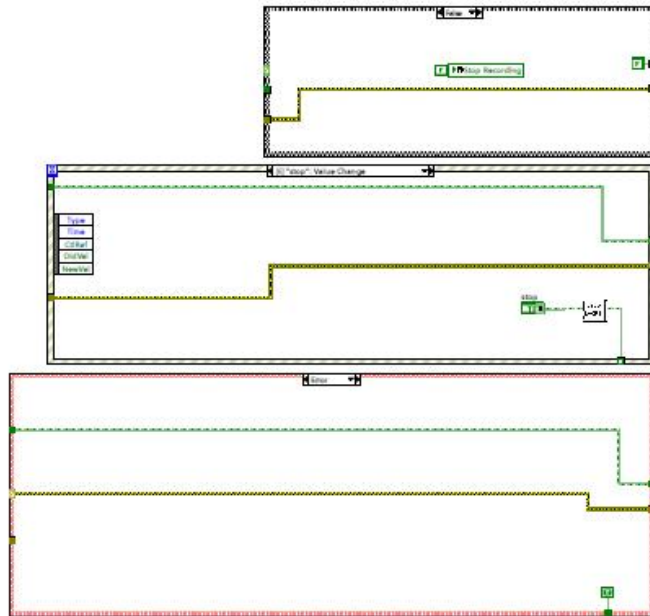
Block Diagram



Evaluation
Harvest Monitor
C:\Users\pj18160\Desktop\Harvest Monitor 2010\Harvest Monitor.vi
Last modified on 11/13/2012 at 8:08 PM
Printed on 11/13/2012 at 8:14 PM

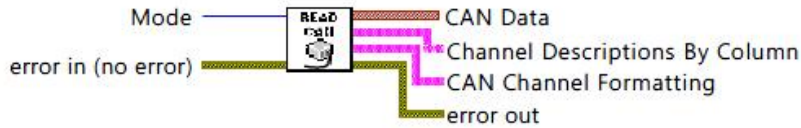






Connector Pane

Read CAN Data.vi



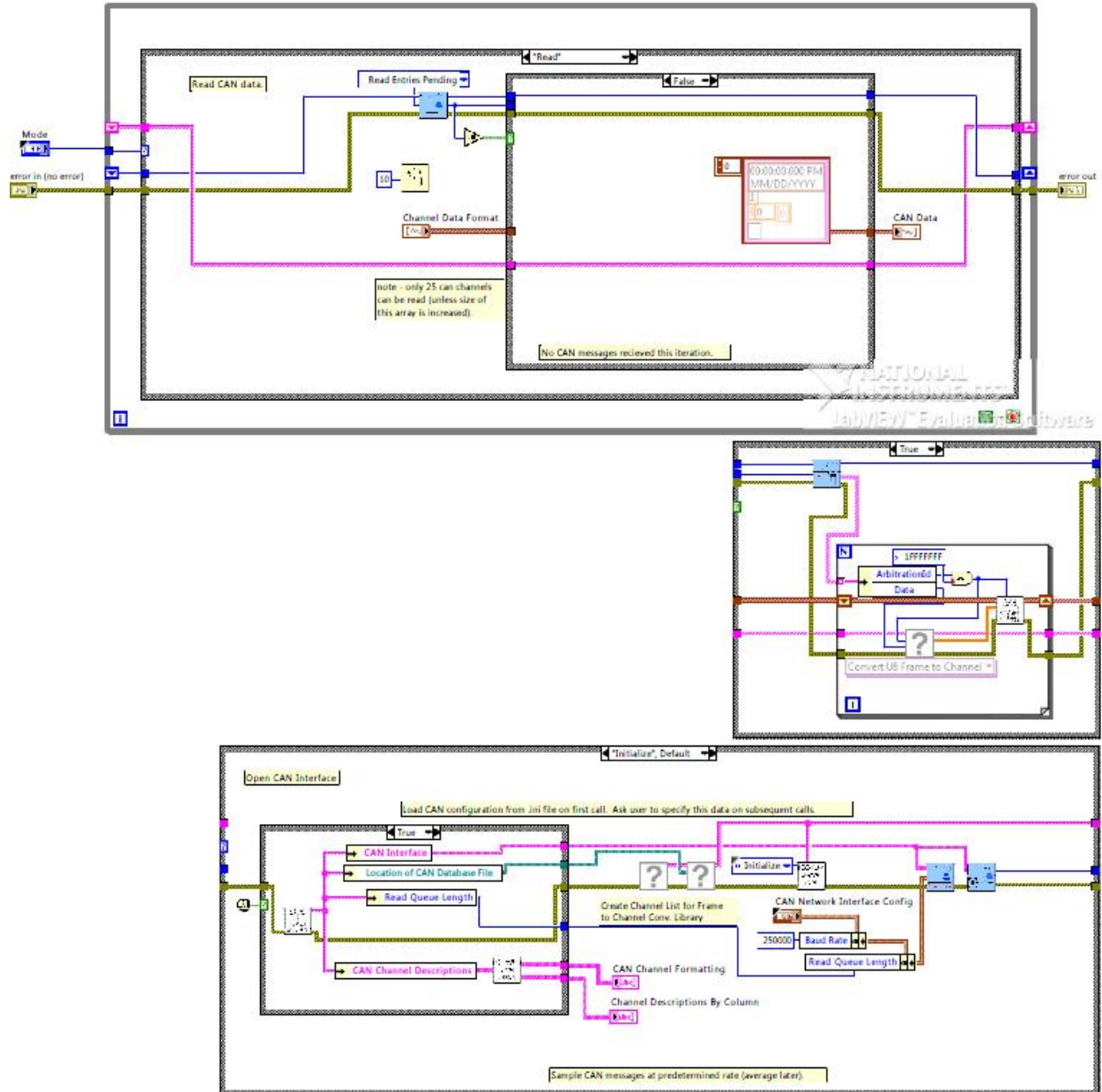
Front Panel

The front panel of the Read CAN Data.vi includes the following elements:

- Mode:** A dropdown menu currently set to "Initialize".
- Channel Descriptions By Column:** A numeric control set to 0.
- CAN Channel Formatting:** A numeric control set to 0.
- error in (no error):** A status indicator with a green checkmark and a numeric code set to 0.
- source:** A list box for selecting the data source.
- Channel Data Format:** A numeric control set to 24, and a table with columns for time (t0), date (dt), and a Y-axis (0).
- CAN Data:** A numeric control set to 0, and a table with columns for time (t0), date (dt), and a Y-axis (0).

At the bottom of the front panel, there is a note: "note - only 25 can channels can be read, unless default size of this array is increased." A watermark for "NATIONAL INSTRUMENTS LabVIEW Evaluation Software" is visible in the background.

Block Diagram

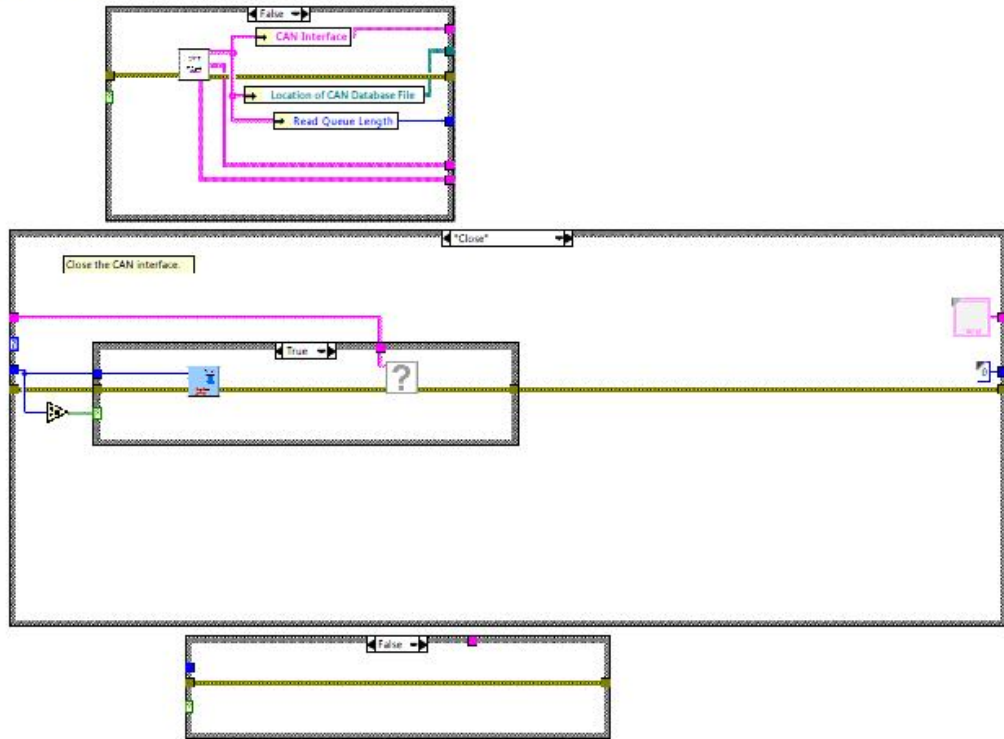




C:\Users\pj18160\Desktop\Harvest Monitor 2010\CAN\Read CAN Data.vi

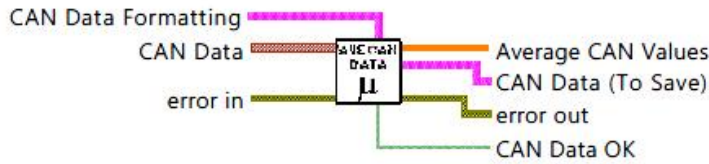
Last modified on 11/13/2012 at 8:08 PM

Printed on 11/13/2012 at 8:14 PM

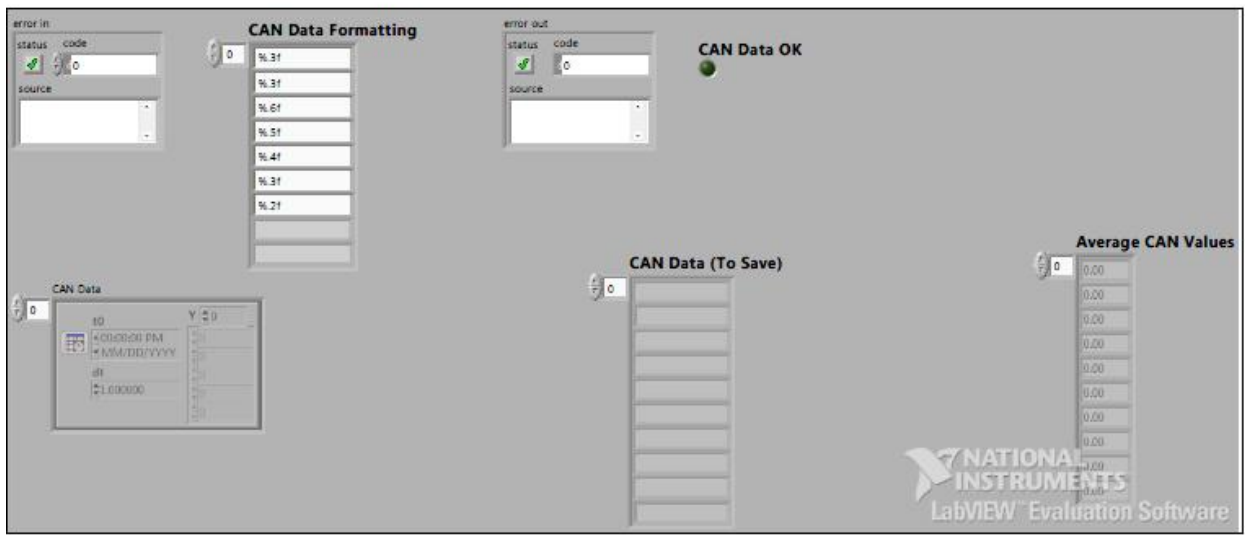


Connector Pane

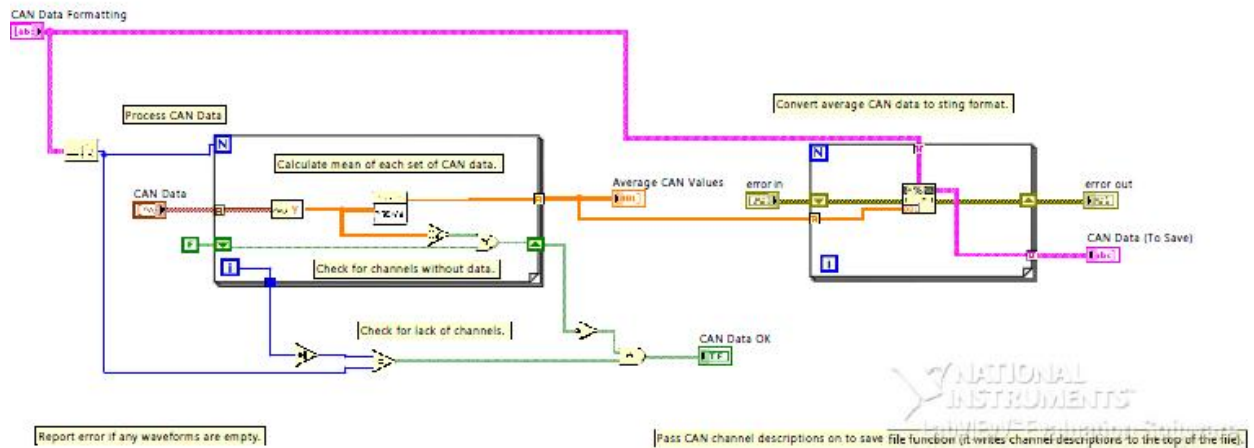
Process CAN Data.vi



Front Panel



Block Diagram

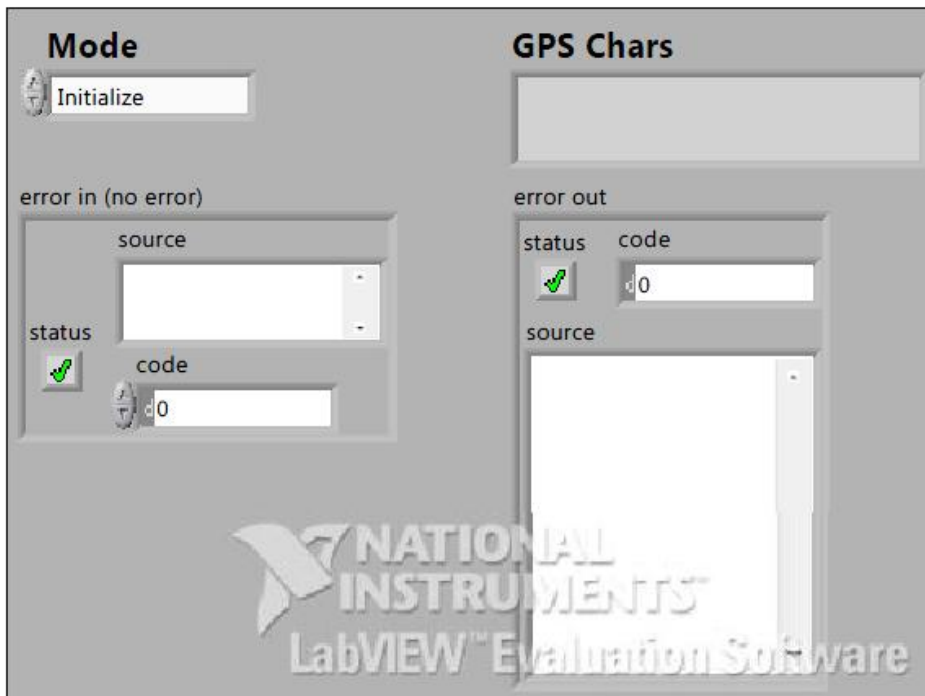


Connector Pane

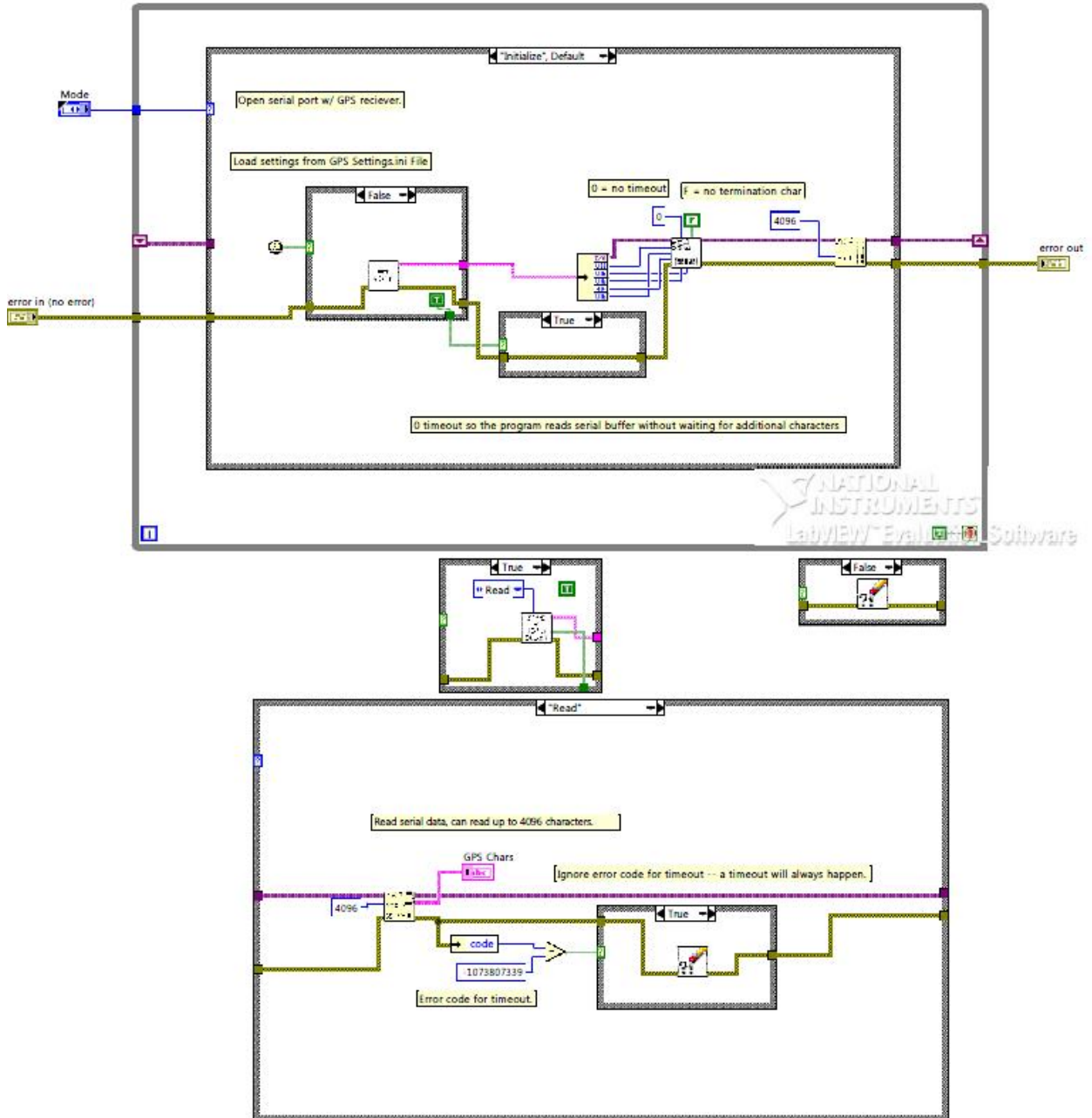
Read GPS Data.vi

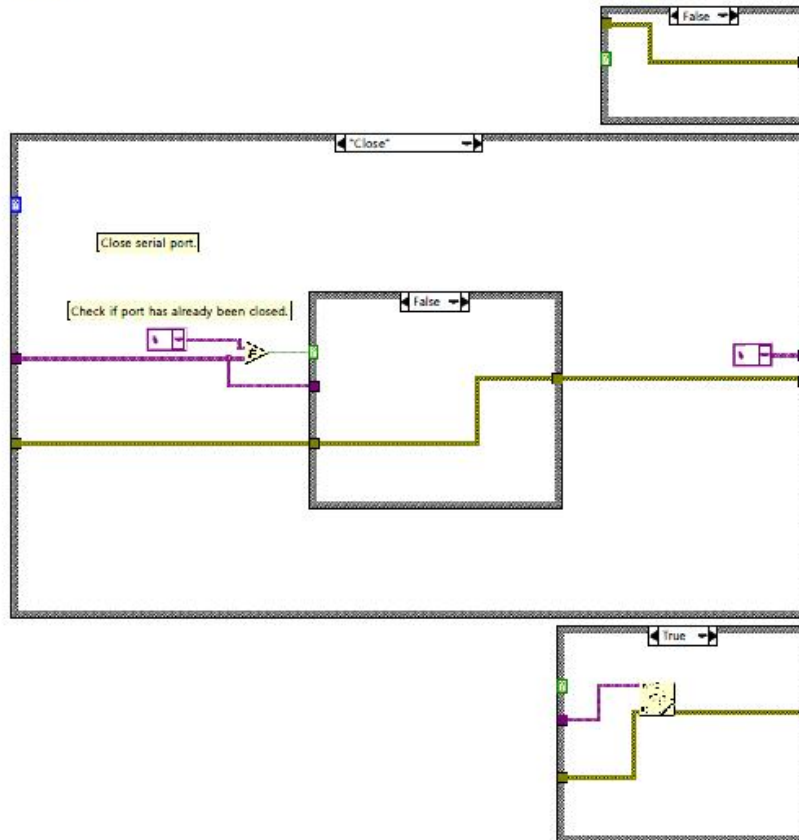


Front Panel



Block Diagram

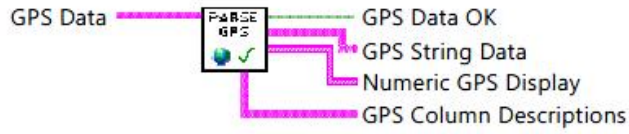







Connector Pane

Process GPS NMEA Strings.vi




Front Panel

GPS Data

GPS Data OK 


Numeric GPS Display

Local Time:
Latitude:
Longitude:
Speed (km/hr):
Fix Type:

Course (degrees): 

GPS Numeric Display

Local Time:
Latitude:
Longitude:
Speed (km/hr):
Fix Type:

Course (degrees): 

GPS Column Descriptions


Local Time HHMMSS.000
Latitude DDMM.DDDD Degrees, minutes, decimal minutes.
N/S
Longitude DDDMM.DDDD Degrees, minutes, decimal minutes.
E/W
Speed (km/hr)
Course, degrees relative to true north.
GPS Fix Type A=OK, V=Bad, 0=Invalid, 1=GPS, 2=DGPS, 4=RTK Fixed, 5=RTK Float

GPS String Data

<input type="text"/>
<input type="text"/>
<input type="text"/>
<input type="text"/>
<input type="text"/>
<input type="text"/>
<input type="text"/>
<input type="text"/>
<input type="text"/>

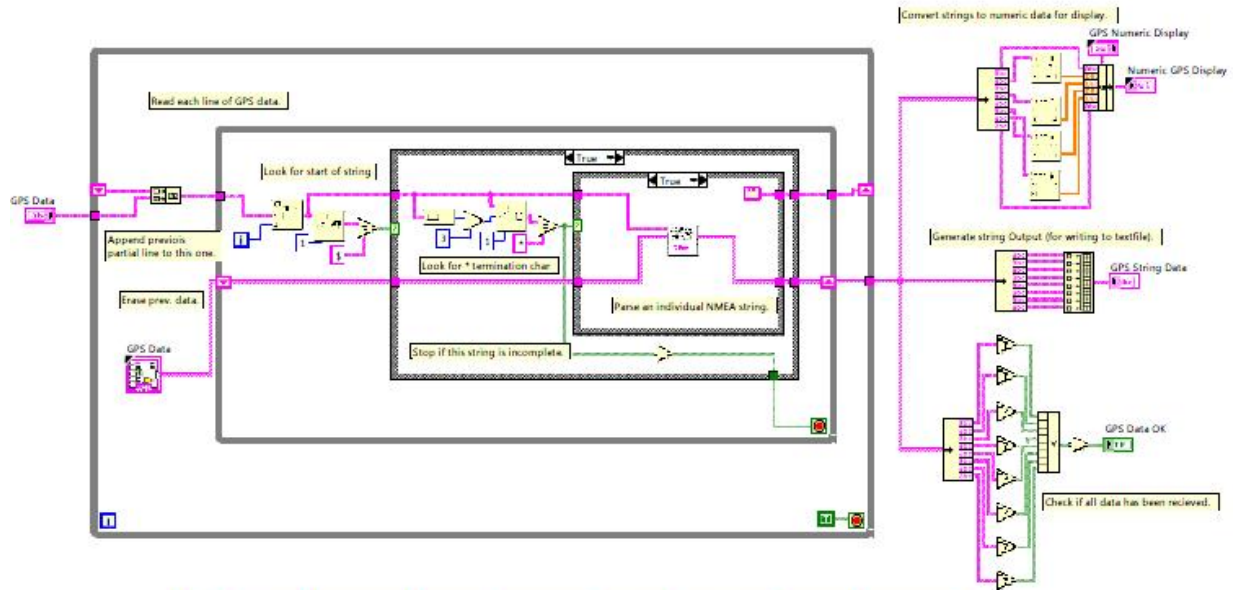
GPS Data

Time:
Latitude:
N/S:
Longitude:
E/W:
Speed (km/hr):
Course:
Fix Type:

 NATIONAL INSTRUMENTS
LabVIEW™ Evaluation Software

C:\Users\pj18160\Desktop\Harvest Monitor 2010\GPS\Process GPS NMEA Strings.vi
 Last modified on 11/13/2012 at 8:08 PM
 Printed on 11/13/2012 at 8:14 PM

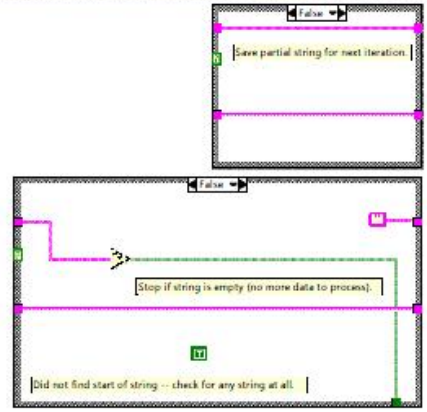
Block Diagram



0	1	2	3	4	5	6	7
Local Time HHMMSS.000	Latitude DDMM.DDDD Degrees, minutes, decimal minutes.	N/S	Longitude DDMM.DDDD Degrees, minutes, decimal minutes.	E/W	Speed (km/hr)	Course, degrees relative to true north.	GPS Fix Type A=OK, V=Bad, 0=Invalid, 1=GPS, 2=DGPS, 4=RTK Fixed, 5=RTK Float

GPS Column Descriptions

[Description of GPS data that is stored in each column. The columns match the order of the string output. Column descriptions are forwarded to the save data files so they can be written to the header.]



APPENDIX C: PROGRAMS USED IN DATA PROCESSING

C.1 Main Matlab® (Mathworks) Script Used to Process High Speed Cutting Data

```
clc; clear all;

%% Constants
%Filename
filename = uigetfile('*.txt', 'Enter Encoder and Force
Dataset');%'cut_40psi_10khz_3_stalks_15-
7mm.txt';%'cut_40psi_10khz_3_stalks_15-7mm.txt
%Experimental Data
sample_rate = 10000; %hz
stalk_diameter = 5.65/1000; %m
blade_radius = .25; %m
%Search Parameters (used to find the cutting event)
start_of_cutting = 0; %degrees
start_angle_cutoff = -140; %degrees
end_angle_cutoff = 35; %degrees
start_vel_cutoff = 2000; %deg/sec
search_window_length = 0.5; %seconds
%Initial Guess For Model
guess_for_b_over_I = 0.4392; %1/s
%Plotting Constants
pfs = 16; %plot font size
ptfs = 22; %plot title font size;
lw = 3.0; %plot line width

%% Fit Model To Recorded Data
%Pack Constants
const = struct('sample_rate', sample_rate, 'sample_time', 1/sample_rate,
...
'stalk_diameter', stalk_diameter, 'blade_radius', blade_radius,
...
'angle_start', start_angle_cutoff, 'angle_end', end_angle_cutoff,
...
'vel_start', start_vel_cutoff, 'search_window_length',
search_window_length, ...
'b_over_I', guess_for_b_over_I, 'angle_cutting',
start_of_cutting, ...
'speed_conversion', pi/180*blade_radius);
%Load File
angle_measured = dlmread(filename);
angle_measured = angle_measured(:,1);
t_measured = linspace(0, (length(angle_measured) - 1)/sample_rate,
length(angle_measured));

%Get Optimum Fit
[model_measured] = fit_coupled_model(angle_measured, const);
v_diff = (model.omega_precut -
model.omega_postcut)*const.speed_conversion;
```

```

%% Measure Sensitivity of Model
  %Sensitivity to Stalk Diameter
  [diam_sensitivity y{1} x{1}] = check_sensitivity('stalk_diameter',
const.stalk_diameter*.5, const.stalk_diameter*5.5, 25, const,
angle_measured);
  %Sensitivity to Start Of Cutting
  [start_cutting_sens y{2} x{2}] = check_sensitivity('angle_cutting',
const.angle_cutting - 4, const.angle_cutting + 2, 25, const, angle_measured);
  %Sensitivity to Start of Test
  [angle_start_sens y{3} x{3}] = check_sensitivity('angle_start',
const.angle_start - 10, const.angle_start + 10, 25, const, angle_measured);
  %Sensitivity to End of Test
  [angle_end_sens y{4} x{4}] = check_sensitivity('angle_end',
const.angle_end - 10, const.angle_end + 10, 25, const, angle_measured);

%% Plot Results
  %Plot Model and Data
  Figure(2); clf;
  subplot(3,1,1); set(gca, 'FontSize', pfs);
  hold on;
  plot(measured.t, measured.theta, 'k', 'LineWidth', lw+lw*.25);
  plot(model.t(model.win_precut), model.theta(model.win_precut), 'r:',
'LineWidth', lw);
  plot(model.t(model.win_cutting), model.theta(model.win_cutting), 'g:',
'LineWidth', lw);
  plot(model.t(model.win_postcut), model.theta(model.win_postcut), 'm:',
'LineWidth', lw);
  lim_1 = axis;
  plot(model.t(model.win_cutting(1))*[1 1], [lim_1(3) lim_1(4)], 'k :',
'LineWidth', lw*.5)
  axis(lim_1);
  h = legend('Measured Response', 'Precut', 'Cutting', 'Postcut',
'Location', 'SouthEast');
  xlabel('Time, s');
  ylabel('Angle, deg');
  title('Measured Response and Dynamic Model', 'FontSize', ptfs);
  %Plot Theoretical Velocity
  subplot(3, 1, 2); set(gca, 'FontSize', pfs);
  hold on;
  speed_conversion = pi/180*const.blade_radius;
  plot(model.t(model.win_precut),
model.omega(model.win_precut)*speed_conversion, 'r:', 'LineWidth', lw);
  plot(model.t(model.win_cutting),
model.omega(model.win_cutting)*speed_conversion, 'g:', 'LineWidth', lw);
  plot(model.t(model.win_postcut),
model.omega(model.win_postcut)*speed_conversion, 'm:', 'LineWidth', lw);
  lim_2 = axis;
  plot(model.t(model.win_cutting(1))*[1 1], [lim_2(3) lim_2(4)], 'k :',
'LineWidth', lw*.5)
  axis([lim_1(1) lim_1(2) lim_2(3) lim_2(4)]);
  legend('Precut', 'Cutting', 'Postcut', 'Location', 'NorthEast');
  xlabel('Time, s');
  ylabel('Blade Speed, m/s');
  title('Model Based Speed', 'FontSize', ptfs);
  %Plot Residuals
  subplot(3, 1, 3); set(gca, 'FontSize', pfs);
  hold on;

```

```

plot(measured.t, model.residuals, 'k', 'LineWidth', lw);
lim_3 = axis;
axis([lim_1(1) lim_1(2) lim_3(3) lim_3(4)]);
plot(model.t(model.win_cutting(1))*[1 1], [lim_3(3) lim_3(4)], 'k :',
'LineWidth', lw*.5)
xlabel('Time, s');
ylabel('Degrees');
title('Model Residuals', 'FontSize', ptfs);
%Plot Sensitivities
%Use Percent Change
%Center Means About Zero
for ii = 1:4
    x{ii} = x{ii} - mean(x{ii});
    y{ii} = (y{ii} - mean(y{ii}))/v_diff*100;    %percent change in
velocity
end
%Use Percent Change In Diameter
x{1} = x{1}/const.stalk_diameter*100;
Figure(20); clf;
subplot(2,2,2); set(gca, 'FontSize', pfs);
plot(x{1}, y{1});
    xlabel('Change In Stalk Diameter, mm');
    ylabel('Change In Velocity Difference, %');
    title('Sensitivity to Change In Stalk Diameter', 'FontSize', ptfs);
subplot(2,2,1); set(gca, 'FontSize', pfs);
plot(x{2}, y{2});
    xlabel('Change In Beginning of Cut, deg');
    ylabel('Change In Velocity Difference, %');
    title('Sensitivity to Start of cutting', 'FontSize', ptfs);
subplot(2,2,3); set(gca, 'FontSize', pfs);
plot(x{3}, y{3});
    xlabel('Change In Start Of Trial, deg');
    ylabel('Change In Velocity Difference, %');
    title('Sensitivity to Start of Trial', 'FontSize', ptfs);
subplot(2,2,4); set(gca, 'FontSize', pfs);
plot(x{4}, y{4});
    xlabel('Change In End Of Trial, deg');
    ylabel('Change In Velocity Difference, %');
    title('Sensitivity to End of Trial', 'FontSize', ptfs);

%% Copy Output To Clipboard
output(1) = model.omega_precut*const.speed_conversion;
output(2) = model.omega_postcut*const.speed_conversion;
output(3) = (output(1) - output(2));
output(4) = diam_sensitivity;
output(5) = start_cutting_sens;
output(6) = angle_start_sens;
output(7) = angle_end_sens;
output(8) = model.rsq;
num2clip(output);

%% Save Data To Mat File
save(filename(1:(end-4)), 'const', 'model', 'measured', 'x', 'y');

```

C.2 Main Matlab® (Mathworks) Script Used To Process In-Field Harvest Data

```
%Each cell is meant to be run independently
clc; %clear all;

    error('The cells in this file should be run individually');

%% Load Excel Control Information
%Control File Information
    clc; control_file.number_header_rows = 14; %range
to be loaded and processed, excel style
    control_file.name = 'File Overview and Matlab Control.xlsx';
%assume file is in same directory
    control_file.sheet = 'Sheet1';
%Read Control File
    datasets = read_excel_control_file(control_file);
    fprintf('Done.\n');

%% Convert Old Excell Files To Improved Format
    clc;
    fprintf('Converting from old xlsx to new xlsx...\n');
    run_input_function_on_each_dataset(@convert_raw_xlsx_to_formatted_xlsx,
datasets);
    fprintf('Done.\n');

%% Convert New Xlsx format To .Mat Structure For Fast Loading and Use
    clc;
    fprintf('Converting from new xlsx to .mat file...\n');
    run_input_function_on_each_dataset(@convert_xlsx_to_mat_file, datasets);
    fprintf('Done.\n');
%% Load .Mat Files
clear test_data;
clc;
fprintf('Loading .mat files into test_data structure array...\n');
for ii = 1:length(datasets)
    path_and_file = [datasets(ii).file.matlabdir
datasets(ii).file.newfile(1:(end-5)) '.mat'];
    test_data(ii) = load(path_and_file);
    fprintf('\tloading: %s\n', test_data(ii).file.name);
end
fprintf('Done.\n');

%% Hand Validate Data
    clc; fprintf('Hand Validating Activity Selection...\n');

run_input_function_on_each_dataset(@verify_activity_and_show_formatted_xlsx,
datasets);
    fprintf('Done.\n');

%% Generate Validation Plots
    clc; fprintf('Generating Validation Plots...\n');
    run_input_function_on_each_dataset(@generate_validation_plot, test_data);
    fprintf('Done.\n');

%% Fix Calculated Data In Each File
```

```

%NOTE: MUST OVERWRITE .MAT DATA FILES FOR THIS TO TAKE EFFECT
%CAN MANUALLY DELETE ALL THE FILES IN THE FOLDER
clc; fprintf('Recalculating Data...\n');

run_input_function_on_each_dataset(@update_calculations_column_of_formatted_x
lsx, datasets);
    fprintf('Done.\n');

%% Open Excel Files For Simple Corrections and Format Checking
clc;
for ii = 1:length(datasets)
    test_info = datasets(ii);
    path_and_file = [test_info.file.newdir test_info.file.newfile];
    exl = actxserver('excel.application');
    exl.visible = 1;
%     exl.heigh = 750;
    exlWkbk = exl.Workbooks;
    %     exlWkbk.Open(path_and_file)
    exlFile = exlWkbk.Open(path_and_file);
    input_loop_running = 1;
    while input_loop_running
        user_input = input('\n\nEnter:  save to save xlsx file or...\n
done to go to next record\n~>', 's');
        switch user_input
            case 'save'
                exlFile.Save();
            case 'done'
                input_loop_running = 0;
            otherwise
                fprintf('Invalid input. ');
        end
    end
    exl.Quit();
    exl.delete;
end
fprintf('Done.\n');

```

```

%Function to generate 2 plots that can be used to easily verify that test
%data is being correctly processed.
%
%Plots are saved as .pdf in directory path option.

function generate_validation_plot(test)

%% Options
fs = 12;    %Figure font size
ls = 16;    %label font size
ts = 20;    %title font size
ms = 20;    %marker size
lw = 4;     %line width

    fprintf('\tPlotting: %s\n', test.file.name);

%% Make Figure To Hold Data
hf = Figure(500); clf;
set(gcf, 'PaperPositionMode', 'auto')
%Maximize Figure (programmatically)
warning('off', 'MATLAB:HandleGraphics:ObsoletedProperty:JavaFrame'); %
disable warning message
jFrame = get(gcf, 'JavaFrame');
pause(0.3);    % unless pause is used error accures orm time to time.
                % I guess jFrame takes some time to initialize
set(jFrame, 'Maximized', 1);
warning('on', 'MATLAB:HandleGraphics:ObsoletedProperty:JavaFrame'); %
enable warning message

%% Plot GPS Of Each Test, Deleinated By Activity
    %Get Proper Zoom
    subplot(2,1,1); set(gca, 'FontSize', fs);
    plot(test.calc.x, test.calc.y, 'w'); zoom_limits = axis; cla;
    plot(1e6, 1e6, 'r .', 'MarkerSize', 25); hold on;
    plot(1e6, 1e6, 'k .', 'MarkerSize', 25);
    plot(1e6, 1e6, 'g .', 'MarkerSize', 25);
    plot(1e6, 1e6, 'b .', 'MarkerSize', 25);
    plot(1e6, 1e6, 'm .', 'MarkerSize', 25);
    plot(1e6, 1e6, 'c .', 'MarkerSize', 25);
    legend('Stopped', 'Turning', 'Working', 'Moving Too Slow', 'Throttle
Too Slow', 'Tractor In Park', 'Location', 'EastOutside');
    plot(test.calc.x, test.calc.y, 'k');
    for jj = 1:test.proc.id(end)
        current_activity = test.proc.activity{jj};
        var_1 = current_activity(1:4);
        switch var_1
            case 'pass',
                plotstyle = 'g .';
            case 'turn',
                plotstyle = 'k .';
            case 'test',
                plotstyle = 'r .';
            case 'stop',
                var_2 = current_activity(6:end);
                switch var_2
                    case 'gndspeed_too_slow',

```



```

        plotstyle = 'b .';
    case 'ptospeed_too_slow'
        plotstyle = 'm .';
    case 'tractor_in_park'
        plotstyle = 'c .';
    end
end
    plot(test.calc.x(jj), test.calc.y(jj), plotstyle);
end
xlabel('UTM Coordinates, x', 'FontSize', 1s);
ylabel('UTM Coordinates, y', 'FontSize', 1s);
name = test.file.name;
for jj = 1:length(name)
    if name(jj) == '_'
        name(jj) = ' ';
    end
end
title(['Activities For Test ' name], 'FontSize', ts);
axis(zoom_limits);

%% Plot Total Energy Vs Groundspeed
%Get Proper Zoom
subplot(2,1,2); set(gca, 'FontSize', fs);
plot(test.rec.gpsspeed, test.calc.totalpower, '.'); zoom_limits =
axis; cla;
plot(1e6, 1e6, 'r .', 'MarkerSize', 25); hold on;
plot(1e6, 1e6, 'k .', 'MarkerSize', 25);
plot(1e6, 1e6, 'g .', 'MarkerSize', 25);
plot(1e6, 1e6, 'b .', 'MarkerSize', 25);
plot(1e6, 1e6, 'm .', 'MarkerSize', 25);
plot(1e6, 1e6, 'c .', 'MarkerSize', 25);
plot(zoom_limits(1:2), test.machine.basepower*[1 1], 'r --',
'LineWidth', 1.5);
legend('Stopped', 'Turning', 'Working', 'Moving Too Slow', 'Throttle
Too Slow', 'Tractor In Park', 'Baseline Power', 'Location', 'EastOutside');
for jj = 1:length(test.proc.id)
    current_activity = test.proc.activity{jj};
    var_1 = current_activity(1:4);
    switch var_1
        case 'pass',
            plotstyle = 'g .';
        case 'turn',
            plotstyle = 'k .';
        case 'test',
            plotstyle = 'r .';
        case 'stop',
            var_2 = current_activity(6:end);
            switch var_2
                case 'gndspped_too_slow',
                    plotstyle = 'b .';
                case 'ptospeed_too_slow'
                    plotstyle = 'm .';
                case 'tractor_in_park'
                    plotstyle = 'c .';
            end
        end
    end
    plot(test.rec.gpsspeed(jj), test.calc.totalpower(jj), plotstyle);

```

```

end
xlabel('Ground Speed, km/hr', 'FontSize', 1s);
ylabel('Total Power KW', 'FontSize', 1s);
title('Total Power vs Ground Speed', 'FontSize', ts);
axis(zoom_limits);

%% Put In Test Activity
%Specify Lines Of Test
name = test.file.name;
for jj = 1:length(name)
    if name(jj) == '_'
        name(jj) = ' ';
    end
end
txstr(1) = {'Filename ' name};
txstr(2) = {sprintf('Crop, Date, Yield, Moisture: %s, %s, %.1f MG/ha
(wet) or %.1f (dry), %.1f %%dm', test.field.crop, test.field.harvestdate,
test.field.yield, test.field.yield_dm, test.field.moisture)};
txstr(3) = {sprintf('Machine, Maxtorque, width: %s, %.1f Nm, %.1f m',
test.machine.type, test.machine.maxtorque, test.machine.width)};
x_pos = (zoom_limits(2) - zoom_limits(1))*0.35 + zoom_limits(1);
y_pos = (zoom_limits(4) - zoom_limits(1))*0.1 + zoom_limits(3);
text(x_pos,y_pos,txstr,'HorizontalAlignment','left',
'BackgroundColor', [1 1 .6]);

%% Save Validation Plot
%Always Overwrite Figures...without checking...they're easy to regenerate
%Save Figure
path_and_file = [test.options.verificationplotsdir
test.file.name(1:(end-4))];
saveas(gcf, path_and_file, 'fig');

%Save .jpg Of Figure
saveas(gcf, path_and_file, 'jpg');

```